University of Stavanger

Faculty of Science and Technology

MASTER'S THESIS

Study program/ Specialization: Petroleum Engineering/Drilling	**Spring semester, 2012** **Open ~~/ Restricted access~~**
Writer: Tanmoy Chakraborty	…… (Writer's signature)
Faculty supervisor: Mesfin Belayneh **External supervisor(s): Dr. Mahbubur Rahman**	
Title of thesis: Performing simulation study on drill string mechanics, Torque and Drag.	
Credits (ECTS): 30	
Key words: Coefficient of friction, Simulation, Realtime data, Drilling, Torque and drag, Hydrodynamic viscous force, Torque and drag monitoring.	Pages: 86 + enclosure:23 Dhaka, 15th June/2012 Date/year

Acknowledgements

The thesis is submitted to Petroleum Engineering department in partial fulfillment of the requirements for the degree of Master of Science (M.Sc.). This thesis work has been carried out from January 2012 to June 2012 under the department of Petroleum Engineering, University of Stavanger, Norway. The work was running under BUET-NTNU linkage program (NOMA scholarship).

I am highly indebted to my main supervisor Mesfin Belayneh, Associate Professor, Department of Petroleum Engineering, University of Stavanger, Norway and external co supervisor Dr. Mahbubur Rahman , Associate Professor, Department of PMRE, BUET, Bangladesh for giving me the opportunity to work on this topic. I am also very grateful to the Santos Sangu Field Limited authority and Matt Davis (General manager, Drilling and Completion) to give me the chance to do my thesis on Sangu field. And above of all I am grateful to the government of Norway to give me the scholarship to study in this masters program.

I would like to express my deepest thanks and gratitude to my advisor Mesfin Belayneh for his cordial help during the tenure of my thesis. His knowledge and idea helped me a lot to give a good shape to my thesis. I'll never forget Matt Davis who gave me the chance to do the simulation myself and rely on my result.

Last of all this is my first work that I have done in my life. The simulation work on Sangu 11 was much more mature than the simulation work on South Sangu 4. I have learned a lot from this thesis work. And I enjoyed when my simulation works match with the real time data and the prediction works well at the time of monitoring real time value in Sanu11.

Abstract

In this thesis work, a simulation and monitoring study was carried based on operational data obtained from two wells. These are South Sangu-4 and Sangu-11, which are situated in block 16.

From the study it was found out that:

Comparing the simulation data and real time data, the tripping in and tripping out coefficient of friction were back calculated .The coefficient of frictions derived from Sangu-4 were used for planning of drilling in Sangu-11.

Calculating the Friction factor ratio on South Sangu-4, it shows an indication of Pack off around 3000m (MD) to 3500m (MD). And eventually the well (South sangu4) took a kick at the depth of 3486m (MD). No real time Torque and Drag monitoring was done there.

Getting the idea of the FF of that block 16, a simulation of drill string stresses, Hook Load and Torque was carried out based on the planned survey data. From the study, it was found that the Torque at higher Friction Factor will cross the limit of make-up torque which may cause the failure of the drill string. Based on the simulation the real time Hook Load and Torque data were monitored. The monitoring results investigated indication of higher Torque in real time for which Lubricant was added in the mud to reduce the Torque in safe limit. One most important observation in 8.5'' section was that the non-rotating protectors were not effectively reducing the Torque. Rather the use of lubricant controls the Torque in desired limit.

Table of contents

List of Figures

List of Tables

List of symbols

B = Buoyancy Factor

$\theta = \alpha$ =Inclination

Φ = Azimuth

Ω = Angular velocity

ρ_{mud} = Mud density

ρ_{steel} =Steel density

N_{re} = Reynold's number

τ = Shear stress.

r_w = Well bore radius.

r_o = Pipe outer radius.

D = Well diameter.

d =Outer diameter of the drill string.

n = Flow behaviour

K = consistency index.

f = Darcy's Friction factor.

V = Velocity

w = weight per unit length

μ = Coefficient of friction

σ_r = Radial stress

σ_a = Axial stress

σ_h = Hoop stress

E = Young's modulus

I = Moment of Inertia

List of abbreviations

DLS = Dog leg severity

HKLD = Hook Load

BHA = Bottom Hole Assembly

DF = Design Factor

SF = Safety Factor

RSS = Rotary Steerable System

WOB = Weight On Bit

FF = Friction Factor

CHFF = Close Hole Friction Factor

OHFF = Open Hole Fricton Factor

Chapter 1: Introduction

Those easy days of extracting oil and gas from simple vertical wells are gone. The petroleum industry is facing with the necessity of drilling more and more directional well as offshore activities continue to increase. Some directional wells have deviations of as much as 70 degree to the vertical and the most drilled directional well is horizontal which makes around 90degree from the vertical. One of the advantages of directional drilling is that the well is exposed to large producing interval length in the reservoir. The second reason is that the number of platforms on new projects will be reduced when wells have long horizontal sections. Recent wells have been drilled more than 12 km. Maersk Oil Qatar had the previous world record in a well with a measured depth of 40,320 ft (12,290 m) including a horizontal reach of 35,770 ft (10,900 m) in the Al Shaheen Field offshore Qatar. On 28 January 2011 the world's longest borehole was drilled at the Odoptu field, Sakhalin-1 situated in the eastern coastland of Russian mainland with a measured total depth 12345 meters and a horizontal displacement of 11475 meters. Torque and drag becomes a very important parameter for these deviated wells as most of the drilling difficulties are occurring due to these. The hard times are coming for the exploration and development field to take the more challenge to extract the oil and gas. The more the challenges is the higher cost of exploration and development of the well. To reduce exploration and development costs, the industry has developed drilling optimizations simulator. Simulation is a must during planning, drilling phases and a post well drilling analysis. Simulation help to design well program and drill string program in order to avoid a possible unwanted well and drill string failures by limiting an operational safe window.

1.1 Back ground for the thesis

The company Santos, the only offshore company in Bangladesh, has planned to drill some wells in the offshore block 16 of Bangladesh. The offshore block 16 is situated in the Bay of Bengal. One of their planned well (Sangu 11) is about 54 degree deviated directional well which is basically a build hold and drop type well. The company was looking to measure the torque and drag value which might be a potential problem for drilling the well safely. To do that, the company decided to produce the prediction of Torque and Drag of that well and monitor the torque and drag while drilling will take place. Before doing that they need a realistic determination of typical average wellbore friction coefficients. This realistic friction coefficient can be calculated from actual drilling situations by using the computer program with drill string surface loads as input data to calculate the friction coefficient for a particular well geometry and drill string. Input data can be pickup weight, slack off weight or torque readings each of which can produce an independent friction coefficient. So it is important to know the coefficient of friction on that block to control the torque and drag of that (Sangu 11) directional deviated well. In order to get an idea about the coefficient of friction of the block the company planned to use their first well South Sangu 4.

1.2 Scope and objective of the thesis

As part of my thesis work I was involved in the drilling campaign at the block 16 of Bangladesh explored by the company Santos Sangu field limited. The scope of this thesis is based on literature study, simulation and monitoring of real time data.

The main objectives are to:

- Analyse the tripping in and tripping out data of South Sangu 4 well to have the idea of coefficient of friction in open hole section on that block.
- Perform simulation study on drill string mechanics of the next deviated well Sangu 11.
- Monitor and study the Torque and drag actual data of Sangu 11 .

Chapter 2: Literature study

2.1 Important role of coefficient of friction in drilling

In this section most of the texts are taken from (Robello Samuel, 2010)

2.1.1 Well path Design

The friction factor between the string and the wellbore is very important for designing the well path. If the friction factor between the string and wellbore is high then we have to be careful in changing the inclination. High inclination in high friction factor region can produce excessive torque and drag which can be the cause of drilling failure. So coefficient of friction is very important in the case of well path design. Normally the sale inclination should be less than the critical inclination, to ensure that the drill string or casing slides downward. For sliding pipe or motor drilling, there is a critical inclination for gravity-driven.

2.2.2 Rotating on/off bottom operation

Friction factor is also affecting many parameters of rotating on bottom and off bottom operation. In on bottom operation coefficient of friction is largely responsible to create high torque along with the geometry of the well. But in the case of hook load the main contributing factors that would cause deviation from the actual hook load include the mud weight variability along the hole, drill string mass, and the well path.. An adjustment of the mud weight and drill string mass will satisfy the condition.

2.1.3 Tripping in/tripping out operation

For tripping in and tripping out operation the coefficient of friction is very important along with mud properties and well geometry. The mud weight properties and well geometry is predefined in the well program so if we can know understand the nature of friction factor in the formation we can alter our well design to avoid the problems in drilling. Though in tripping in and tripping out operations, the up and down drag forces are not linearized reversals of one another for various reasons, such as drill string geometry, formation geometry , position , and the path traversed when the pipe is tripped . This results due to different friction factor which occurs due to different contact point.

2.1.4 Swab and Surge analysis

The friction forces are accounted in the correct direction to estimate the axial tension for calculating the dynamic swab and surge pressures due to pipe movement. The influence of coefficient of friction is evident in the overall results in estimating the position of the pipe, as well as in solving the dynamic pressure-flow equation. The figure below shows the effect of friction factor on the dynamic wellbore pressures. These results are for a ''J''-type directional well with the maximum angle o 60 degree and dogleg 3 degree/100 ft, and show simulated swab results at the bottom of the well at 20,000ft with and without friction forces.

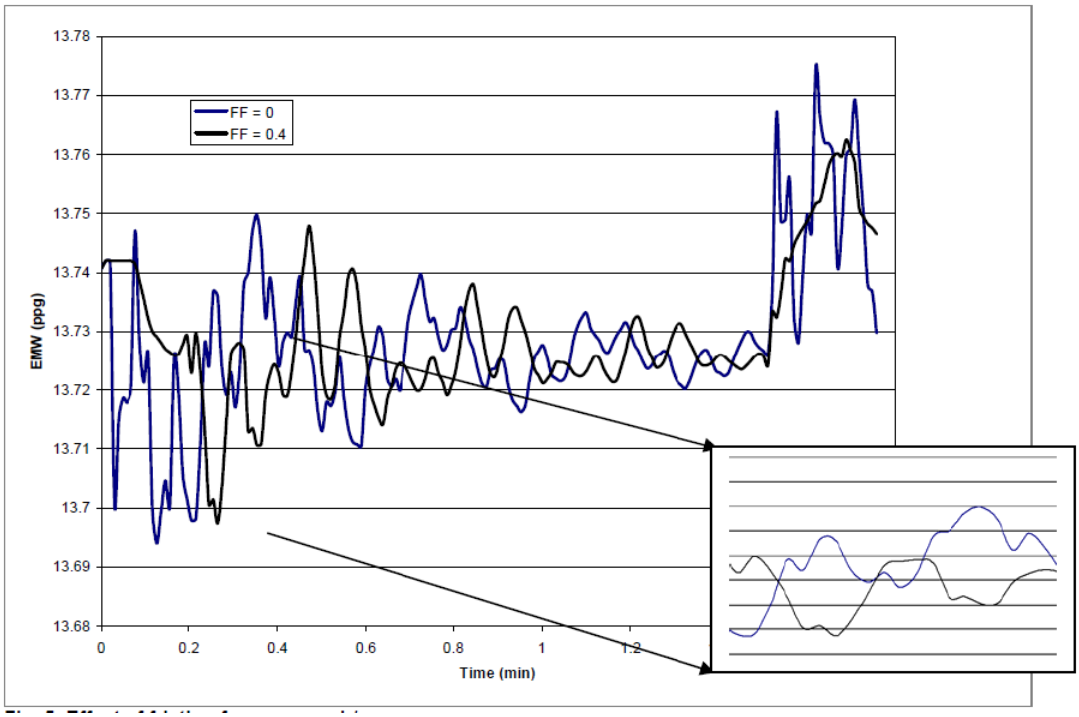

Figure 2.1 : Effect of friction on well Pressure (Robello Samuel, 2010)

2.1.5 Drill ahead analysis

The forces are generated in three directions as the bit is progressed in the wellbore. Bending characteristics of the bottom hole assembly confined in a well bore will result in a bit tilt in both the inclination and azimuth axes. The interaction of these variables will determine the wellbore trajectory. While calculating these forces , the friction forces, the friction factor used in the form of coefficient of friction is important.

2.1.6 Stuck force estimation

The drilling string is assumed to be a series of blocks with weightless string attached. Torque and drag calculations are usually use to predict the over pull and slack off forces for freeing stuck pipe and to apply force and torque for backing off.

2.2 Torque and Drag modelling

2.2.1 Model assumptions

For the modelling of Toque and drag, the following are most common assumptions.

- **Slack string:** This assumes that the drill string is lying on the wellbore (a drill string is in a continuous contact with the wellbore).
- **Coulomb friction:** The friction force against the drill string is due to the wallbore and the drilling fluid.
- **Soft string:** For a vertical and an inclined straight well section, the contact force is due to the normal component of the weight of the drill string.
- **Fluid flow effect** : the fluid flow in the annulus has an effect on the drag force.

2.2.2 Well friction torque and Drag in straight section

The wellbore friction models are basically derived based on the above assumptions. The figure defines the forces free diagram on a string and an inclined plane (Aadnøy 2006):

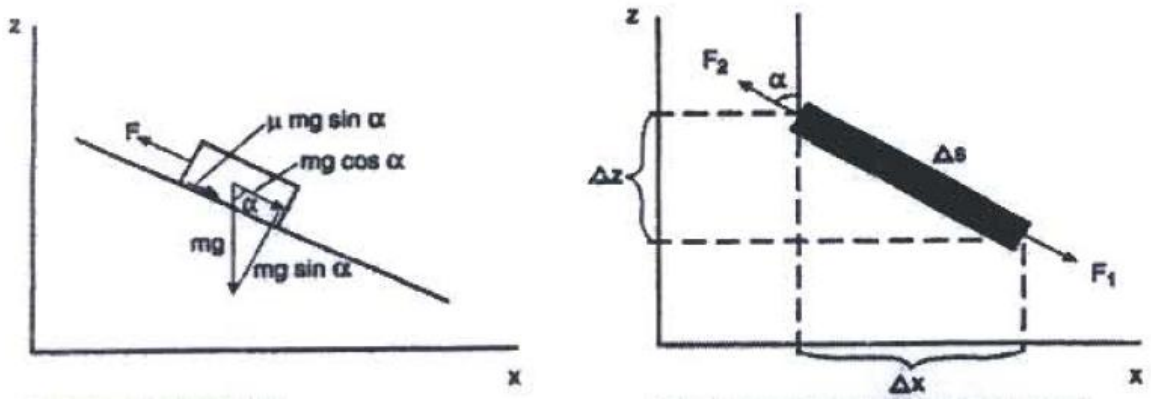

Figure 2.2 a) Forces on inclined object 2.2 b) Geometry and forces for straight inclined hole.(Aadnøy, 2006)

The force required to pull a string along an inclined plane is

$$F = mg\cos\alpha + \mu mg\sin\alpha \qquad 1$$

In case of lowering the drill string the friction force will act opposite to the direction of motion and hence the equation become

$$F = mg\cos\alpha - \mu mg\sin\alpha \qquad 2$$

This is a coulomb friction model. From a stationary position, increasing or decreasing the load an equal amount will be lead to upward or downward movement of the drill string. For a drill string of weight mg= (wΔs) and an inclination α , the axial weight and the drag force in a straight inclined section becomes :

$$F_2 = F_1 + w\Delta s\,(\cos\alpha \pm \mu\sin\alpha) \qquad 3$$

The plus sign defines pulling of the pipe, whereas the minus sign defines lowering of the pipe. The first term inside the bracket defines the weight of the pipe and the second term defines additional frictional force required to move the pipe. The change in force when initiating the motion either up or downward is found by subtracting the weight from the forces defined above. The weight is

$$w\Delta s\cos\alpha \qquad 4$$

The same principle also applies for the rotating friction , the torque. The applied torque is equal to the normal moment (wΔsr) multiplied with the friction factor μ . The torque then becomes

$$T = \mu w \Delta s r \sin\alpha \quad (5)$$

The unit mass of the drill pipe or the weight must always be rrected for buoyancy. The buoyancy factor is given by

$$\beta = 1 - \frac{\rho_{mud}}{\rho_{pipe}} \quad (6)$$

And the buoyed weight must be

$$w = \beta w drill\ \ pipe \quad (7)$$

2.2.3 Torque and drag in bends

Drop off bends

We will in the following derive equations to calculate the drag forces when a drill string is pulled or lower through a bend. **Figure 2.3** shows the forces acting when a pipe is pulled through a drop-off section. Before doing the actual analysis, a few parameters need to be defined. Due to the bend, a normal force N results between the drill string and the hole. While pulling the string, a frictional force Q resists the motion. The weight of the string is the unit weight w multiplied with the length of the differential element, wRdα. Choosing an x, z reference system the weight can be decomposed into the following components

$$P = wRd\alpha\cos\alpha \ and\ O = wRd\alpha\sin\alpha \quad (8)$$

Performing a force balance in the x and z direction results in the following equations

$$\sum Fx = 0: \ (F + dF)\cos d\alpha/2 - F\cos d\alpha/2 - Q - P = 0 \quad (9)$$

$$\sum Fz = 0: \quad N - O - (F + dF)\sin\alpha/2 - F\sin d\alpha/2 = 0 \quad (10)$$

The resulting friction force Q is equal to the coefficient of friction μ multiplied with the resulting normal force, that is : Q= μN. Furthermore, for small arguments, cos dα/2 = 1, and sin dα/2 = dα/2. The force balance above can be shown to becomes:

$$dF = Q + P = Q + wRd\alpha\cos\alpha \quad (11)$$

$$N = Fd\alpha + O = Fd\alpha + wRd\alpha\sin\alpha \quad (12)$$

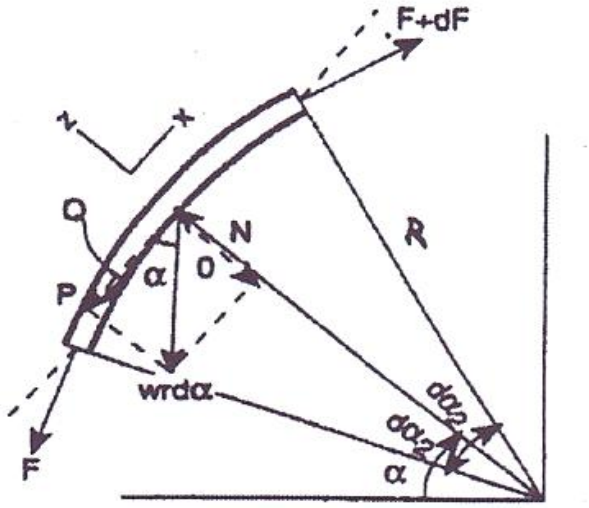

Figure 2.3: Drag forces in drop off bends (Aadnøy,2006)

Combining the equations above, the equation for the tension in the drill string becomes:

$$dF = \{\mu F + wR(\mu \sin\alpha + \cos\alpha)\}d\alpha \qquad 13$$

Integrating equation 13, the final solution for the additional force through the bend is given by :

$$F_2 = F_1 e^{\mu(\alpha 2-\alpha 1)} + \frac{wR}{1+\mu^2}\begin{Bmatrix}(1-\mu^2)(\sin\alpha_2 - e^{\mu(\alpha_2-\alpha_1)}\sin\alpha_1) \\ -2\mu(\cos\alpha_2 - e^{\mu(\alpha_2-\alpha_1)}\cos\alpha_1))\end{Bmatrix} \qquad 14$$

Here F1 refer to the tension at the bottom and F2 to the tension at the top of the bend.

The above equation is valid for the case of pulling the drill string upwards. If the drill string is lowered into the well, the forces F and F+dF interchanges place in **figure 2.2**, and the friction force Q changes direction. The force balance now becomes:

$$dF = Q - P = Q - wrd\alpha\cos\alpha \qquad 15$$

$$N = Fd\alpha + O = Fd\alpha + wRd\alpha\sin\alpha, \qquad 16$$

Resulting in the following differential equation:

$$dF = \{\mu F + wR\{\mu\sin\alpha - \cos\alpha\}da, \qquad 17$$

Which gives the solution

$$F_2 = \{F_1 e^{\mu(\alpha_2-\alpha_1)} + wR\{\sin\alpha^2 - e^{\mu(\alpha_2-\alpha_1)}\sin\alpha_1\} \qquad 18$$

Note that the forces have for this case been redefined. F2 is always referring to the force in the top of the string.

The frictional Torque is equal to the normal force multiplied with the pipe radius, integrated over the length of the bend, ds = rdα. The tension in the pipe for a static position is:

$$F = F_1 - wR(\sin\alpha - \sin\alpha_1) \tag{19}$$

The general expression for the torque becomes,

$$T = \int \mu r N \tag{20}$$

Integrating the equation above, the resulting torque for drop off bend becomes :

$$T = \mu r\{F_1 + wR\sin\alpha_1\}(a_2 - a_1) - 2\mu r wR(\cos\alpha_2 - \cos\alpha_1) \tag{21}$$

Build up bends

Figure 2.4 shows the forces in the build up section. The basic definitions are the same as for the previous case. A force balance now results in :

$$\sum Fx = 0: \ (F + dF)\cos d\alpha/2 - F\cos d\alpha/2 - Q - P = 0 \tag{22}$$

$$\sum Fz = 0: \ N + O - (F + dF)\sin d\alpha/2 - F\sin d\alpha/2 = 0 \tag{23}$$

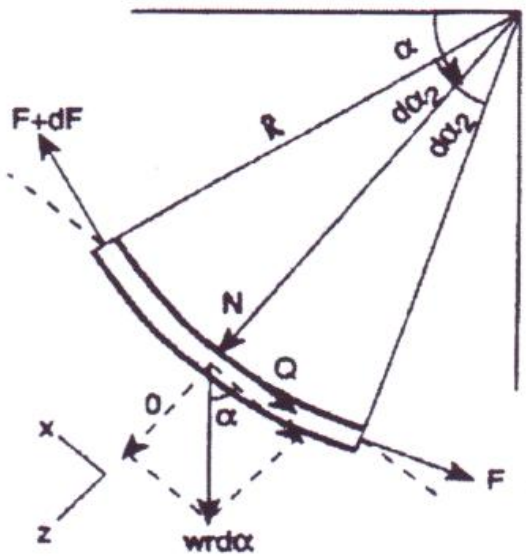

Figure 2.4 : Drag forces in buildup bends (Aadnøy,2006)

Repeating the previous analysis , the force balance above becomes :

$$dF = Q + P = Q + wrd\alpha\cos\alpha \quad (24)$$

$$N = Fd\alpha - O = Fd\alpha - wRd\alpha\sin\alpha \quad (25)$$

Repeating the previous analysis, it can be shown that pull force is now defined by :

$$dF = \{\mu F - wR(\mu\sin\alpha + \cos\alpha)\}d\alpha \quad (26)$$

$$F_2 = F_1 e^{-\mu(a_2 - a_1)} - wR\{\sin\alpha_2 - e^{-\mu(a_2 - a_1)}\sin\alpha_1\} \quad (27)$$

Finally for the case of lowering the pipe through the build-up bends results in: dF=Q-P

$$dF = \{\mu F - wR(\mu\sin\alpha + \cos\alpha)\}d\alpha \quad (28)$$

Which solved again defining F2 as the top force becomes :

$$F_2 = F_1 e^{\mu(a_2 - a_1)} - \frac{wR}{1+\mu^2}\begin{Bmatrix}(1-\mu^2)(\sin\alpha_2 - e^{\mu(a_2 - a_1)}\sin\alpha_1) \\ -2\mu(\cos\alpha_2 - e^{\mu(a_2 - a_1)}\cos\alpha_1)\end{Bmatrix} \quad (29)$$

Repeating the process for buildup bends the Torque becomes

$$T = \mu r\{(F_1 + wR\sin\alpha_1)|a_2 - a_1|\} + 2\mu wRr(\cos\alpha_2 - \cos\alpha_1) \quad (30)$$

Side bends

In side bend another complexity arise, which can be described as follows .

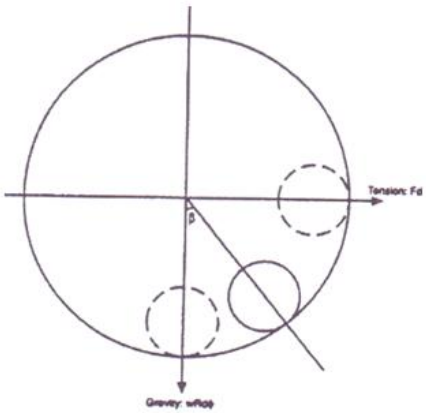

Figure 2.5 : Position of the drill pipe in the borehole for a side bend (Aadnøy,2006)

Figure 2.5 shows the situation. One extreme is that the drill pipe is weightless. For this case pure tension applies, and the pipe will assume a position in the middle of the borehole. Based on previous derivations, we can define the end force of the bend due to tension as:

$$F_{2t} = F_1 e^{\mu(\phi_2 - \phi_1)} \quad (31)$$

The normal force on the borehole is the tension multiplied by the angle, or :

$$dN_t = F d\phi \quad (32)$$

The other extreme would be to assume the pipe weight is the deforming factor, resulting in the pipe lying on the bottom of the hole. The normal force is then:

$$dN_g = wF d\phi \quad (33)$$

In reality, neither of the two extreme exists. The drill pipe may assume a position at the bottom of the hole when entering the bend, and move towards β = 90◦ at the exit of the bend. We will assume that the resultant normal force is

$$dN = \sqrt{dN^2{}_t + dN^2{}_g} \quad (34)$$

The friction in the borehole is equal to the resultant normal force, multiplied with the coefficient of friction, or :

$$dF = \mu \sqrt{F^2 + (wR)^2}\, d\phi \quad (35)$$

Integrating equation 37, the general solution is :

$$In\left\{F + \sqrt{F^2 + (wR)^2}\right\} = \mu\phi + c \quad (36)$$

The constant of integration, c, is determined by inserting the initial condition (F_1,ϕ_1). Applying the other end condition, the tension at the upper end of the side bend is given by

$$F_2 = \frac{1}{2}\left\{F_1 + \sqrt{F^2{}_1 + (wR)^2}\right\} e^{\mu(\phi_2 - \phi_1)} - \frac{1}{2}\frac{(wR)^2 e^{-\mu(\phi_2 - \phi_1)}}{2F_1 + \sqrt{F^2{}_1 + (wR)^2}} \quad (37)$$

A similar expression results for lowering of the pipe. The difference is that the change in the exponent sign. The pipe position on the borehole wall can be determined by defining a tangential force balance as seen for the figure 5 :

$$\tan\beta = \frac{F_1 e^{\mu(\phi - \phi_1)}}{wR} \quad (38)$$

Inserting zero friction equation 37, one observe that F2 = F1. For pure rotation, the torque is generated by a constant normal force (weight) as defined in equation 37.The total Torque becomes:

$$T = \mu r \sqrt{F^2{}_1 + (wR)^2}\,(\phi_2 - \phi_1) \quad (39)$$

2.2.4 Three dimensional (3D) Friction model

In this section most of the texts and figures are taken from Bernt S. Aadnøy,M. Fazaelizadeh,Geir Hareland, 2010

The equations derived here define the Hook Loads for hoisting and lowering operations and also Torque for a string in a wellbore. There are two sets of equations, one for straight well sections and another for arbitrary well orientation.

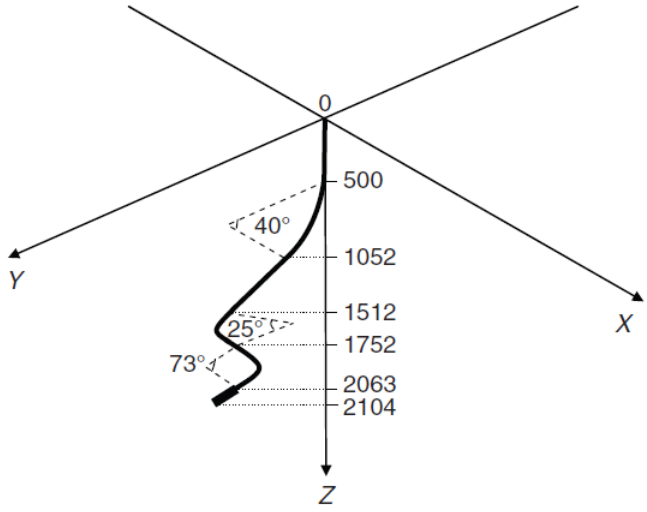

Figure 2.6: A 3D well shape

Drag for straight inclined wellbore sections without pipe rotation:

A characteristic of a straight wellbore is that pipe tension is not contributing to the normal pipe force, and hence not affecting friction. Straight sections are weight dominated as only the normal weight component gives friction. The top force F2 of an inclined pipe is given by:

$$F_2 = F_1 + \beta \Delta L w \{\cos\alpha \pm \mu \sin\alpha\}, \quad (40)$$

Where, "+" means hoisting and "- " means lowering of the pipe.

Torque for straight inclined wellbore sections without axial pipe rotation:

The torque is defined as the normal weight component multiplied by the coefficient of friction and the pipe tool joint radius. The result is:

$$T = \mu r \beta w \Delta \sin\alpha\,. \quad (41)$$

Drag for curved wellbore sections without pipe rotation:

For curved borehole sections, the normal contact force between string and hole is strongly dependent on the axial pipe loading. This is therefore a tension dominated process. In, for instance, a short bend, the tension is often much larger than the weight of that pipe inside the bend. In the following derivation we will assume that the pipe is weightless when we compute the friction, but add the weight at the end of the bend.

Furthermore, The Dogleg and angle depends both on the wellbore inclination and the azimuth. Because the pipe will contact either the high side or the low side of the wellbore, its contact surface is given by the Dogleg plane.

For build up, drop off**,** side bends or combination of these , the axial force becomes :

$$F_2 = F_1 e^{\pm\mu|\theta_2-\theta_1|} + \beta w \Delta L \left\{ \frac{\sin\alpha_2 - \sin\alpha_1}{\alpha_2 - \alpha_1} \right\} \quad 42$$

Where, "+" means hoisting and "-" means lowering of the pipe.

Torque for curved wellbore sections without axial motion:

The Torque for the bend is defined as:

$$T = \mu r N = \mu r F_1 |\theta_2 - \theta_1| . \quad 43$$

Friction for any wellbore shape can thus be computed by dividing the well into straight and curved elements.

The forces and Torques are summed up starting from bottom of the well. Equation 1 and 3 give the drag whereas equations 2 and 4 give the Torque.

Combined Axial motion and Rotation :

The previously described solutions must be modified if a combined motion takes place. Aadnoy and Andersen showed how the frictional capacity is decomposed into two directions, axial motion and rotation. The effect of combined motion is well known, for example when rotating a liner. A high rotational speed reduces the axial drag.

During the combined motion, the axial velocity is V**h** and the tangential pipe speed is V**r**. These give a resultant velocity of V. The angle between the axial and tangential velocity is:

$$\psi = \tan^{-1}\left(\frac{V_h}{V_r}\right) = \tan^{-1}\left(\frac{60 V_h (m/s)}{2\pi N_r (rpm)\, r(m)}\right) \quad 44$$

The Torque and drag for combined operation in a straight section **is:**

$$F_2 = F_1 + \beta w \Delta L \cos\alpha \pm \mu \phi w \Delta L \sin\alpha \sin\psi \quad 45$$

$$T = r\mu\beta w \Delta L \sin\alpha \cos\psi \quad 46$$

And the torque and drag for combined operation in a curved section **is:**

$$F_2 = F_1 + F_1\left(e^{\pm\mu|\theta_2-\theta_1|} - 1\right)\sin\psi + \beta w \Delta L \left\{ \frac{\sin\alpha_2 - \sin\alpha_1}{\alpha_2 - \alpha_1} \right\} \quad 47$$

$$T = \mu r N = \mu r F_1 |\theta_2 - \theta_1| \cos\psi \quad 48$$

2.2.5 Curvature dependent 3D T& D model

Figure 2.7 illustrates loads on the drill sting. Johancsik et al (1984) has derived a 3D model, which is a function of variation in inclination and azimuth. According to the authors, the normal force per unit length is given as:

$$N_i = \sqrt{\left(\beta w_i \sin\left(\frac{\theta_{i+1}+\theta_i}{2}\right) - F_i\left(\frac{\theta_{i+1}-\theta_i}{S_{i+1}-S_i}\right)\right)^2 + \left(F_i \sin\left(\frac{\theta_{i+1}+\theta_i}{2}\right)\left(\frac{\varphi_{i+1}-\varphi_i}{S_{i+1}-S_i}\right)\right)^2} \quad 49$$

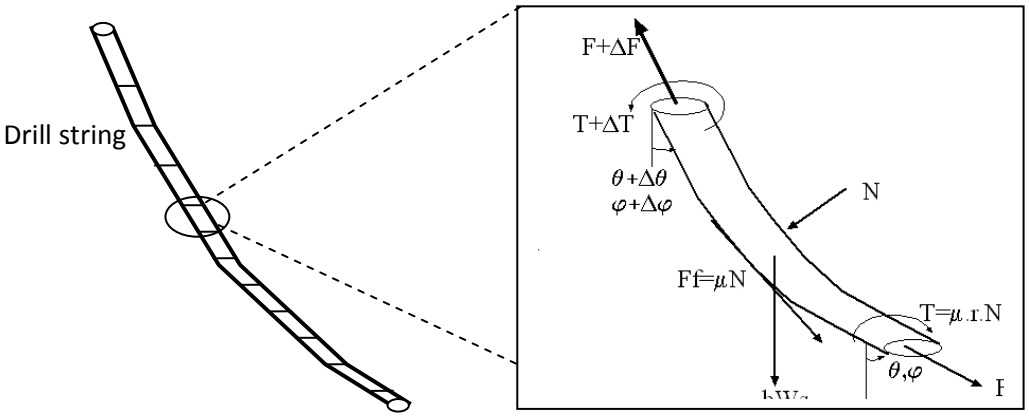

Figure 2.7: Illustration of drill string and loadings

In addition, we are drilling at various angular rotational speeds and when tripping in/out a drilling string at various axial speeds. These dynamics parameters affect the axial and tangential coefficients of friction. These will be considered in the torque and drag mode as the following.

The axial friction factor, μ_a, is given as:

$\mu_a = \mu \sin\alpha$ Where the angle α is given by $\tan\alpha = \frac{v_a}{r\Omega}$, r is the local drill string radius, Ω is the angular velocity of rotation and v_a is the axial speed. Sing conventions are chosen as (v_a is defined positive for tripping in and drilling, and negative for pulling out).

$$F_{i+1} = F_i + \sum_{i=1}^{n}\left[\beta w_i \cos\left(\frac{\theta_{i+1}+\theta_i}{2}\right) \pm \mu_{ai} N_i\right](S_{i+1}-S_i) \quad 50$$

F_i is the bottom weight when integrating from the bottom to top type. The sign of the fiction force is always opposite to the direction of the applied axial load on a tube. When axial load is in the direction of the component of the weight of the tube (i.e. run into the hole), the friction causes a compressive (negative) force to be added. When the axial load is in the opposite direction of the component of the tube along the axial direction (i.e. when pull out of the hole), the friction causes a tensile (positive) force to be added.

2.2.6 Effect of hydrodynamics viscous force

Applying the condition of equilibrium along the axial and the normal directions, the effective force along the axial direction reads:

$$\frac{dF}{ds} = \pm\mu_a N + \beta w_s \cos\bar{\theta} + \frac{dF_{fl}}{ds} \qquad 51$$

Where the fist term is the contact force given by Eq.14 and the second term is the axial component of the weight of the drill string and the third term is the fluid flow effect, given as (Bhalla & Walton, 1998)

$$\frac{dF_{fl}}{ds} = \frac{2\pi r_i r_o}{r_o^2 - r_i^2}(r_o\tau_0 - r_i\tau_i) \qquad 52$$

Where, τ_o and τ_w are the outer tube and the wellbore shear stress and r_w is the wellbore radius, r_o is the pipe outer radius, and τ_w and τ_o are the corresponding wall shear stresses due to fluid flow. The latter two quantities are defined positive for fluid flow up the annulus. In this theory the wall shear stress τ_i on the pipe inner wall does not affect the force balance.

Maidla and Wojtanowicz (1987, a) also derived the effect of viscous pressure gradient for each pipe element. The hydrodynamic viscous drag force can be calculated by to be included in the drag equation:

$$F_{fl} = \frac{\pi}{4}\sum_{i=1}^{n}\left(\frac{\Delta P}{ds}\right)\Delta s_i d_i^2 \qquad \mathbf{53}$$

Where, the pressure loss term with fluid velocity and density in the annulus is given as

$$\frac{\Delta P}{ds} = \frac{f\rho V_{av}^2}{D-d} \qquad 54$$

Where D = well diameter, d = outer diameter of the drill string

The friction factor is calculated based on the flow regimes
For laminar

$$f = \frac{16}{N_{\mathrm{Re}}} \quad (55)$$

For turbulent,

$$f = \frac{0.0791}{N_{\mathrm{Re}}^{0.25}} \quad (56)$$

Where, N_{Re} is the Reynolds number and determined based on the flow regimes and rheology of the drilling fluid. It is given as according to Power-law model:

$$N_{\mathrm{Re}} = 10.9x10^{4}\,\frac{\rho V_{an}^{2-n}}{k}\left(\frac{D-d}{48}\,x\,\frac{n}{2n+1}\right)^{n} \quad (57)$$

For laminar flow: $N_{Re} \leq 3470 - 1370xn$ (58)

For turbulent flow: $N_{Re} \geq 420 - 1370xn$ (59)

Where n is flow-behavior index and k = consistency index *dyne.s/100 cm*^{2}

2.3 Buckling

In a circularly constrained well, a tube can be buckling either sinusoidally or helically. The following presents the two modes of tube deformations. All these critical load formulas are taken from Mesfin Belayneh, A Review of Buckling in Oil Wells, 2006

2.3.1 Sinusoidal buckling

The sinusoidal mode of deformation is the first phase of buckling , the pipe buckling in an oil wellbore encounters lateral encounters along the length of the tube. The shape of the initial buckling will look like as sinusoidal as seen from the top side shown in the **figure2.8** But the end view of the initial bucking is off course a curve , when viewed from the axial direction of the wellbore. As the length increases, the weight increases thus the force required pushing it , increases. For the initial distance the CT remains straight, forming a trough at the bottom of the casing. Once the force required to push the tubular reaches a certain amount (load) , the tubular will begin to “snake” in a

sinusoidal form. The load is called the “sinusoidal buckling load”. In drill pipes , it is often referred to as the “ critical buckling load”. The amplitude is not greater than the inner diameter of the casing.

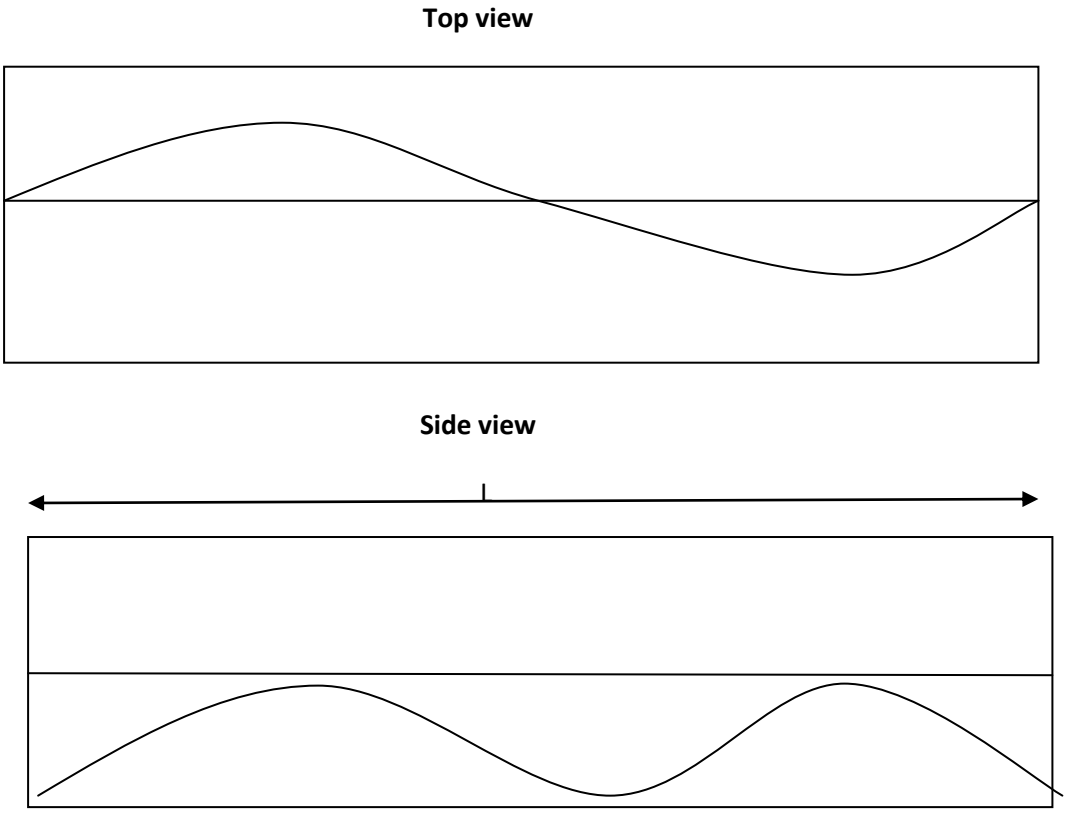

Figure 2.8: Sinusoidal critical buckling of pipe in oil well

Critical load for sinusoidal buckling in vertical well:

When a compressive load exceeds the critical (sinusoidal) buckling load , the coiled will buckle. For long pipe, Lubiniski derived a critical buckling load for drill strings in a vertical well

$$F_{cri} = 1.94(EIw^2)^{1/3} \quad 60$$

This equation is valid with a length equivalent to 7.94 dimensionless unit. For the greater length of this Lubiniski showed that

$$F_{cri} = 1.88(EIw^2)^{1/3} \quad 61$$

Wu et al (1992) proposed the vertical sinusoidal buckling as:

$$F_{cri,b} = 2.55(EIw^2)^{1/3} \quad 62$$

Critical load for sinusoidal buckling in inclined well :

Paslay and Bogy , (1964) gave the sinusoidal buckling equation for inclined well as :

$$F_{cri} = 2\left(\frac{EI\rho Ag\sin\theta}{r}\right)^{0.5} \quad 63$$

2.3.2 Helical buckling

Helical buckling is the second phase and the critical tube buckling. By increasing sufficient load, a certain load is reached that makes the tube form a helix inside the casing. This load is referred to as the "Helical buckling load". The reason for this buckling type change is that the cylindrical wall of the wellbore constrains the sinusoidal buckling development within the wellbore and the helix takes on the post buckling shape that has the minimum total potential energy. This buckling shape is called the helical buckling. **Figure 2.9** is the side view and the top view of the helical buckling.

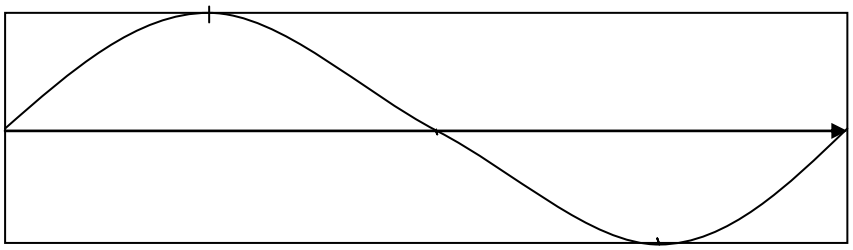

(a)Top view

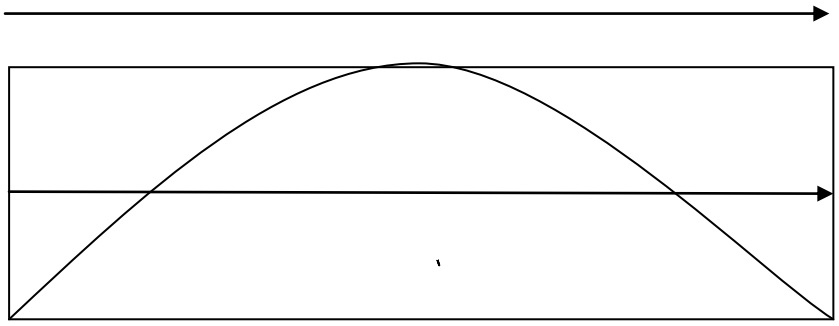

(b)Side view

Figure 2.9: Helical buckling of a pipe in a wellbore

Critical load for Helical buckling in vertical well :

Wu et. al., (1993) have derived a new helical buckling load equation through an energy analysis to predict the occurrence of helical buckling in vertical well bores. They have proposed the vertical helical buckling as :

$$F_{cri,b} = 5.55(EIw^2)^{1/3} \quad 64$$

Critical load for Helical buckling in inclined well :

Chen et. al. ,(1989) using energy principle, derived an equation for the helically buckling in horizontal wells (α=90°):

$$F_{hel} = 2\sqrt{2}(EI)^{0.5}(w)^{0.5}(\frac{1}{r})^{0.5} \quad 65$$

Wu and Juvkam-wold (1993) derived the helical buckling force for inclined and horizontal wells. The true critical load is given by:

$$F_{hel} = 2(2\sqrt{2}-1)(EI)^{0.5}(w)^{0.5}(\sin\alpha / r)^{0.5} \quad 66$$

Lubiniski and Woods fits n equation to experimental data collected in 1953. The fitted equation was:

$$F_{hel} = 2.85(EI)^{0.504}(\rho Ag)^{0.496}(\sin\theta / r)^{0.511} \quad 67$$

Dellinger et. Al. 1983 presented similiar equation as:

$$F_{hel} = 2.93(EI)^{0.479}(\rho Ag)^{0.522}(\sin\theta / r)^{0.436} \quad 68$$

2.3.3 Lockup

The phenomenon of “lock-up” of a tubular is the situation when the tubular cannot be pushed further into the well bore. This is due to the fact that pushing the formed helix into the casing will increase the wall contact forces. This eventually increases the friction with the wall of the casing. The coiled tube has now 3 sections. First there is a straight section up to the point where the sinusoidal

buckling load is reached. This is followed by a sine mode deformation until the helical buckling load reached. Finally there is a section of the tubular buckled into a helix. It is only this third, helical section in which the additional wall contact forces are generated.

The development of coiled tubing helical buckling and the frictional drag are different for different well bores. In horizontal wellbore, helical starts from pushing the top, while in vertical well bore the helical buckling starts from the bottom (the kick point). In order to avoid the possible lock-up condition, we need to operate within the safe operational limits. The criteria for the lock-up operational limits are (Aasen and Aadnoy, 2002) :

1. The ratio of the change in output (bottomhole weight) to the change in input (change in surface weight) should not be less than 1%.
2. The Von Mises' effective tubing stress shall not exceed 80% of the yield strength of the material.

2.4 Stresses in drill string

Figure **2.10** is drill pipe with wall thickness, *t*, and inner radius, *r*. The pipe is pressurized internally and externally with P_i and P_o, respectively. It is also loaded axially with load F and possible applied with torque. The figure shows an element of material subjected to stress σ_x, σ_y, and σ_z in three perpendicular directions is said to be in a state of triaxial stress. Tubes subjected to axial load and pressure (external and/or internal pressure).

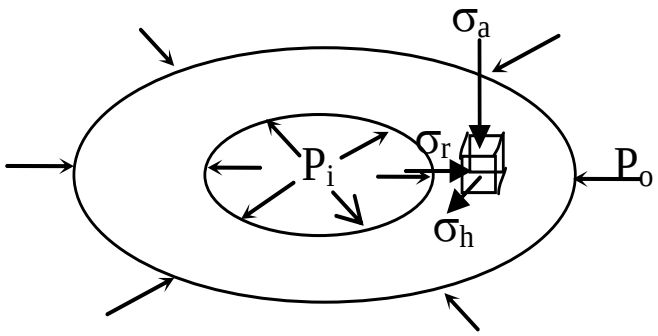

Figure 2.10 : A drill pipe with axial load and torque

2.4.1 Radial stress

Radial stress is stress towards or away from the central axis of a curved member. The walls of pressure vessels generally undergo triaxial loading. For cylindrical pressure vessels, the normal loads on a wall element are the longitudinal stress, the circumferential (hoop) stress and the radial stress.

The radial stress for a thick walled pipe is given by

$$\sigma_r = \frac{p_i r_i^2 - p_o r_o^2}{r_o^2 - r_i^2} - \frac{r_i^2 r_o^2}{(r_o^2 - r_i^2) r^2}(p_i - p_o) \qquad 69$$

where,

- r_i is the inner radius,
- r_o is the outer radius,
- p_i is the inner pressure and
- p_o is the outer pressure.

2.4.2 Hoop stress

This is the stress which is set up in resisting the bursting effect of the applied pressure and can be most conveniently treated by considering the equilibrium of the cylinder.

$$\sigma_\theta = \frac{p_i r_i^2 - p_o r_o^2}{r_o^2 - r_i^2} + \frac{r_i^2 r_o^2}{(r_o^2 - r_i^2) r^2}(p_i - p_o) \qquad 70$$

2.4.3 Axial stress

Compressive stress is axial stress that tends to cause a body to become shorter along the direction of applied force. Tensile stress is axial stress that tends to cause a body to become longer along the direction of applied force.

From the perspective view mentioned in the figure 2.10

The axial stress can be written as,

$$\sigma_a = \frac{F_a}{A} + \frac{p_i r_i^2 - p_o r_o^2}{r_o^2 - r_i^2} \qquad 71$$

Where., σ_a = Axial stress, F_a = total axial force and A = cross sectional area

2.4.4 Shear stress /Torsion

When a shaft is subjected to a torque or twisting, a shearing stress is produced in the shaft. The shear stress varies from zero in the axis to a maximum at the outside surface of the shaft.

In the presence of torque, *T*, the average shear stress will be given as:

$$\tau = \frac{3T}{\pi(r_o^3 - r_i^3)} \qquad 72$$

- σ = shear stress (MPa, psi)
- T = torque (Nmm, in lb)
- ro, and ri = outer and inner radii of drill string (mm, in)

2.4.5 Tensile limit :

Tensile load is a maximum allowable load applied on a drill string before reaching to yielding. This tensile load is called tensile limit. The tensile load is given as:

$F_{tensile}$= (Yield stress x Crosssectional area)/SF

2.5 Collapse and Burst of drill string

There exist a variety of models and techniques available to estimate burst and collapse pressures of pipe used for drilling, completion and intervention. The results obtained using the different methods are not always easy to compare since the underlying theories differ. Here a three dimensional (3D) yield model is described. (This section is summarised from the paper Jan A. Aasen, Bernt S. Adnoy, 2006)

2.5.1 Triaxial well design

Well tubular are subjected to a variety of loads during installation and services. Tensile and compressive axial stresses are produced by axial loads and bending of the pipe. Pressures inside and outside of the tubular gives rise of radial and hoop stresses. Pipe may also experience shear stresses if torque is applied. Tensile stress is positive, and a negative sign indicates compression throughout the paper. Neglecting the shear stresses, the axial stress σ_z, the radial stress σ_r, the hoop stress σ_h, are principal stresses. These stresses may be combined to a single equivalent stress σ_{VME}, using the Von Mises distortion energy theorem

$$2\sigma_{VME}^2 = (\sigma_z - \sigma_r)^2 + (\sigma_z - \sigma_h)^2 + (\sigma_r - \sigma_h)^2 \quad 73$$

The yield strength of well tubular is experimentally determined from simple uniaxial tensile tests. Two of the three principal stresses are zero for this case (σ_r and σ_h). The Von-Mises equivalent (VME) stress for this situation is given as:

$$\sigma_{VME} = \sigma_y \quad 74$$

We design the design factor (DF) as the ratio of the allowable stress to the working stress (σ_y/σ_{VME}). Oil countries tubular goods are manufactured according to the API tolerances. There are manufacturing tolerances for both dimensional and material (yield strength) properties. The allowable stress is taken as the yield strength of the pipe, while the applied stress is the VME stress. The theory predicts DF=1 at failure. The higher the DF is , the higher the margins against failure.

$$DF = \frac{\sqrt{2}\sigma_y}{\sqrt{(\sigma_z - \sigma_r)^2 + (\sigma_z - \sigma_h)^2 + (\sigma_r - \sigma_h)^2}} \quad 75$$

Current triaxial design is based on methodology developed by Kastor (1986). He incorporated the thick walled Lame solution in the Von Mises failure model. In addition he incorporated the hydrostatic fluid pressure with depth. This pioneering work yields a correct solution , but is somewhat cumbersome to use.

So the simplified procedure is by solving the equations for (i) zero inside pressure for collapse and (ii) zero outside pressure for burst. The result was obtained by adding the inside or outside pressure respectively. In general terms, the Johnson et al. Solution can be formulated as :

$$P_{Collapse} = P_i + g(o, \sigma_z, \beta, \sigma_y)$$

$$P_{burst} = P_0 + h(o, \sigma_z, \beta, \sigma_y) \quad 76$$

The functionality in equation (76) are nonlinear. Although a clever way to solve a non-linear problem, they are introducing an error by simply superimposing the inner or outer pressures. Implicitly they are assuming thin walled solution of the pipe.

Various approaches were attempted to solve this rather complex nonlinear problem. Using dimensional analysis we can get a rather simple solution. In the following derivation no torque or bending are assumed.

The Lame solution for radial and hoop stresses in a thick walled pipe is used (Timoshenko and Goodier, 1970). Investigation of the equations revealed that both burst and collapse failures would initiate on the inner surface of the pipe. Introducing the following geometry factor

$$\beta = \frac{2r_0^2}{r_0^2 - r_i^2} = \frac{(d_0/t)^2}{2(d_0/t - 1)} \quad (77)$$

The radial and hoop stress formulations at the inside pipe wall become:

$$\sigma_r = -P_i \quad (78)$$

$$\sigma_h = \beta(P_i - P_o) - P_i \quad (79)$$

Including the bending, the axial stress is calculated as :

$$\sigma_z = \frac{F_a}{F_s} + \sigma_b = \sigma_a + \sigma_b \quad (80)$$

Performing a dimensional analysis and collecting terms, the following dimensionless variables were found :

$$x = \frac{(P_i + \sigma_z)}{\sigma_y} \quad (81)$$

$$y = \frac{\beta(P_i - P_0)}{\sigma_y} \quad (82)$$

Inserting these equations into equation (75), the design factor is expressed as:

$$z = DF = \frac{1}{\sqrt{x^2 - xy + y^2}} = \frac{\sigma_y}{\sigma_{VME}} \quad (83)$$

This is an exact solution to the burst and collapse calculations, which will replace the approximate solution of equation (76). If z=DF is assigned, this equation describes a surface (x,y,z) that totally represents the loads caused by axial stress, inside pressure and outside pressure seen in relation to the yield limit of the pipe.

The 3D yield surface is shown in the **figure 2.11** If z is equal to one, this combination of σ_z, σ_r, and σ_h gives a loading on the pipe that is equal to its yield strength. The part of the surface that lies below z=1, identifies loading in excess of the yield strength. If the z coordinate is greater than one, the calculated VME stress is lower than the yield strength of the pipe and the design s in order. We

notice that the pipe is infinitely strong at x=y=0 as the denominator in equation (83) is zero at this point. This condition implies that σ_z=-P_i and P_i=P_0, also called a hydrostatic stress state.

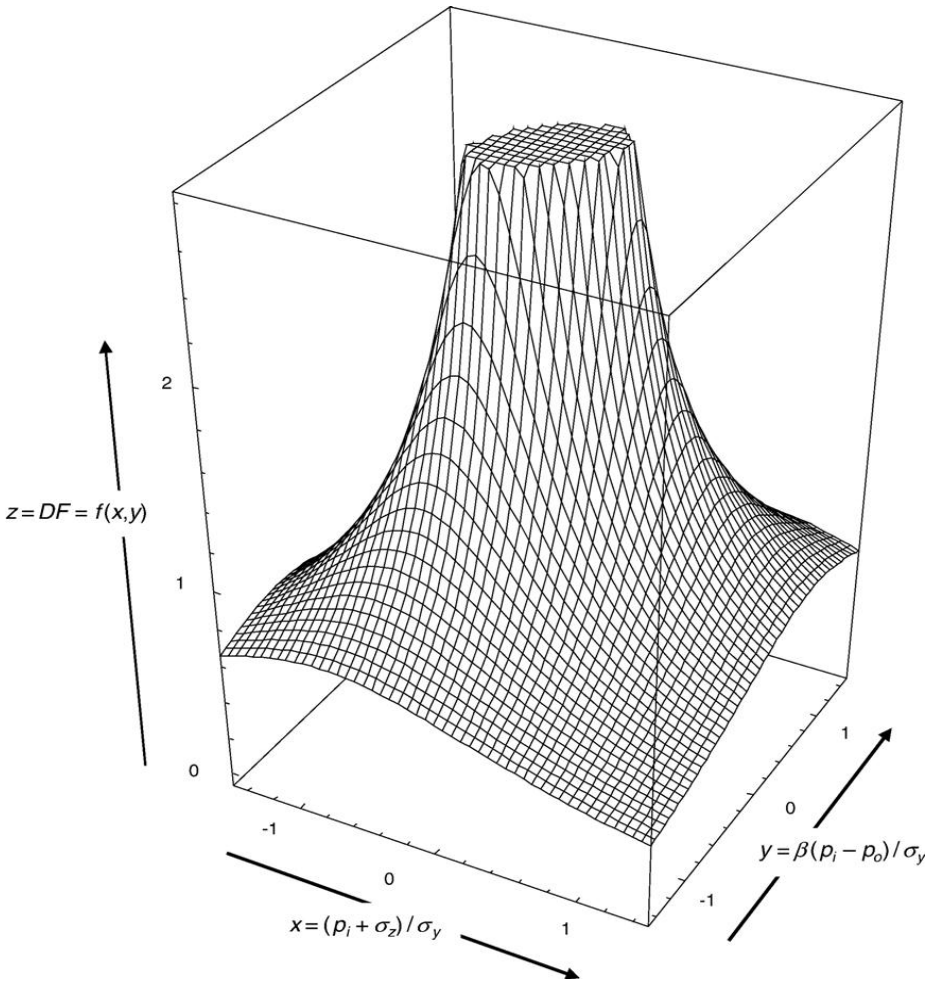

Figure 2.11 : Three dimensional (3D) yield field.
(Reference: Jan A. Aasen, Bernt S. Adnoy, 2006)

In **figure 2.12** we look at a 2D plot obtained by intersecting the 3D yield surface by horizontal planes through different values of z. In this plot the envelopes for burst and collapse become smaller than the design factor increases. Any load path describing the service loads on casing or tubing over time needs to remain inside the ellipse. It is also necessary to plot the VME stresses associated with the occurrence of possible leak situations and emergency scenarios. The upper half of the ellipse corresponds to burst,, while the bottom half describes collapse pressure. All needed parameter to

describe a pipe (P_i, Po, σz, do/t, σ_y) are included in this 2D dimensionless plot. It is not necessary to normalize the equations by selecting P_i=0(collapse) or P_o=0 (burst), as is the case in conventional triaxial well design.

Solving for y in equation (83):

$$y = \frac{x}{2} \pm \sqrt{\frac{1}{DF^2} - \frac{3}{4}x^2} \qquad 84$$

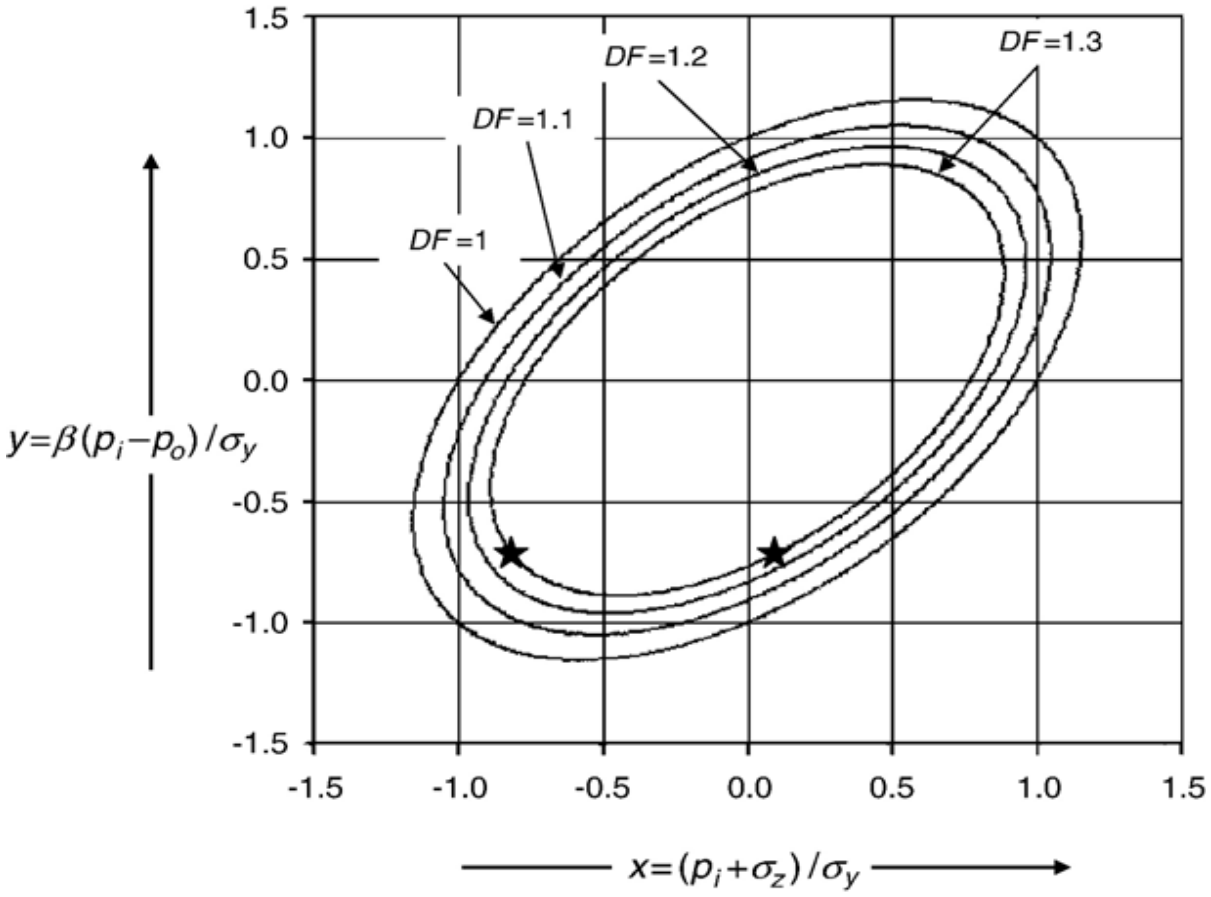

Figure 2.12: Three dimensional design factors projected on a two dimensional plane
(Reference: Jan A. Aasen, Bernt S. Adnoy, 2006)

The plus sign defines the tensile hoop stress for burst calculation, while the negative sign defines the compressive hoop stress for the collapse pressure calculation. Consider DF=1 in the following. Substitute equations (81) and (82) for x and y in this equation and obtain the

collapse pressure:

$$P_{Collapse} = \frac{P_i(2\beta - 1) - \sigma_z + \sqrt{4\sigma_y^2 - 3(P_i + \sigma_z)^2}}{2\beta} \quad 85$$

The burst pressure may be calculated as:

$$P_{burst} = \frac{\beta P_0(2\beta - 1) + \sigma_z(\beta - 2) + \sqrt{4\sigma_y^2(\beta^2 - \beta + 1) - 3\beta^2(P_0 + \sigma_z)^2}}{2(\beta^2 - \beta + 1)} \quad 86$$

The theory presented here so far for burst and collapse is based on the assumption that pipe fails by yielding at inner wall. There are situations where this situation may not be true. If the pipe is bent, either by buckling or in cured sections of the well, it is necessary to analyze the bending stress at the outside wall. Collapse experiments on oil-country tubular (API 5C3, 1994) show that yield failure, as described in this study, is valid for pipe with small and moderate d_o/t ratios. As a rule of thumb (Craft et al., 1962), the limiting d_o/t value for yield collapse is about 14.

2.6 Short study on drill string

The drill string is an important part of the rotary drilling process. It is the connection between the rig and the drill bit. Although the drill string is often a source of problems such as washouts, twist-offs, and collapse failures, it is seldom designed to prevent these problems from occurring. In many cases, a few minutes of drill string design work could prevent most of the problems.

2.6.1 Purposes of drill string

The drill string serves several general purposes, including the following:

- provide a fluid conduit from the rig to the bit
- impart rotary motion to the drill bit
- allow weight to be set on the bit

- lower and raise the bit in the well

In addition, the drill string may serve some of the following specialized services:

- Provide some stability to the bottom-hole assembly to minimize vibration and bit jumping,
- Allow formation fluid and pressure testing through the drill string,
- Permit through-pipe formation evaluation when logging tools cannot be run in the open hole,

2.6.2 Components of drill string

The drill string consists primarily of the drill pipe and bottom-hole assembly (BHA). The drill pipe section contains conventional drill pipe, heavyweight pipe and occasionally a reamer. The BHA may contain the following items: drill collars (several types and sizes)- stabilizers-jars-reamers-shock subs-bit, and bit sub. Special tools in the BHA or drill pipe may include monitor-while-drilling (MWD) tools, drill stem testing tools, and junk baskets.

Drill Pipe:

The longest section of the drill string is the drill pipe. The BHA is usually no longer than 1,000 ft. Each joint of drill pipe includes the tube body and the tool joint, which connects the sections of drill pipe. Although aluminium drill pipe is sometimes used in special projects, it will not be presented in this section. However, it does have important applications in remote areas where airfreight is required and where otherwise the rig would have insufficient hoisting capacity. Drill pipe is available in several sizes and weights (Table 3-1). Common sizes include the following:

- 3 ½ in.-13.30 lb/ft nominal
- 4 ½ in.-16.60 lb/ft nominal
- 5 in. -19.50 lb/ft nominal

Various types of tool joints may increase the average weight per foot, i.e.,16.60-18.60 lb/ft for 4.5-in. pipe. However, it is still termed as 16.60-lb/ft pipe. The grade of drill pipe describes the minimum yield strength of the pipe. This value is important because it is used in burst, collapse, and tension calculations. Common grades are as follows:

Table 1 Common Grades of Drill Pipes

Letter Designation	Alternative Designation	Yield Strength (psi)
D	D-55	55000
E	E-75	75000
X	X-95	95000
G	G-105	105000
S	S-135	135000

In most drill string design, the pipe grade will be increased for extra strength rather than increase the pipe weight. This approach differs somewhat from casing design. Drill pipe is unlike most other oil-field tubular, such as casing and tubing, because it is used in a worn condition. Casing and tubing are usually new when installed in the well. As a result “classes” are given to drill pipe to account for wear. Therefore, drill pipe must be defined according to its nominal weight, grade and class. The API has established guidelines given below:

1. **New** = No wear and has never been used.
2. **Premium** = Uniform wear and a minimum wall thickness of 80%.
3. **Class 2** = Allows drill pipe with a minimum wall thickness of 65% with all wear on one side so long as the cross-sectional area is the same as premium class; that is to say, based on not more than 20% uniform wall reduction.
4. **Class 3** = Allows drill pipe with a minimum wall thickness of 55% with all wear on one side.

Drill pipe classification is an important factor in drill string design and use since the amount and type of wear affect the pipe properties and strengths. Drill pipe is available in several length ranges:

Table 2:Ranges of Drill Pipes

Range	Length (ft)
1	18-22
2	27-30
3	38-40

Heavy Weight Drill Pipe:

The use of heavy weight drill pipe in the drilling industry has become a widely accepted practice. The pipe is available in conventional drill pipe outer diameters. However, its increased wall thickness gives a body weight 2-3 times greater than regular drill pipe. Heavy weight drill pipe provides three major benefits to the user.

- Reduces drilling cost by virtually eliminating drill pipe failures in the transition zone. Significantly increases performance and depth capabilities of small rigs in shallow drilling areas through the case of handling and the replacement of some of the drill collars.
- Provides substantial savings in directional drilling costs by replacing the largest part of the drill-collar string, reducing down hole drilling torque, and decreasing tendencies to change direction.

Most heavy-wall drill pipe has an integral centre upset acting as a centralizer and wear pad. It helps prevent excessive tube wear when run in compression. This pipe has less wall contact than drill collars and therefore reduces the chances of differential pipe sticking.

Drill Collars:

Drill collars are the predominant components of the bottom-hole assembly. Some of the functions of the collars are as follows:

- provide weight for the bit
- provide strength needed to run in compression
- minimize bit stability problems from vibrations, wobbling, and jumping
- minimize directional control problems by providing stiffness to the BHA

Proper selection of drill collars (and BHA) can prevent many drilling problems. Drill collars arc available in many sizes and shapes, such as round, square, triangular, and spiral grooved. The most common types are round (slick) and spiral grooved. Large collars offer several advantages.

- fewer drill collars are needed for required weight
- fewer drill collar connections are required.
- less time is lost handling drill collars during trips
- factors governing good bit performance favor close fitting stiff members
- straighter holes can be drilled

2.6.3 Drill Pipe Selection

Drill pipe is used for several purposes, including providing a fluid conduit for pumping drilling mud, imparting rotary motion to the drill bit, and conducting special operations such as drill stem testing and squeeze cementing. The controlling criteria for drill string design are collapse, tension, slip crushing and dogleg severity. Collapse and tension are used to select weights, grades and couplings. Typically- higher-strength pipe is required in the lower sections of the string for collapse resistance, while tension dictates the higher strength pipe at the top of the well. The following design criteria will be used to select a suitable drill string: a) tension, (b) collapse, (c) torsion.

Chapter 3: Simulation study in South Sangu– 4

3.1 Simulation arrangement

The simulation is of South Sangu 4 is the continuation of my last semester project. On that project I finished only the analysis of tripping out data of 12.25'' section to get an idea about the Friction factor of the block.

In my thesis part I have analyzed the 8.5'' section of the well for both Tripping in and Tripping out operation data and 12.25'' section for tripping in operation data. I have taken the result of 12.25'' section Tripping in operation to finish the analysis of whole depth for my thesis part.

For simulation purpose I used the licensed copy of Landmark software of Halliburton. In the Landmark I used the well plan section to simulate my project input data which I got from the drilling program. Various parameters used for the simulation is briefly described below.

3.1.1 Hole section Editor

This part defines the hole section including the last casing , liner, and the open hole section. Here by default the friction factor for cased section is 0.2 and friction factor for open hole section is 0.3 is assigned. If we want to change the friction factor we can change it from here. But it will be wise to change the friction factor by using the "run parameter" button at the end of the simulation to see the sensitivity of different curves with the change of friction factor. According to the drilling program we have to enter the length of the cased section and open hole section as input in this editor.

3.1 .2 String editor

Table 1 shows the total drill string components and Bottom Hole assembly data used for the simulation of 12.25 inches section. If the component from the default library is found then we can do it directly from there otherwise we have to change the properties of the component that is not present in their library. In that case we have to put the mass per unit, ID, OD and the measured length of the component. We used the following string with the BHA specially while the tripping out operation was carried out.

Table 3:Description of String including BHA

Section Type	Length (m)	Measured Depth (m)	OD (mm)	ID (mm)	Weight (kg/m)
Drill Pipe	2663.789	2663.79	139.7	118.62	42.96
Heavy Weight	37.45	2701.24	139.7	82.55	86.46
Jar	9.85	2711.09	158.75	57.15	135.24
Heavy Weight	95	2806.09	139.7	82.55	86.46
Sub	1.524	2807.61	201.17	76.2	218.76
MWD	26.61	2834.22	203.2	82.55	579.57
Stabilizer	1.524	2835.75	209.55	76.2	234.94
Sub	1.524	2837.27	209.55	76.2	238.11
Mud Motor	9.29	2846.56	244.47	132.33	260.19
Bit	0.439	2847	311.15		413.3

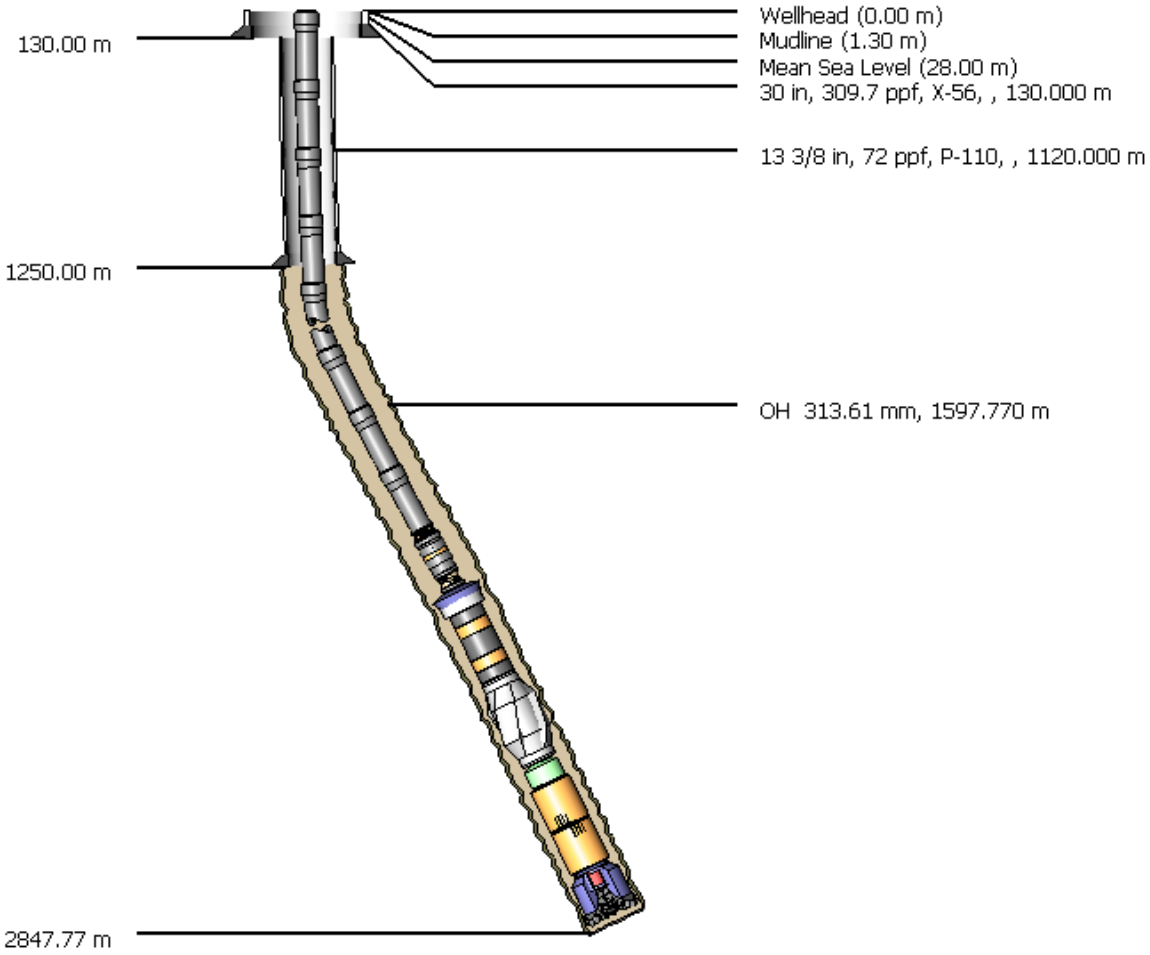

Figure 2.1 : Schematic view of Full String

3.1.3 Well path Editor

In the drilling program a certain well path is designed to reach the target. The inclination and azimuth is very important in this point which is directly related to the drag and torque. Here to find out the real time friction factor we are using the real time survey data to calculate the real time coefficient of friction. The real time survey report given in Appendix A and corresponding graph of vertical section, DLS, inclination and azimuth is given below accordingly.

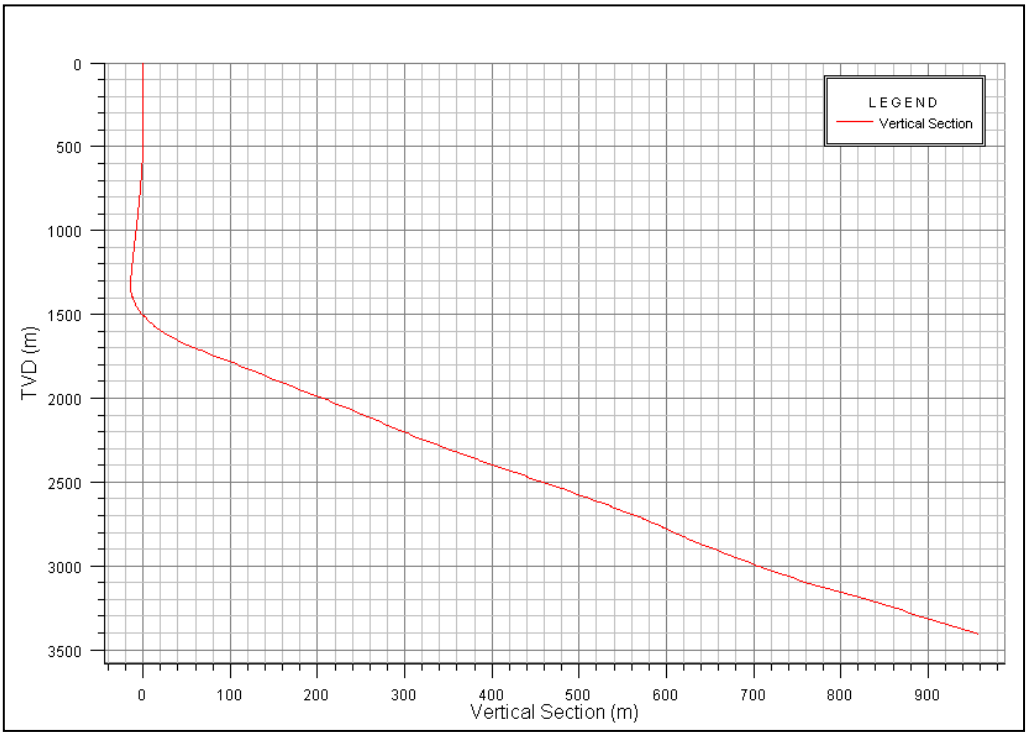

Figure 3.2 : Graphical presentation of Vertical section

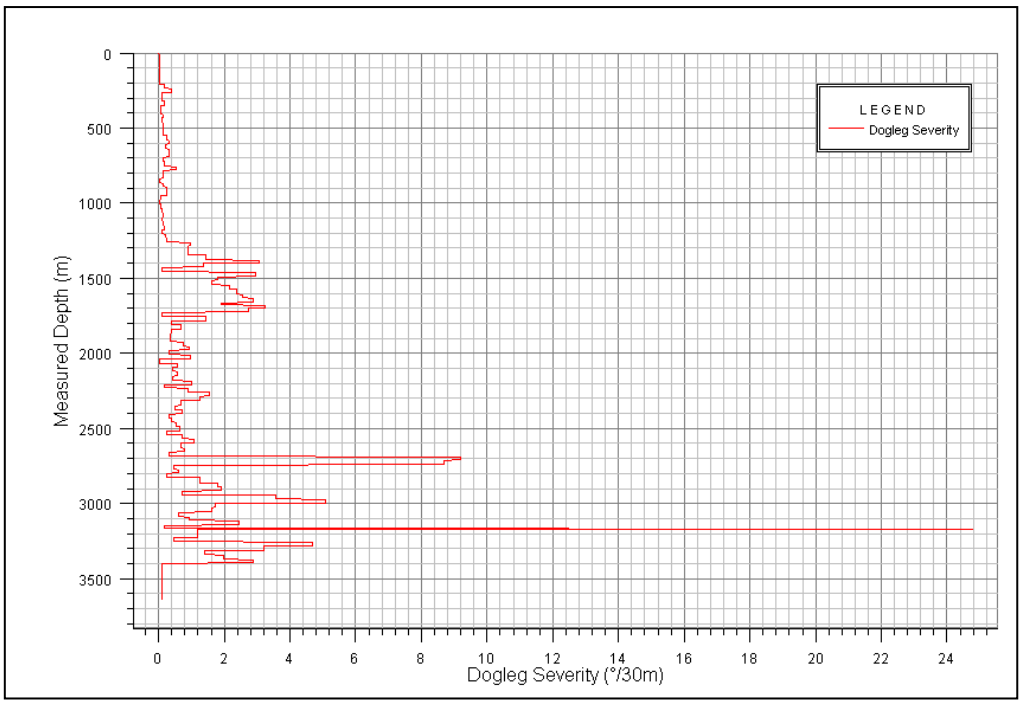

Figure 3.3 : Graphical presentation of DLS

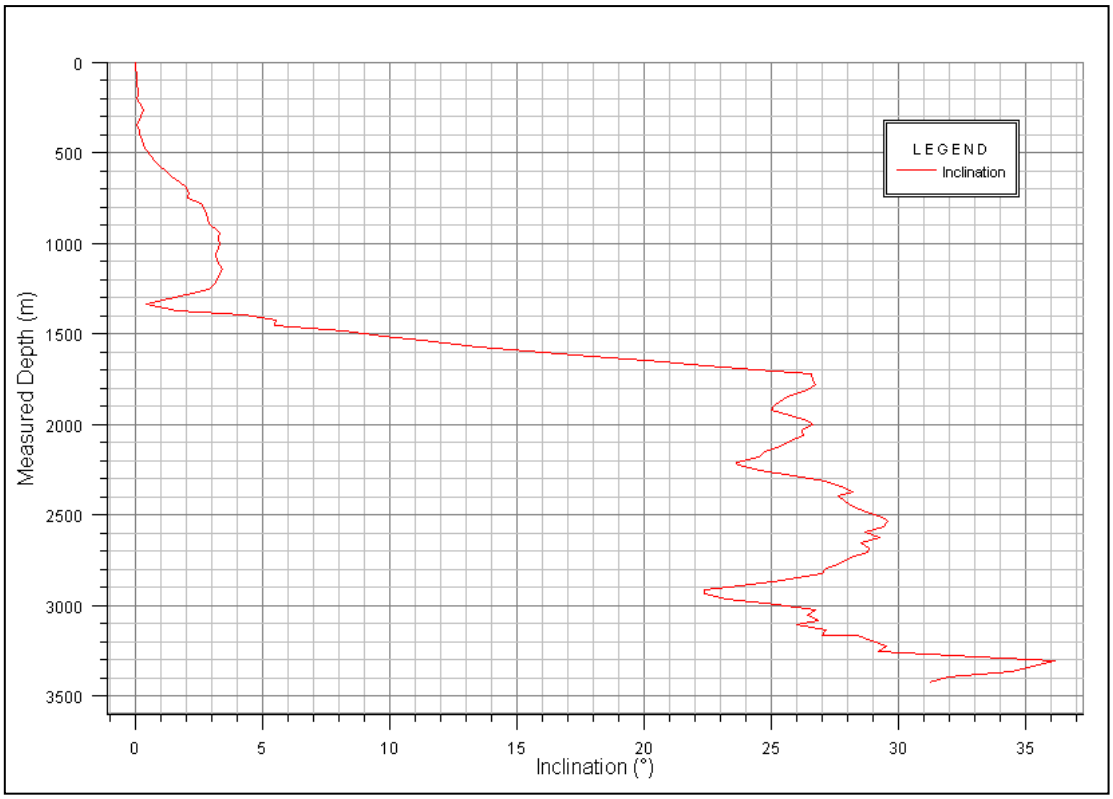

Figure 3.4 : Graphical presentation of Inclination.

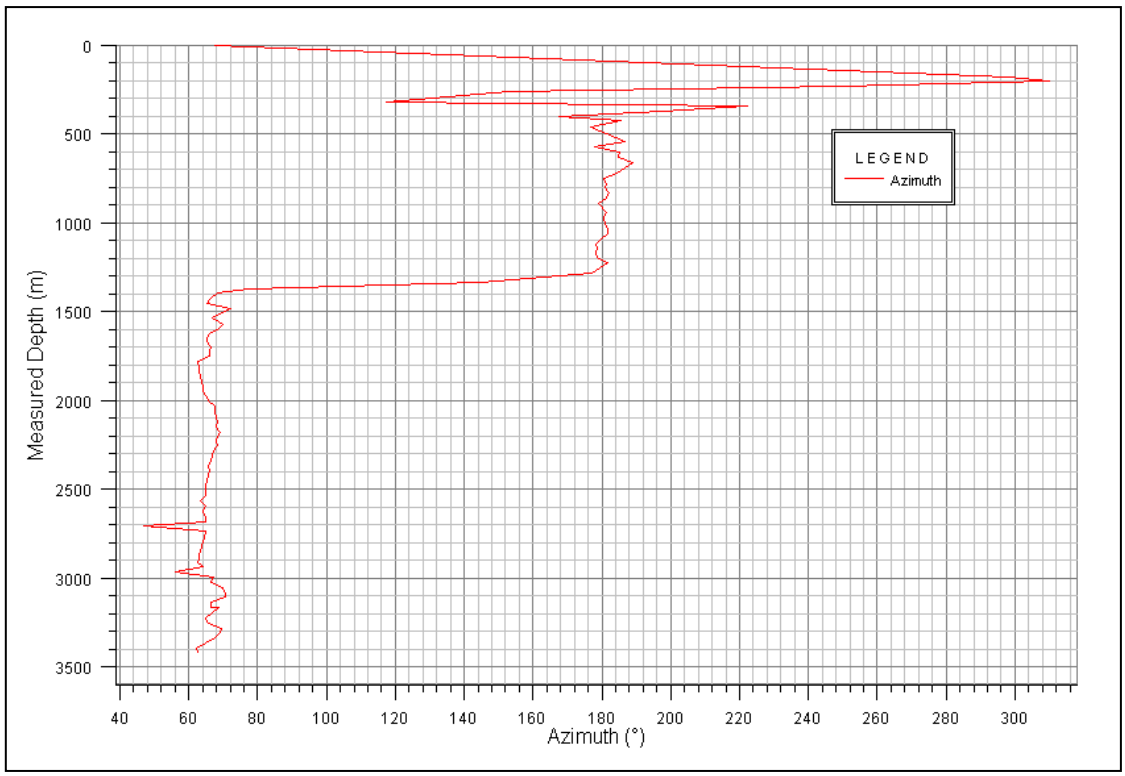

Figure 3.5: Graphical presentation of Azimuth.

3.1.4 Fluid Editor

In this section we have to put the properties of mud use in the drilling. In our drilling well, we used 9.7 ppg of water based mud where the plastic viscosity is 24 cp and yield point is 12lbf/100 ft2. Figure 10 shows the shear stress as a function of shear rate.

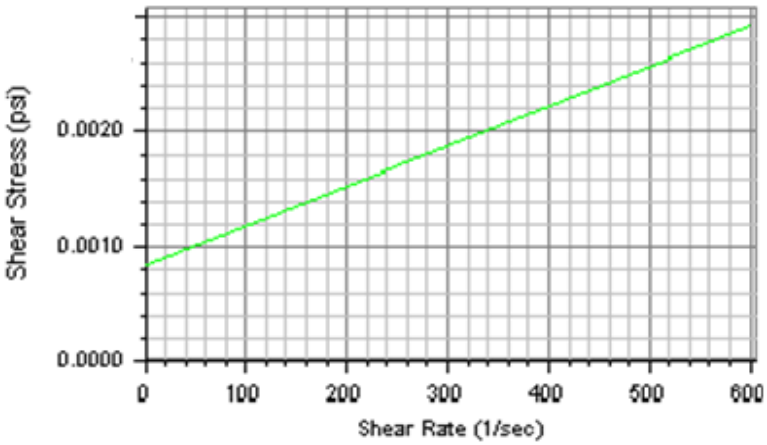

Figure 3.6 : Stress vs Shear rate graph of fluid.

3.1.5 Geothermal gradient

In this stage of simulation we need to input the data of temperature of ambient as well as the mud line. The gradient of temperature is also necessary in this input section. The surface ambient

temperature is 80 ^{o}F and the mud line is 40 ^{o}F. The geothermal gradient is 1.5 ^{o}F/100ft. The temperature at 11188,9ft is 207.77^{o}F

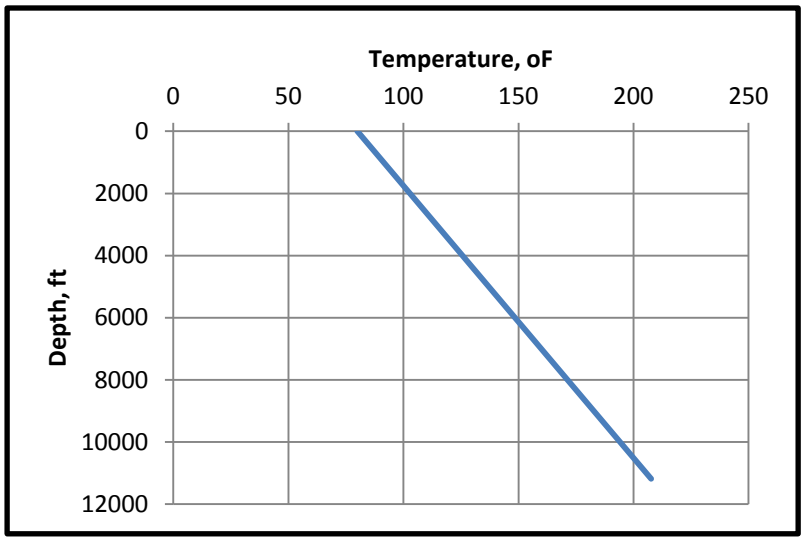

Figure 3.7: Formation Temperature profile.

3.2 Back calculated coefficient of friction from the analysis

3.2.1 12.25" section (Tripping in condition)

The simulated Tripping in Hook Load data for different friction factor (0.2 to 0.4) from 0 m (MD) to 2850 m (MD) and corresponding manually filtered real time data is graphed below:

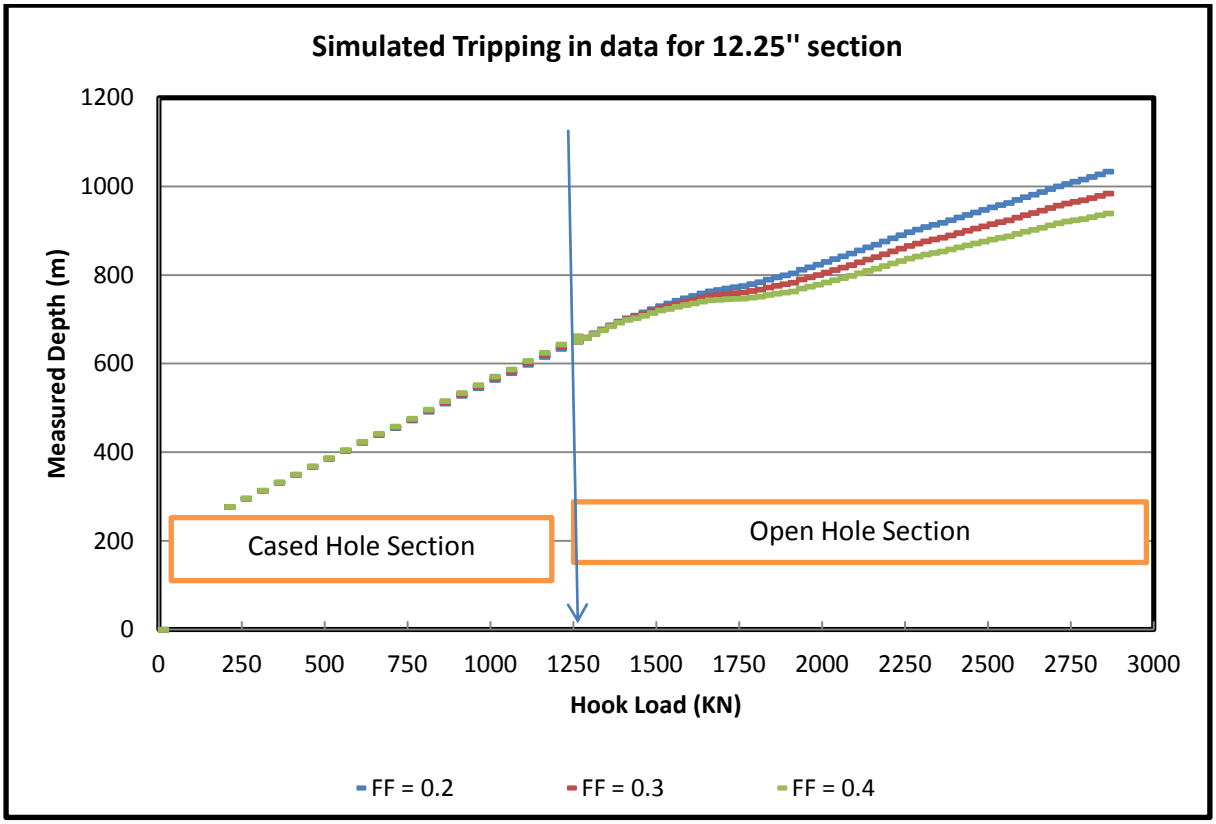

Figure 3.8: Simulated Hook Load graph for different FF in cased and open hole section (Tripping in)

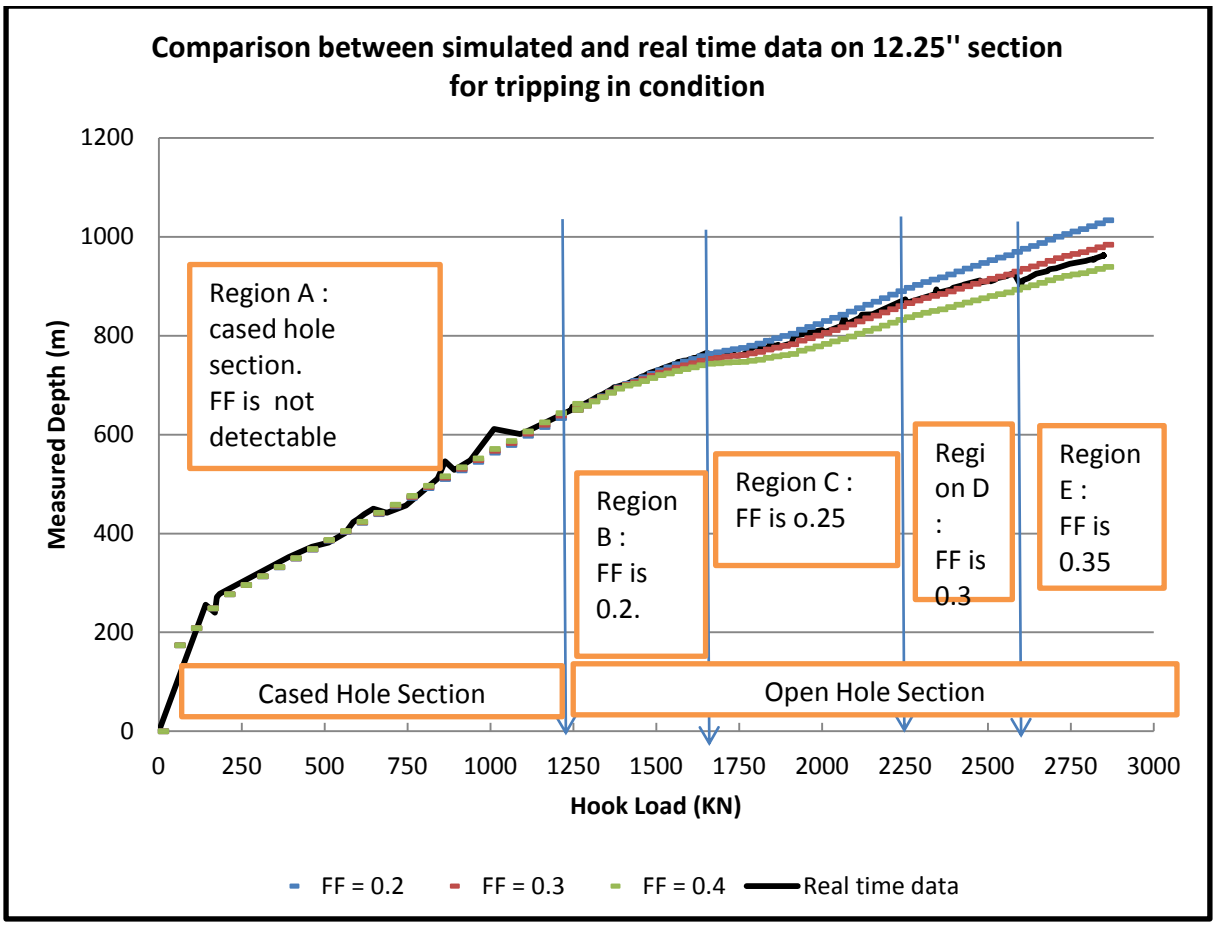

Figure 3.9: Comparison of Hook Load data with Real time data (Tripping in)

Analyzing the real time data : (Tripping in 12.25" section)

1. **Region A**: From the above figure it is clear that the cased section from 0m to 1250 m has no impact of friction factor on Hook Load as the well is vertical throughout the casing section. The real time data shows a bit higher value than the simulated one due to hydrodynamic viscous force which is already discussed in the theory part.
2. **Region B :** In this open hole region the real time tripping in data is matched with the simulated data having the FF 0.20. The region extends from 1250 m(MD) to 1650 m(MD).
3. **Region C:** In this open hole region the open hole real time tripping in data is matched with the simulated data having the FF 0.25.The region extends from 1650 m (MD) to 2250 m (MD).
4. **Region D :** In this open hole region the real time tripping in data is matched with the simulated data having the FF 0.30. The region extends from 2250 m (MD) to about 2625 m (MD).
5. **Region E** : In this region from the depth of around 2625 m (MD)the Hook Load data increased and show the FF 0.35 for the rest of the open hole part.

3.2.2 12.25" section (Tripping out condition)

The simulated Tripping out Hook Load data against the measured depth (MD) for different friction factor (0.2 to 0.4) from 0 m (MD) to 2850 m (MD) and corresponding manually filtered real time data is graphed below:

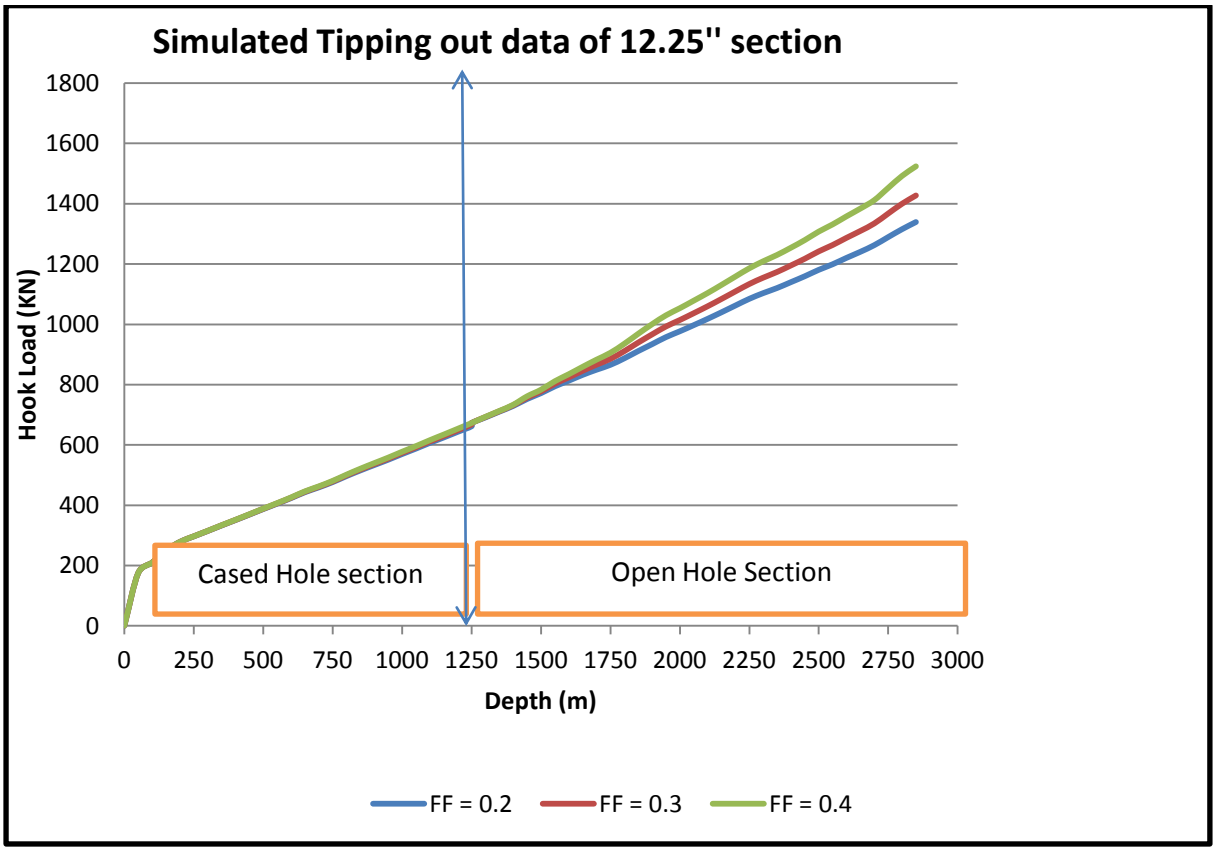

Figure 3.10 : Simulated Hook Load graph for diff. FF in cased and open hole section (Tripping out)

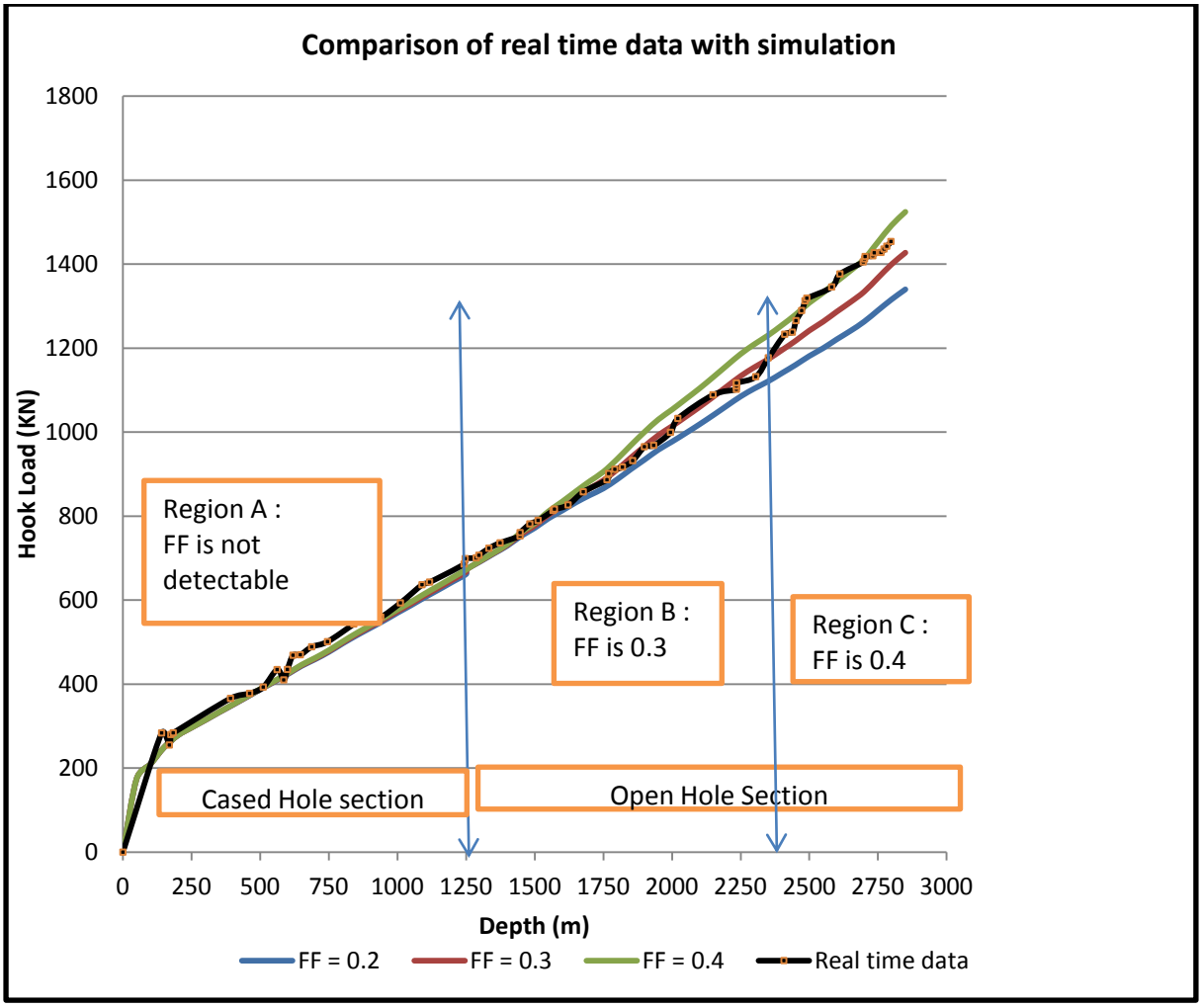

Figure 3.11: Comparison of Hook Load data with Real time data (Tripping out)

Analyzing the real time data : (Tripping out 12.25" section)

1. **Region A**: From the above figure it is clear that the cased section from 0m to 1250 m has no impact of friction factor on Hook Load as the well is vertical throughout the casing section. The real time data shows a bit higher value than the simulated one due to hydrodynamic viscous force which is already discussed in the theory part.
2. **Region B:** In this open hole region the real time tripping out data is matched with the simulated data having the FF 0.30. The region extends from 1250 m(MD) to 2375 m(MD).
3. **Region C:** In this open hole region the open hole real time tripping out data is matched with the simulated data having the FF 0.4 .The region extends from 2375 m (MD) to 2850 m (MD).

3.2.3 8.5" section (Tripping in condition)

The simulated Tripping in Hook Load data (Open hole section) for different friction factor (0.2 to 0.4) from 2850 m (MD) to 3450 m (MD) is shown below. As some adjustment to overcome the input error in simulator constant 90 KN hook load is added with the original simulated data and the corrected simulated data also is expressed below :

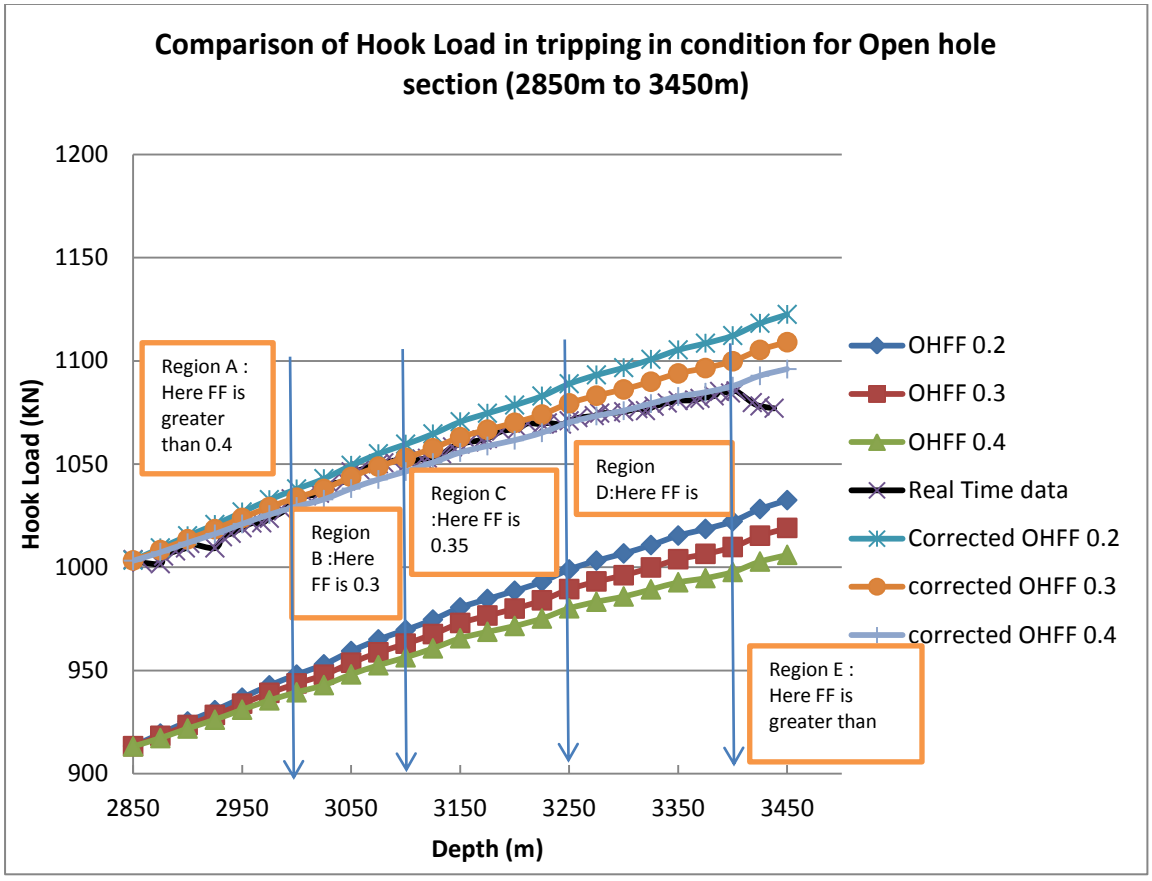

Figure 3.12: Comparison of Hook Load data with Real time data (Tripping in)

Analyzing the real time data : (Tripping in 8.5" section)

Region A: In this open hole region real time hook load data does not match with any corrected simulated data but showing FF greater than 0.4. This open hole region extends from 2850 m(MD) to 2990m (MD).

Region B: In this open hole region real time hook load data is matched with the corrected simulated data of FF 0.3. this open hole region extends from 2990 m (MD) to 3100 m (MD).

Region C: In this open hole section the real time hook load data is matched with the corrected simulated data of FF 0.35. This open hole region is extends from 3100 m (MD) to 3250m (MD).

Region D: In this open hole region the real time data hook load data is matched with the corrected simulated data of FF 0.4. This region extends from 3250 m (MD) to 3400 m (MD).

Region E: In this region from the depth of 3400 m (MD) the Hook Load increases sharply indicating the FF to be more than 0.4.

3.2.4 8.5" section (Tripping out condition)

The simulated Tripping out Hook Load data (Open hole section) for different friction factor (0.2 to 0.4) from 2850 m (MD) to 3450 m (MD) is shown below. As some adjustment to overcome the input error in simulator is needed, aconstant 115 KN hook load is added with the original simulated data. Both original simulated data and corrected simulated data are plotted with the real time data below:

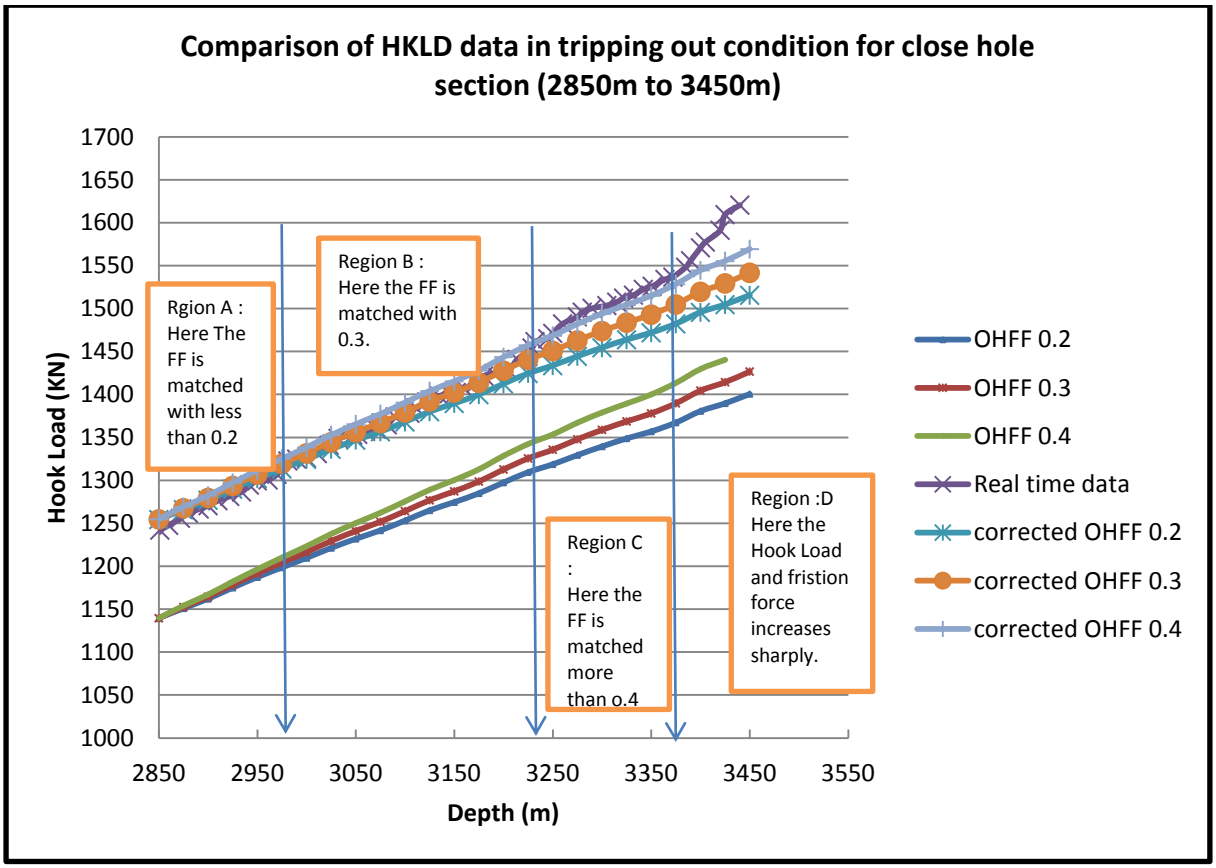

Figure 3.13 : Comparison of Hook Load data with Real time data (Tripping out)

Analyzing the real time data : (Tripping out 8.5" section)

Region A: In this open hole region real time tripping out hook load data is matched with the corrected simulated data of FF 0.2. This open hole region extends from 2850 m(MD) to 2975m (MD).

Region B: In this open hole region real time hook load data is matched with the corrected simulated data of FF 0.3. this open hole region extends from 2975 m (MD) to 3230 m (MD).

Region C: In this open hole section the real time hook load data is matched with the corrected simulated data of FF 0.4. This open hole region is extends from 3230 m (MD) to 3375m (MD).

Region D: In this open hole region the real time hook load data is gone above the simulated line of FF 0.4 which shows the FF in this region is greater than 0.4. This region extends from 3375 m (MD) to the rest of the depth.

3.2.5 Summary of the result

Finding out an average coefficient of friction in South sangu 4 is basically divided into two parts. First part is 12.25'' section where the well bore (open hole) extends from 1250 m to 2850 m and the second part is 8.5'' section where the open hole section was extended from 2850 upto the 3450m. The summary of the result is given below

12.25'' section

For Tripping in condition the minimum and maximum FF is found 0.2 and 0.35 respectively. And for Tripping out condition the minimum value and maximum value we get is 0.2 and 0.4.

From the above result we can come to a conclusion that the FF in this section will vary from 0.2 to 0.4.

8.5'' section

For Tripping out condition the minimum and maximum FF is found to be o.2 and greater than 0.4 respectively. In Tripping in condition the minimum and maximum value of FF are 0.3 and greater than 0.4 respectively. In both cases we observe the higher value of FF which is more than 0.4 at the lower part of the section.

From the above result we can come to an end that the FF in this section varies from 0.2 to 0.5 or higher.

From the above result a profile of Friction factor is graphed below for the open hole section. And one FF ratio graph is plotted where the ratio greater than 1 is a very clear indication of pack off.

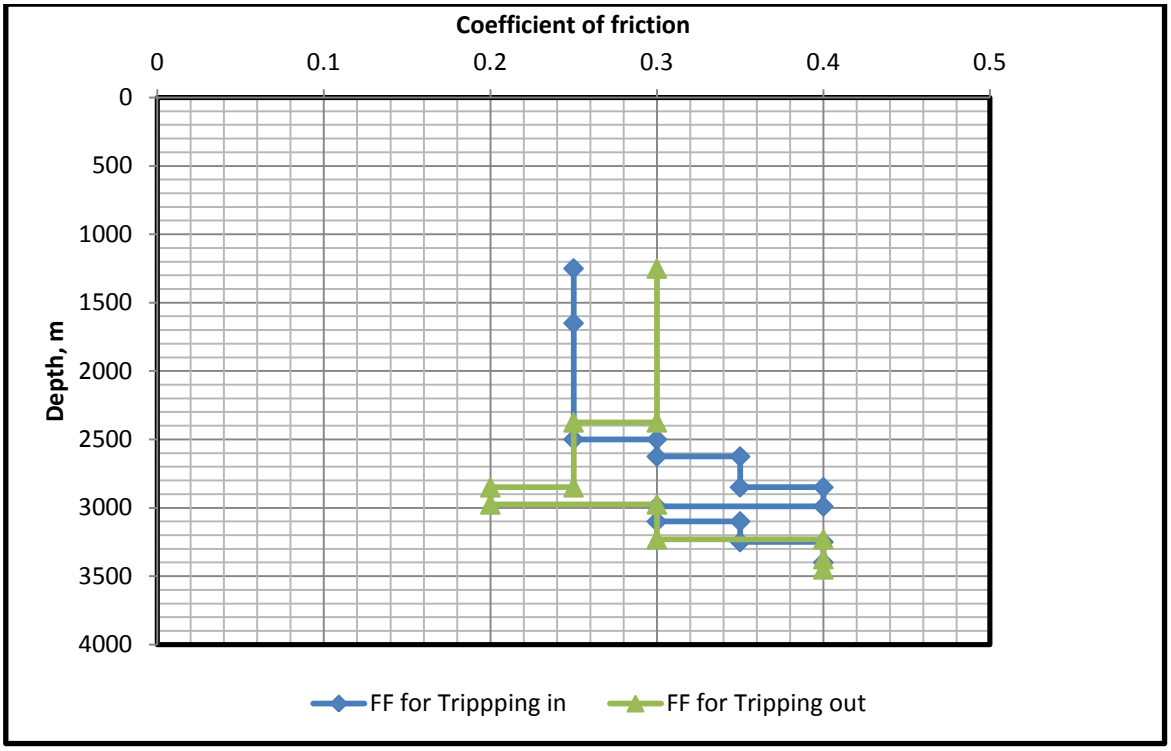

Figure 3.14: FF profile for both Tripping in and Tripping out operation in Open Hole

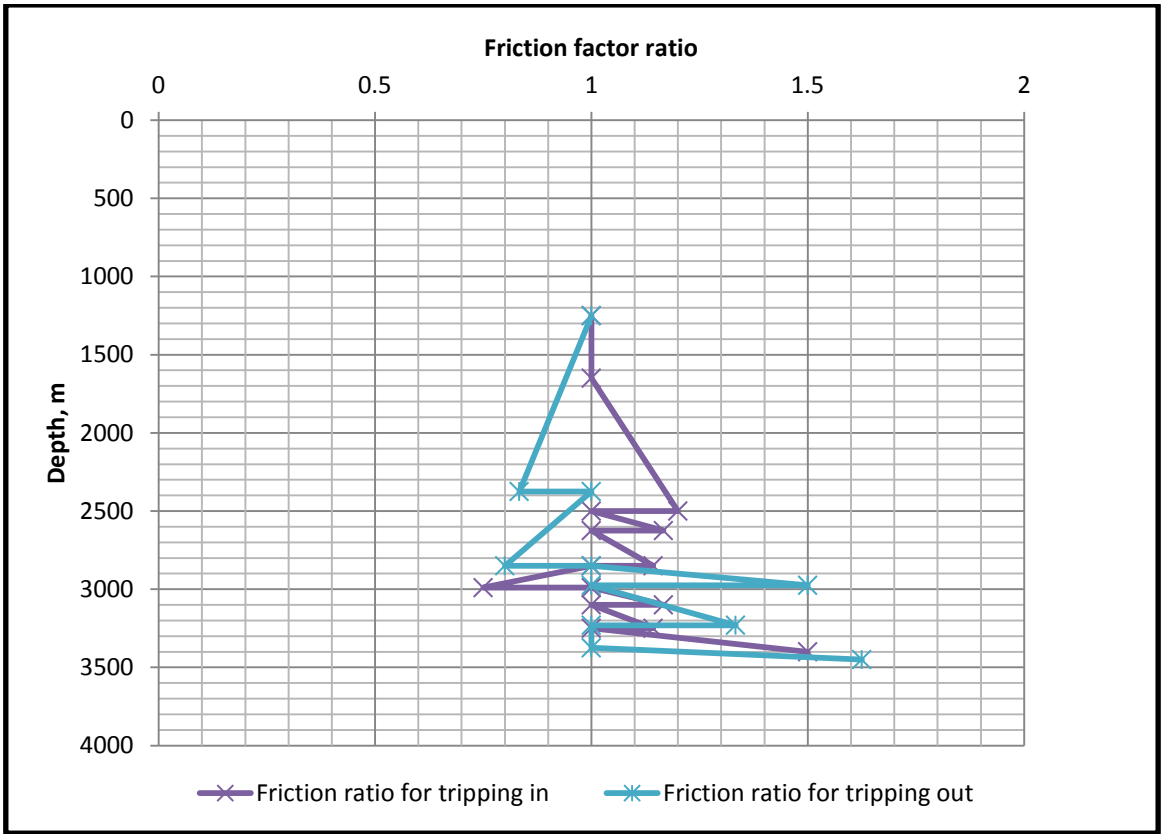

Figure 3.15: ratio of FF in Tripping in and Tripping out

Chapter 4: Monitoring and Simulation study in Sangu– 11

4.1 Overview of Sangu 11

4.1.1 Well Information

Well Name : Sangu-11
Well Type : Development

Field : Santos Sangu Field

Rig Name : Offshore Resolute
Rig Type : Jack Up

RKB Elevation : 49.38m relative to MSL
Water Depth : 11.60m

Final Depth MD : 4260m
Final Depth TVD: 3143.99m

Well Co-ordinates :

UTM Coordinates
Y: N 2435283.700 m
X: E 347723.200 m

Geographical Coordinates
Latitude : N 22° 0' 55.99833"
Longitude : E 91° 31' 28.93676"

Geomagnetic Data:

Magnetic Field Strength : 45551.941 nT

Magnetic Dip Angle : 32.222 °

Magnetic Declination : -0.612 °

Total Correction MN>TN : -0.0584 °

4.1.2 Planned survey data

The planned trajectory , The plan view and the view of vertical section of Sangu 11 is shown below:

(a)Planned Trajectory :

Table 4:Planned Trajectory of Sangu 11

Sangu-11 Plan					
Field:	Bangladesh Block 16				
Structure / Slot:	Sangu Platform / Slot 8				
Well:	Sangu-11				
Borehole:	Sangu-11				
Survey Name:	Sangu-11 Plan				
Coordinate Reference System:	UTM Zone 46 - WGS84, Meters				
Location Lat / Long:	N 22° 0' 55.99833", E 91° 31' 28.93676"				
Location Grid N/E Y/X:	N 2435283.700 m, E 347723.200 m				
Comments	**MD (m)**	**Incl (°)**	**Azim Grid (°)**	**TVD (m)**	**DLS (°/30m)**
Tie-In	0.00	0.00	339.71	0.00	N/A
Seabed	*67.20*	*0.00*	*339.71*	*67.20*	*0.00*
30" Conductor	*130.00*	*0.00*	*339.71*	*130.00*	*0.00*
KOP	140.00	0.52	339.71	140.00	0.00
305 Anomaly	*270.20*	*2.34*	*339.71*	*269.70*	*2.00*
EOC #1 (3D-S)	912.66	52.50	339.71	812.70	2.00
13-3/8" Casing	*1366.25*	*52.50*	*339.71*	*1095.00*	*0.00*
1240 Anomaly	*1598.75*	*52.50*	*339.71*	*1239.70*	*0.00*
KOP #2	3213.09	52.50	339.71	2244.42	0.00
A Target	3760.78	15.00	339.00	2694.70	2.00
9-5/8" Casing	*3799.39*	*15.00*	*339.00*	*2732.00*	*0.00*
B Target	*3869.48*	*15.00*	*339.00*	*2799.70*	*0.00*
C Target	*4086.89*	*15.00*	*339.00*	*3009.70*	*0.00*
TD	4262.89	15.00	339.00	3179.70	0.00

(b)Plan View of Sangu 11

WELL	FIELD	STRUCTURE
Sangu-11	Bangladesh Block 16	Sangu Platform

Magnetic Parameters				Surface Location				Miscellaneous			
Model: BGGM 2011	Dip: 32.222°	Date: May 20, 2011		Lat: N 22 0 55.996	Northing: 2435283.70 m	Grid Conv: -0.55313360°	UTM Zone 46N - WGS84, Meters	Slot: Slot 8	TVD Ref: Rotary Table(49.7m above MSL)		
	Mag Dec: -0.612°	FS: 45551.9nT		Lon: E 91 31 28.937	Easting: 347723.20 m	Scale Fact:0.99988651		Plan: Sangu-11 Plan Rev 7	Srvy Date: May 20, 2011		

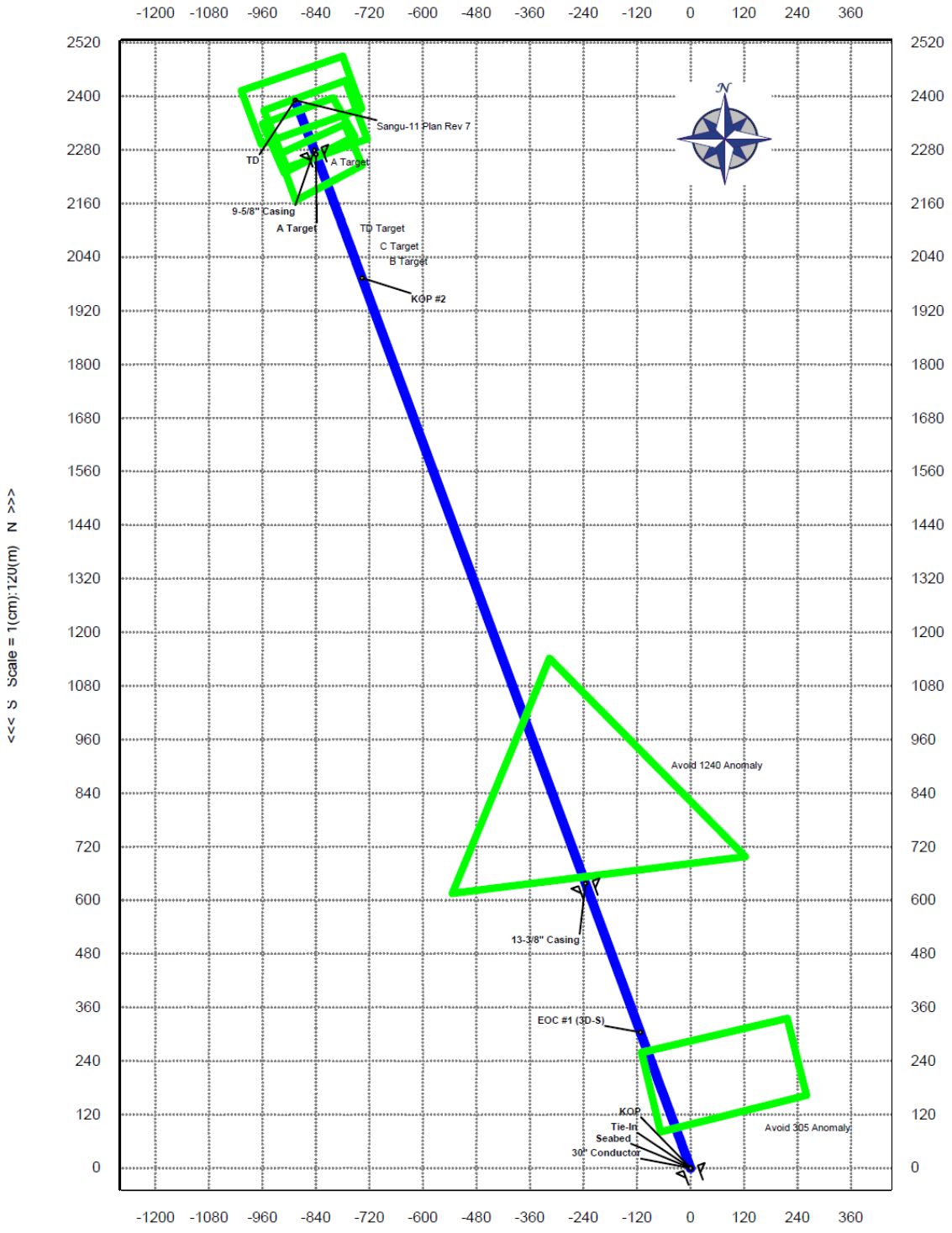

Figure 4.1: Plan view of Sangu 11 (Source : Schlumberger)

(c)Vertical section of Sangu 11

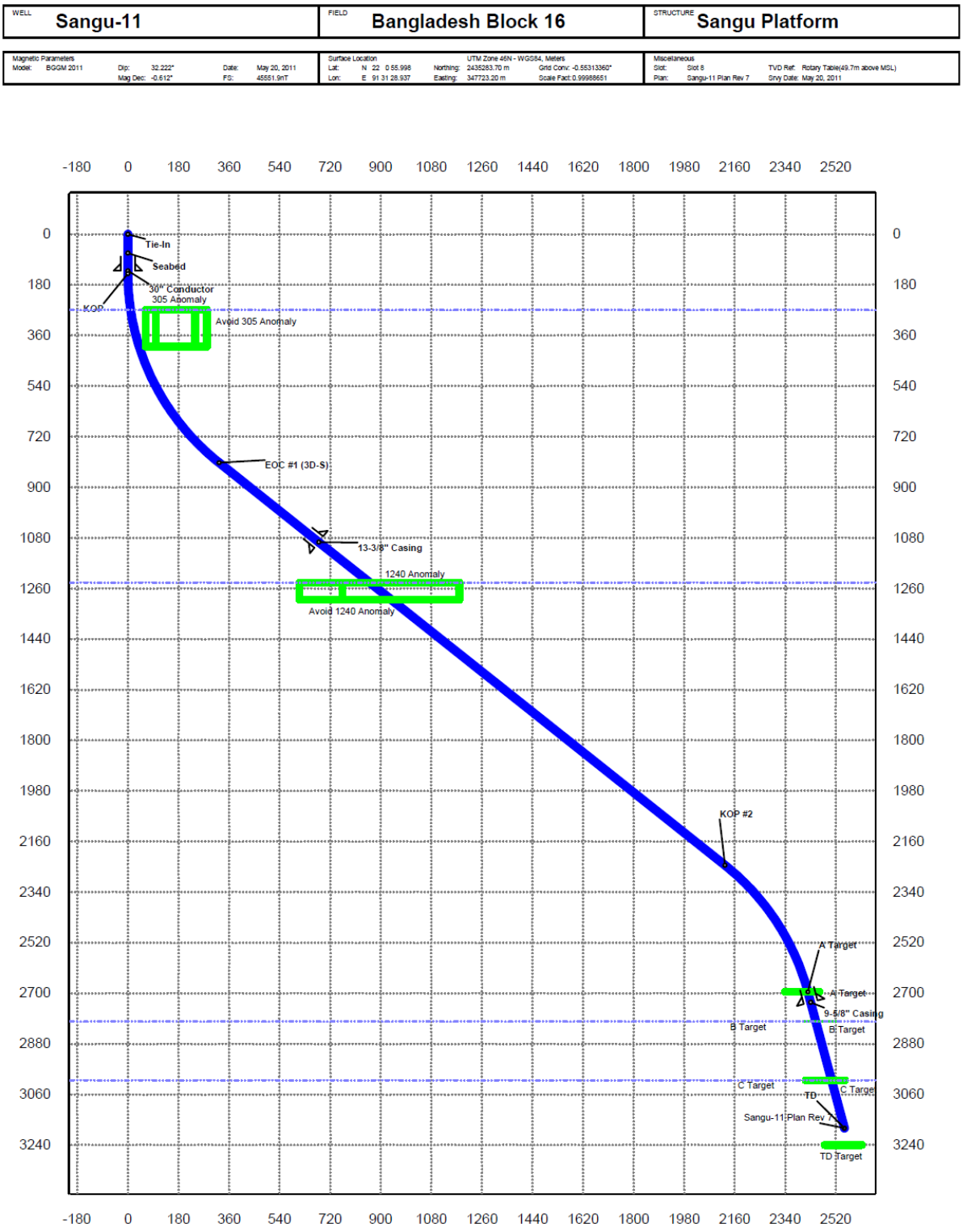

Figure 4.2: Vertical section of Sangu 11 (Source: schlumberger)

4.1.3 Position of Sangu 11 in the block 16

(a) Sangu 11 Location map :

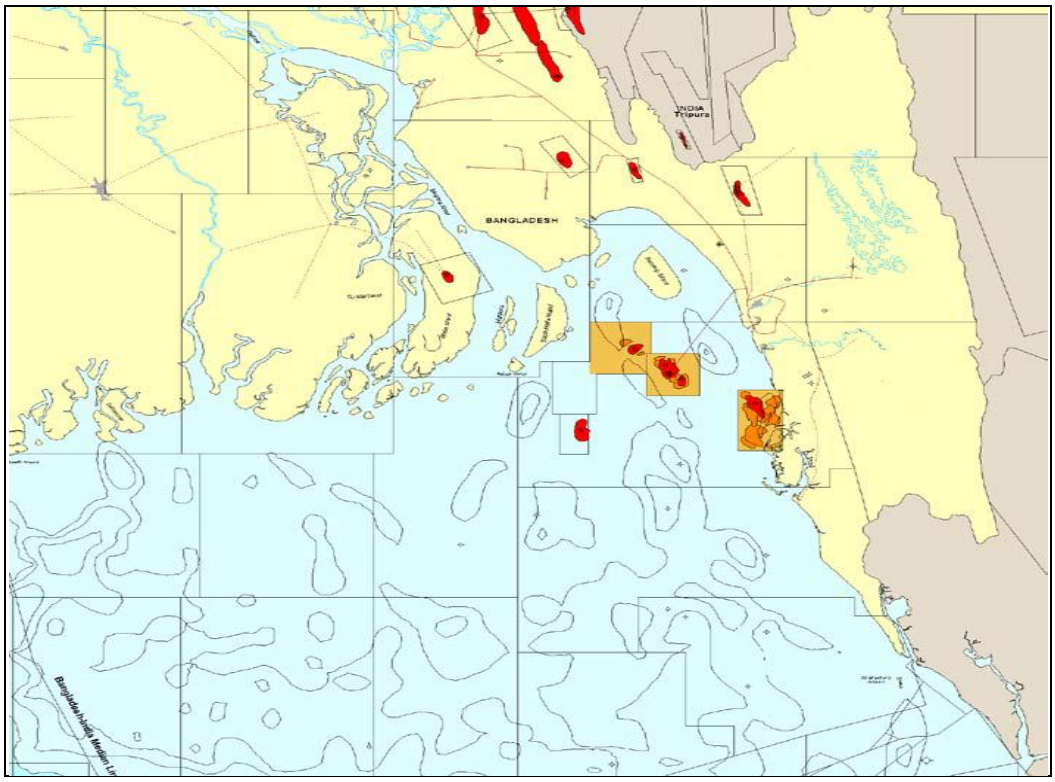

Figure 4.3 : Sangu location map

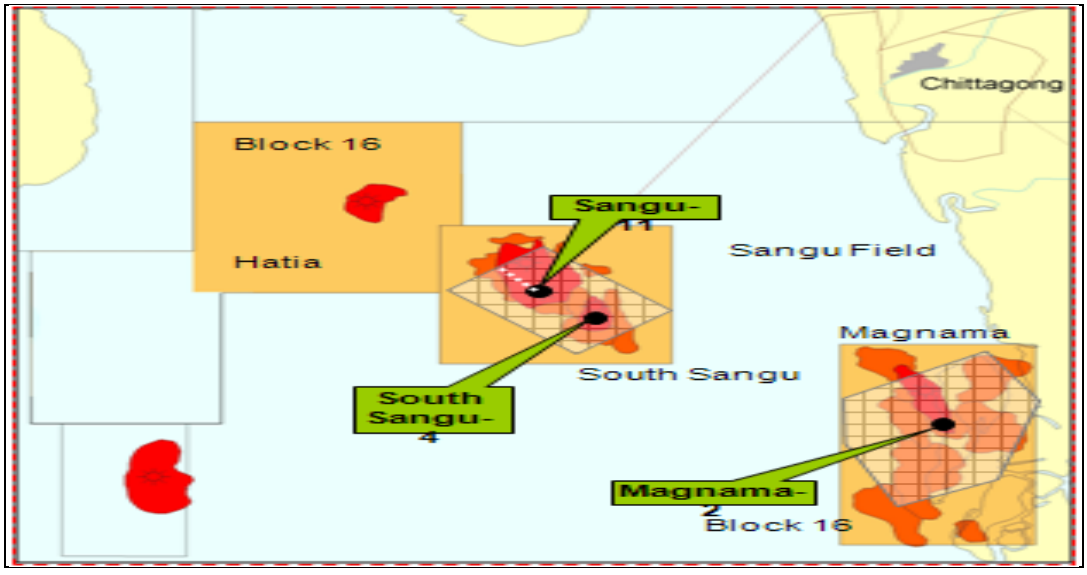

Figure 4.4: Relative position of Sangu 11 and South Sangu

(b)Position of Sangu 11 in the platform:

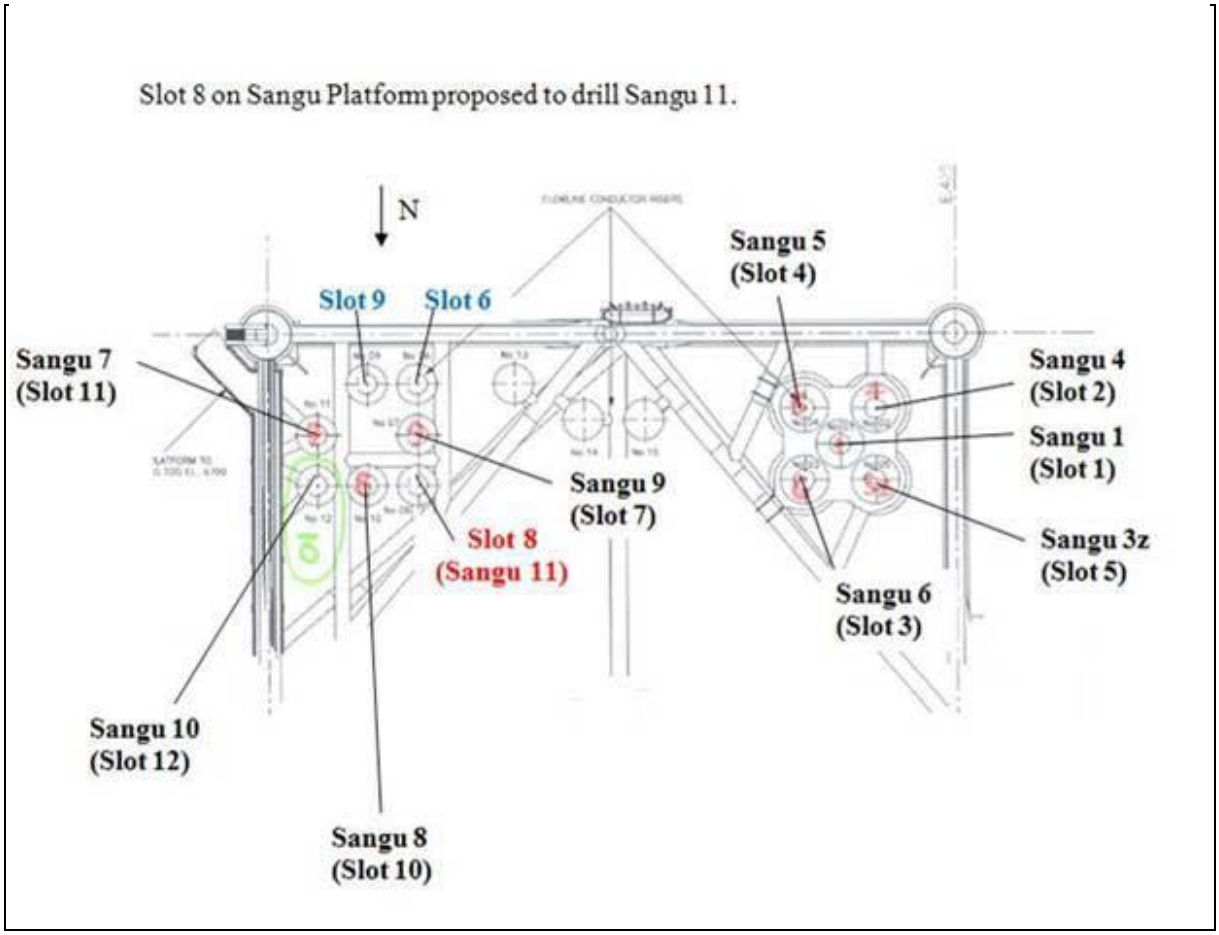

Figure 4.5: Naming convention and position of Sangu 11

NOTE:
1) SLOT FOR SANGU-11 LOCATION IS KBR SLOT 8
2) Platform North is directionally Due South

4.1.4 Drilling string and fluid information

Different types of Bottom Hole Assembly was used both in the 12.25 inches section and 8.5 inches section in different depth. The summary of the BHA used in the different depth is given below

Table 5: Different BHA used in the different section of Sangu11

Section	12.25 inches		
Run	Bottom Hole Type	Start Depth	Stop Depth
1	Motor BHA	1164 m	1726 m
2	RSS BHA	1726 m	3017 m
3	Rotary BHA with power drive	3017 m	3503 m

Section	8.5 inches		
Run	Bottom Hole Type	Start Depth	Stop Depth
1	RSS Vortex BHA	3503 m	4260 m

The details of the Boottom Hole assembly and related mud properties of the different sections are stated in the following pages. (The information has taken from the Drilling Program of Sangu-11, Santos Sangu Field Limited)

Block 16	Well name	SANGU 11
	BHA Name	12.25'' Motor BHA
	Borehole name	12.25"

	Desc.	OD (in) / ID (in)	Max OD (in)	Bot. (in) / Top. (in)	Length (m)	Cum. Length (m)	Cum. Weight (1000 lbm)
1	12 1/4 " Bit	8.000 / 3.250	12.250	6.625	0.44	0.44	0.4
2	A962M5640XP Motor	9.625 / 7.880	12.125	6.625 / 6.625	9.29	9.73	6.5
3	Float Sub	8.250 / 3.000	8.250	6.625 / 6.625	1.52	11.25	7.3
4	String Stabilizer	8.250 / 3.000	12.000	6.625 / 6.625	1.52	12.78	8.1
5	ARC-8	8.250 / 2.810	9.100	6.625 / 6.625	5.49	18.26	10.9
6	Telescope 825 HF	8.250 / 5.900	8.410	6.625 / 6.625	7.53	25.79	14.0
7	StethoScope 825 w/ 12" Stabilizer	8.250 / 5.900	12.000	6.625 / 6.625	9.60	35.39	18.3
8	sonicVISION 825	8.250 / 4.000	9.130	6.625 / 6.625	6.89	42.28	21.7
9	SADN-8	8.250 / 3.250	12.000	6.625 / 6.625	6.71	48.98	24.3
10	Cross Over	8.000 / 3.000	8.000	6.625 / 5.500	1.52	50.51	25.0
11	Heavy Weight Drill Pipe	5.500 / 3.250	7.250	5.500 / 5.500	97.00	147.51	44.1
12	Cross Over	8.000 / 3.000	8.000	5.500 / 4.500	1.52	149.03	44.9
13	JAR	6.500 / 2.250	6.630	4.500 / 4.500	10.10	159.13	48.0
14	Cross Over	8.000 / 3.000	8.000	4.500 / 5.500	1.52	160.66	48.7
15	Heavy Weight Drill Pipe	5.500 / 3.250	7.250	5.500 / 5.500	38.80	199.46	56.3
16	5-1/2 " 24.70 DPS, Premium	5.334 / 4.670	7.000	5.500 / 5.500	10.00	209.46	57.3

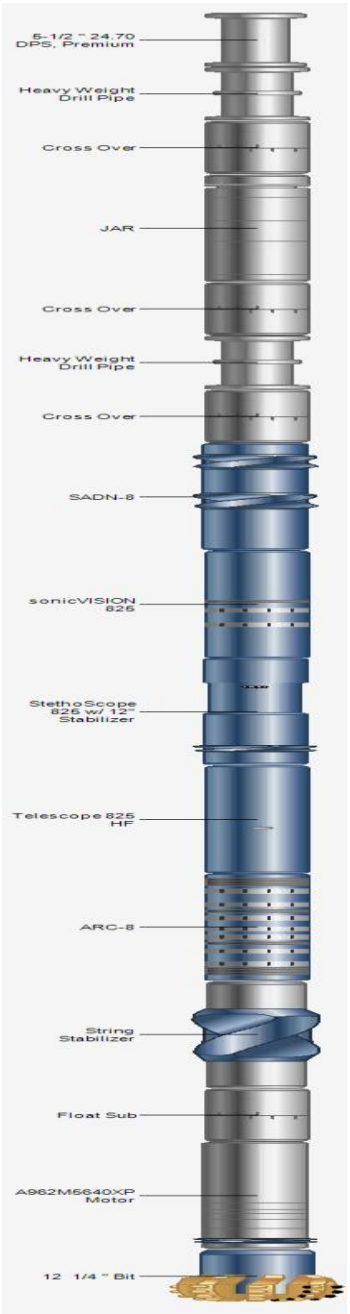

Figure 4.6 : 12.25'' motor BHA

Table 6:Stabilizer Summary of 12.25'' Motor BHA

Stabilizer Summary	
Blade Length (m)	Blade Mid-Pt to Bit (m)
0.457	1.155
0.610	11.710
0.695	27.249
1.091	45.309
0.993	47.771
Bend Summary	
Bend Angle (deg)	Bend to Bit (m)
0.780	2.810

Table 7:Mud Properties of 12.25'' section with Motor BHA

Mud Properties			
Mud Weight (lbm/gal)	9.5	YP (lbf/100ft2)	20
Funnel Viscosity (s)	45	PV (cP)	20

Block 16	Well name	SANGU 11
	BHA Name	12.25'' RSS BHA
	Borehole name	12.25"

	Desc.	OD (in) / ID (in)	Max OD (in)	Bot. (in) / Top. (in)	Length (m)	Cum. Length (m)	Cum. Weight (1000 lbm)
1	12 1/4 " Bit	8.000 / 3.250	12.250	6.625	0.44	0.44	0.4
2	PD 900 X5	9.000 / 5.125	11.960	6.625 / 6.625	4.21	4.65	2.9
3	E-Mag Receiver w / stab 12-1/4"	8.250 / 3.000	12.125	6.625 / 6.625	1.52	6.17	3.7
4	Inline Flex	6.625 / 2.813	8.250	6.625 / 6.625	3.00	9.17	4.9
5	ARC-8	8.250 / 2.810	9.100	6.625 / 6.625	5.49	14.66	7.7
6	Telescope 825 HF	8.250 / 5.900	8.410	6.625 / 6.625	7.53	22.18	10.7
7	sonicVISION 825	8.250 / 4.000	9.130	6.625 / 6.625	6.89	29.07	14.1
8	SADN-8	8.250 / 3.250	12.000	6.625 / 6.625	6.71	35.78	16.7
9	Cross Over	8.000 / 3.000	8.000	6.625 / 5.500	1.52	37.30	17.5
10	10 X 5 1/2" HWDP	5.500 / 3.250	7.250	5.500 / 5.500	97.00	134.30	36.6
11	Cross Over	8.000 / 3.000	8.000	5.500 / 4.500	1.52	135.82	37.3
12	JAR	6.500 / 2.250	6.630	4.500 / 4.500	10.10	145.92	40.4
13	Cross Over	8.000 / 3.000	8.000	4.500 / 5.500	1.52	147.45	41.2
14	4 X 5 1/2" HWDP	5.500 / 3.250	7.250	5.500 / 5.500	38.80	186.25	48.8
15	5-1/2 " 24.70 DPS, Premium	5.334 / 4.670	7.000	5.500 / 5.500	10.00	196.25	49.7

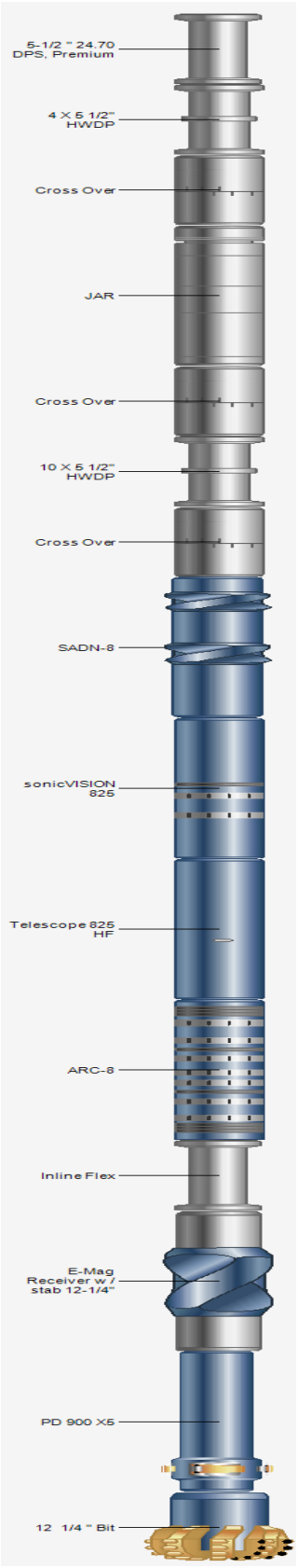

Figure 4.7 : 12.25'' RSS BHA

Table 8:Stabilizer summary of 12,25'' RSS BHA

Stabilizer Summary	
Blade Length (m)	Blade Mid-Pt to Bit (m)
0.610	5.102
1.091	32.099
0.993	34.562

Table 9: Nozzle Summary 12.25'' RSS BHA

BHA Nozzle Summary			
Bit Nozzle		Reamer Nozzle	
Count	1/32 in	Count	1/32 in
6	18.000		
		TFA (in2)	
		PD Flow Restrictor	
		(1/32 in)	42.000
		Rotor By Pass Nozzle	
TFA (in2)	1.491	(1/32 in)	

Table 10:Mud Properties of 12.25'' section with RSS BHA

Mud Properties			
Mud Weight (lbm/gal)	9.5	YP (lbf/100ft2)	20
Funnel Viscosity (s)	45	PV (cP)	20

Block 16	Well name	SANGU 11
	BHA Name	12.25'' Rotary BHA
Borehole name		12.25"

	Desc.	OD (in) / ID (in)	Max OD (in)	Bot. (in) Top. (in)	Length (m)	Cum. Length (m)	Cum. Weight (1000 lbm)
1	12 1/4 " Bit	8.000 / 3.250	12.250	6.625	0.44	0.44	0.4
2	Near bit Stab	8.250 / 3.000	12.120	6.625 / 6.625	1.52	1.96	1.2
3	8.25" Collar	8.250 / 2.813	8.250	6.625 / 6.625	27.43	29.39	15.6
4	String Stab	8.250 / 3.000	12.120	6.625 / 6.625	1.52	30.92	16.3
5	ARC-8	8.250 / 2.810	9.100	6.625 / 6.625	5.49	36.41	19.1
6	Telescope 825 HF	8.250 / 5.900	8.410	6.625 / 6.625	7.53	43.93	22.2
7	StethoScope 825 w/ 12" Stabilizer	8.250 / 5.900	12.000	6.625 / 6.625	9.60	53.53	26.5
8	sonicVISION 825	8.250 / 4.000	9.130	6.625 / 6.625	6.89	60.42	29.9
9	SADN-8	8.250 / 3.250	12.000	6.625 / 6.625	6.71	67.13	32.5
10	Cross Over	8.000 / 3.000	8.000	6.625 / 5.500	1.52	68.65	33.3
11	Heavy Weight Drill Pipe	5.500 / 3.250	7.250	5.500 / 5.500	97.00	165.65	52.4
12	Cross Over	8.000 / 3.000	8.000	5.500 / 4.500	1.52	167.17	53.1
13	JAR	6.500 / 2.250	6.630	4.500 / 4.500	10.10	177.27	56.2
14	Cross Over	8.000 / 3.000	8.000	4.500 / 5.500	1.52	178.80	57.0
15	Heavy Weight Drill Pipe	5.500 / 3.250	7.250	5.500 / 5.500	38.80	217.60	64.6
16	5-1/2 " 24.70 DPS, Premium	5.334 / 4.670	7.000	5.500 / 5.500	10.00	227.60	65.5

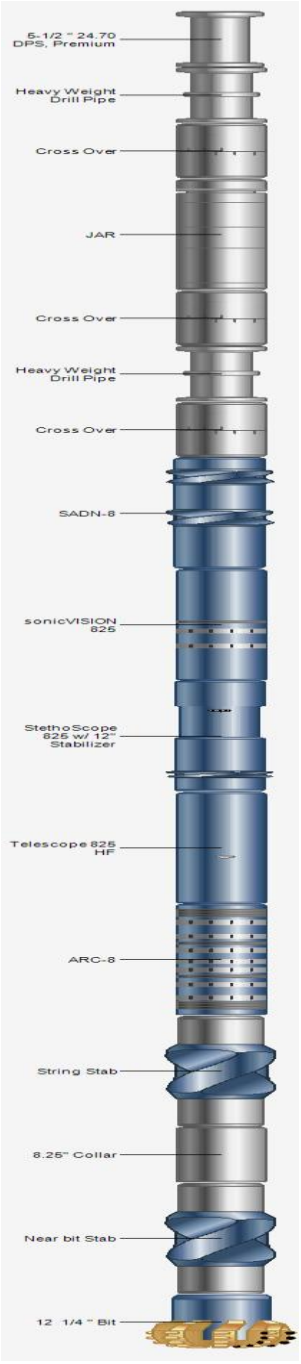

Figure 4.8: 12.25'' Rotary BHA

Table 11:Nozzle Summary of 12.25'' Rotary BHA

BHA Nozzle Summary			
Bit Nozzle		Reamer Nozzle	
Count	1/32 in	Count	1/32 in
6	18.000		
		TFA (in2)	
		PD Flow Restrictor	
		(1/32 in)	
		Rotor By Pass Nozzle	
TFA (in2)	1.491	(1/32 in)	

Table 12:Stabilizer Summary of 12.25'' Rotary BHA

Stabilizer Summary	
Blade Length (m)	Blade Mid-Pt to Bit (m)
0.610	0.896
0.610	29.852
0.695	45.391
1.091	63.450
0.993	65.913

Table 13:Mud Properties of 12.25'' section with Rotary BHA

Mud Properties			
Mud Weight (lbm/gal)	9.5	YP (lbf/100ft2)	20
Funnel Viscosity (s)	45	PV (cP)	20

Block 16	Well name	SANGU 11
	BHA Name	8.5" RSS Vortex BHA
Borehole name		8.5"

	Desc.	OD (in) / ID (in)	Max OD (in)	Bot. (in) / Top. (in)	Length (m)	Cum. Length (m)	Cum. Weight (1000 lbm)
1	8 1/2 " Bit	6.000 / 2.250	8.500	/ 4.500	0.30	0.30	0.1
2	PD 675 X5 AB 8 1/2" Stabilized CC	6.750 / 4.200	8.375	4.500 / 5.500	4.11	4.41	1.5
3	E-mag Receiver	6.750 / 3.250	6.750	5.500 / 5.500	9.14	13.55	4.3
4	PLF6C-AA Flex Collar	5.220 / 4.000	7.000	5.500 / 5.500	2.96	16.51	4.8
5	Filter Sub	6.750 / 2.875	6.750	5.500 / 4.500	1.52	18.04	5.3
6	A700M5682GT	7.000 / 5.500	7.000	4.500 / 4.500	9.31	27.35	8.5
7	Cross over	6.750 / 2.813	6.750	4.500 / 5.500	1.52	28.87	9.0
8	GVR-6 2 x 8 1/4" Stabilizers	6.750 / 4.880	8.250	5.500 / 5.500	3.08	31.96	10.2
9	EcoScope w/ 8 1/4" Stabilizer	6.875 / 2.000	8.250	5.500 / 5.500	8.04	40.00	13.0
10	Telescope 675 NF	6.750 / 5.109	6.890	5.500 / 5.500	7.53	47.52	15.1
11	StethoScope 675 w/ 8 1/4" Stabilizer	6.750 / 2.810	8.250	5.500 / 5.500	9.45	56.97	17.9
12	sonicVISION 675	6.750 / 3.290	7.500	5.500 / 5.500	7.25	64.23	20.4
13	String Stabilizer	6.750 / 2.813	8.375	4.500 / 4.500	1.52	65.75	20.9
14	Cross over	6.750 / 2.813	6.750	4.500 / 5.500	1.52	67.27	21.4
15	10 X 5 1/2" HWDP	5.500 / 3.250	7.250	5.500 / 5.500	100.00	167.27	41.6
16	Cross over	6.750 / 2.813	6.750	5.500 / 4.500	1.52	168.80	42.1
17	Jar	6.750 / 2.500	6.910	4.500 / 4.500	6.86	175.66	44.4
18	Cross over	6.750 / 2.813	6.750	4.500 / 5.500	1.52	177.18	44.9
19	4 X 5 1/2" HWDP	5.500 / 3.250	7.250	5.500 / 5.500	40.00	217.18	53.0
20	5-1/2 " 24.70 DPS,	5.417 / 4.670	7.000	5.500 / 5.500	10.00	227.18	53.9

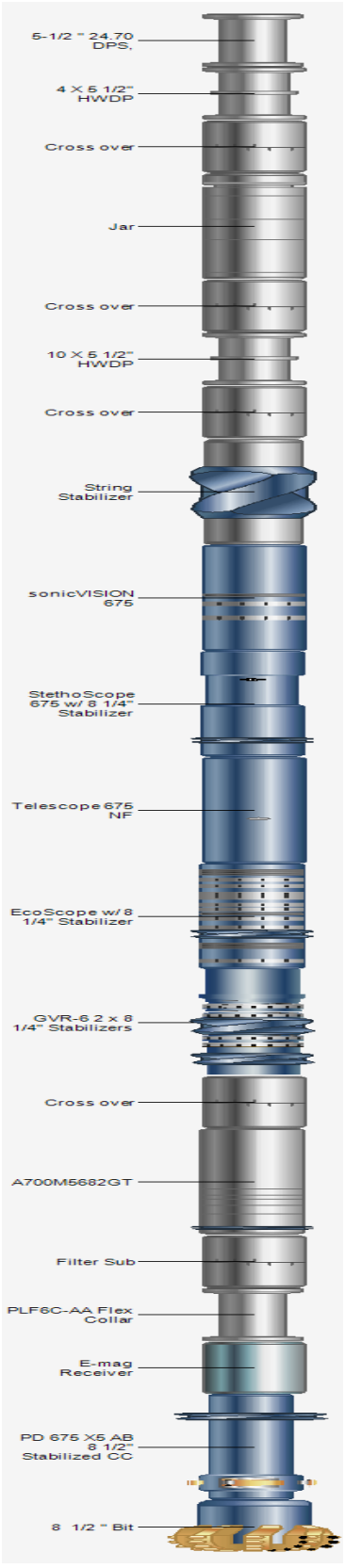

Figure 4.9: 8.5'' RSS Vortex BHA

Table 14:Stabilizer Summary

Stabilizer Summary	
Blade Length (m)	Blade Mid-Pt to Bit (m)
0.213	3.511
0.357	18.568
0.366	29.331
0.518	30.291
0.716	34.589
0.588	48.975
0.610	64.684

Table 15:Stabilizer Summary

BHA Nozzle Summary			
Bit Nozzle		Reamer Nozzle	
Count	1/32 in	Count	1/32 in
3	14.000		
2	13.000		
		TFA (in2)	
		PD Flow Restrictor	
		(1/32 in)	0.000
		Rotor By Pass Nozzle	
TFA (in2)	0.710	(1/32 in)	0.000

Table 16:Mud Properties

Mud Properties			
Mud Weight (lbm/gal)	10	YP (lbf/100ft2)	20
Funnel Viscosity (s)	45	PV (cP)	20

4.5 Drill string simulation of Sangu 11

The more we are pressured to maximize productivity, the more we push the most expensive item in our operation - our drill string - to its limit. Unfortunately, the harder we push it, the more stress we apply to each length of drill pipe. Hoop stresses, radial stresses, torsional stresses, tensional stresses and compression stresses can all build up during the punishing drilling process, resulting in microscopic fatigue cracks. Unless these tiny cracks are detected by a thorough inspection, they propagate - accelerated by stress concentrators like corrosion pitting, mashes and dents - until they cause a washout and the premature failure of our entire drill string. Which can mean extensive downtime from tripping and fishing or even loss of the entire well. That's why it is very necessary to perform a simulation study of the stresses of drill string to make sure that the predicted stress formation will be far away from the stress limit of the drill string in use.

The stresses generally evolved during the drilling operation in drill string is discussed below with the simulated plot of Sangu 11.

4.3.1 Radial stress of drill sting in Sangu 11 well:

The simulated Radial stress plot of Sangu 11 is shown below

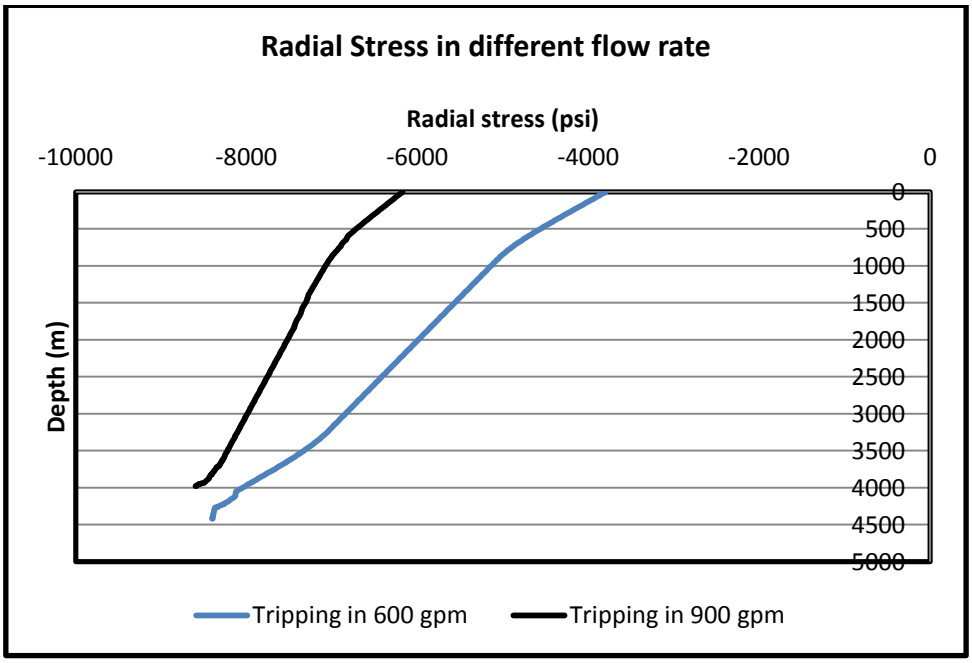

Figure 4.10 : Radial stress in different flow rate

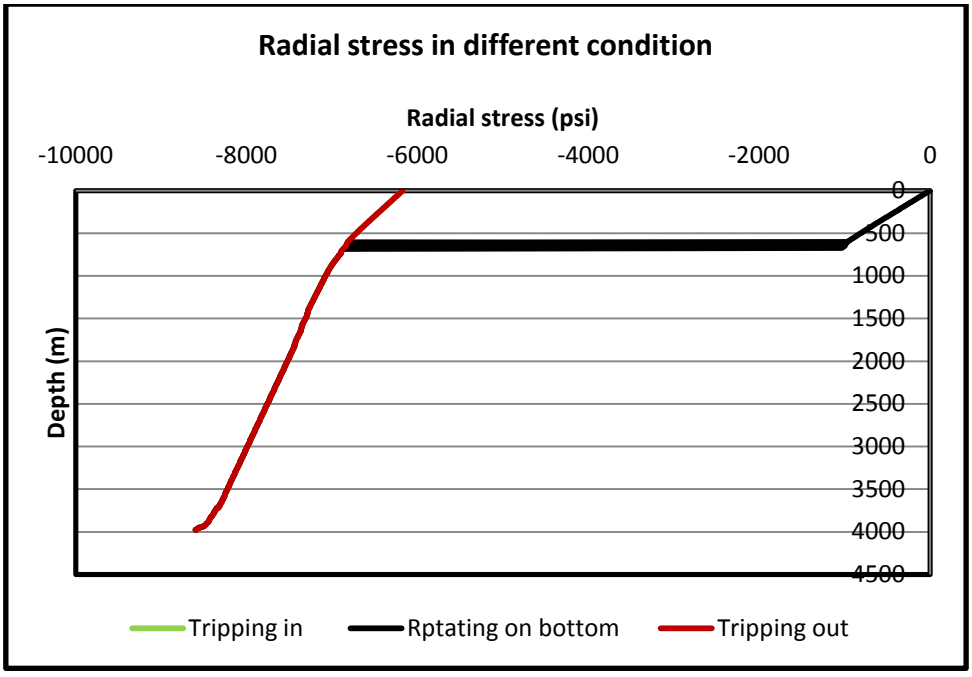

Figure 4.11 : Radial stress in 12.25'' section with 900 gpm flow rate

Observation from radial stress simulation :

From the above graph it is clear that for a certain flow rate the radial stress is same for both Tripping in and Tripping out operation but as the flow rate changes the radial stress is also changed.

4.3.2 Hoop stress of drill sting in Sangu 11 well

The simulated Hop stress plot of Sangu 11 is shown below :

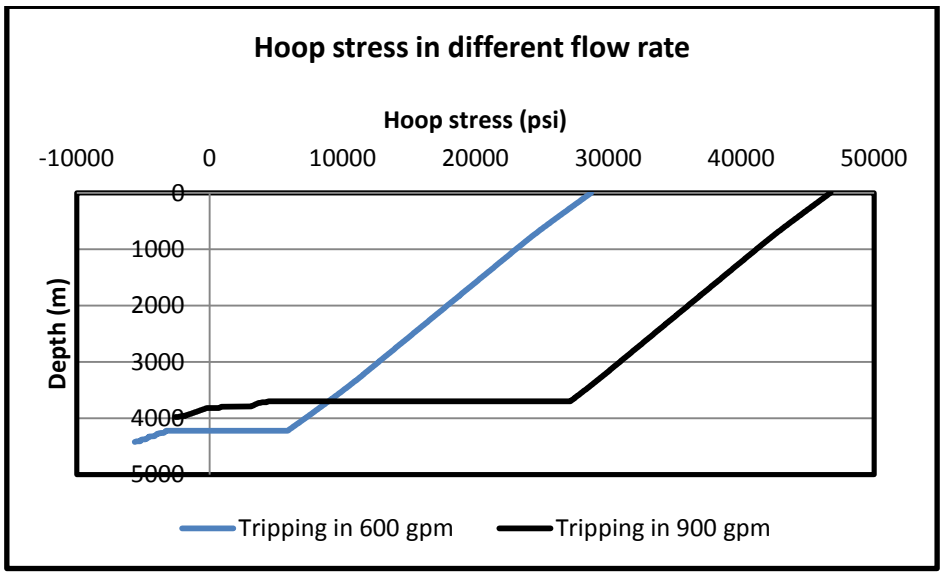

Figure 4.12 : Hoop stress in different flow rate

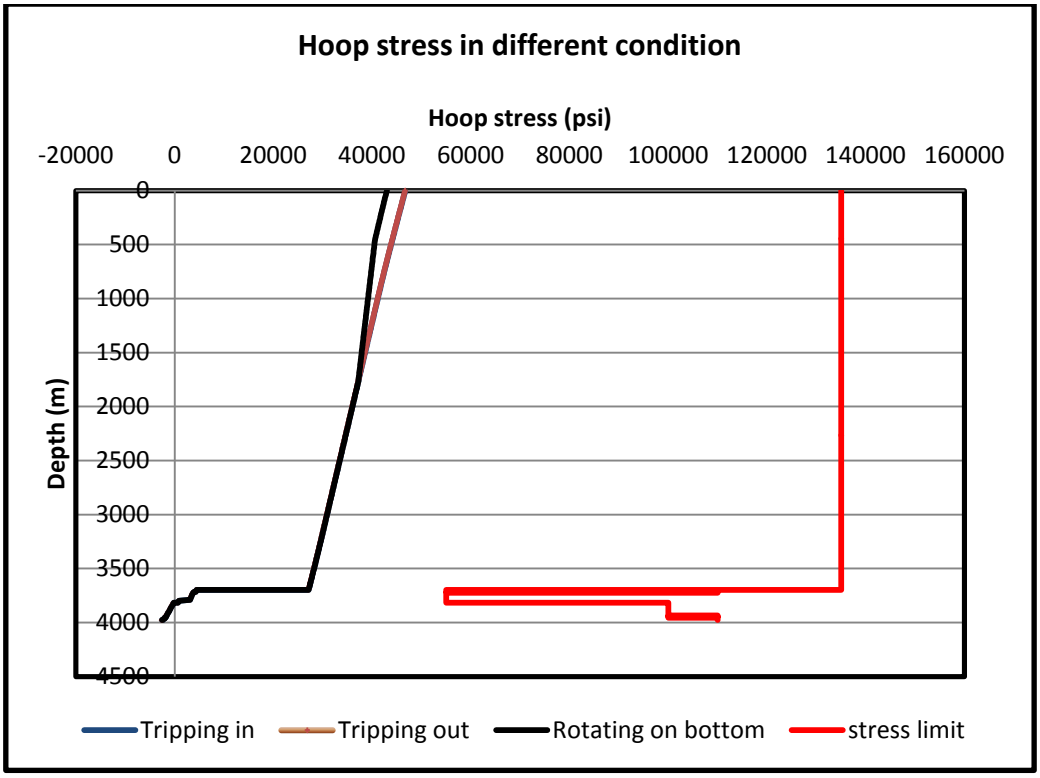

Figure 4.13: Hoop stress in 12.25'' section with 900 gpm flow rate

Comment on Hoop Stress simulation :

As like as the radial stress the Hoop stress is also same for a certain flowrate but changes for rotate on bottom operation. And from the graph it is also clear that the Predicted Hoop stress develop during the drilling is quite lower than the stress limit and there is no chance of drill string failure due to the development of Hoop stress.

4.3.3 Axial stress of drill sting in Sangu 11 well

Various simulated plot of Axial stress regarding Sangu 11 is shown below

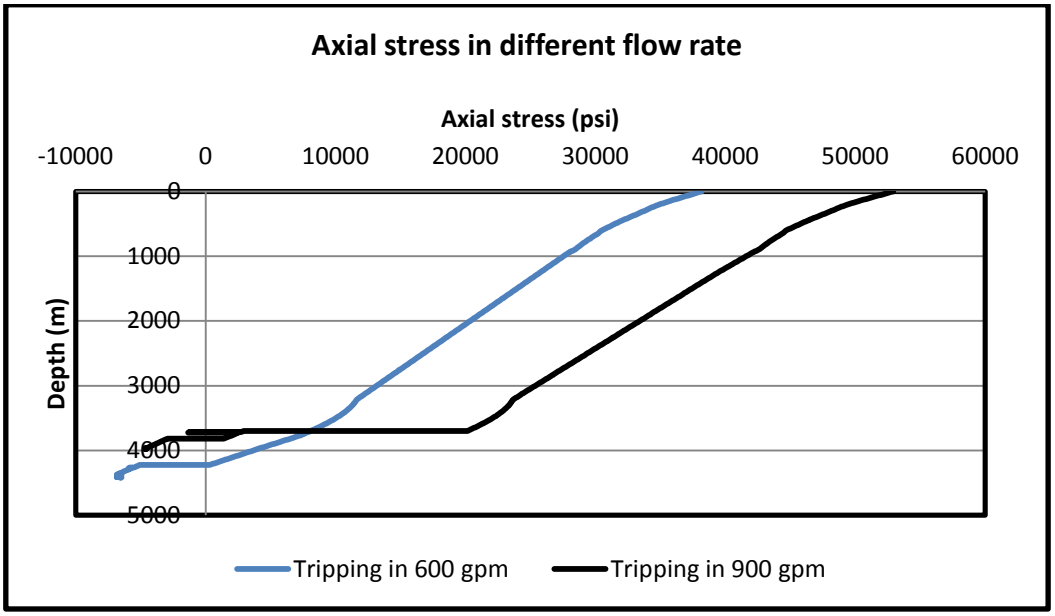

Figure 4.14: Axial stress in different flow rate

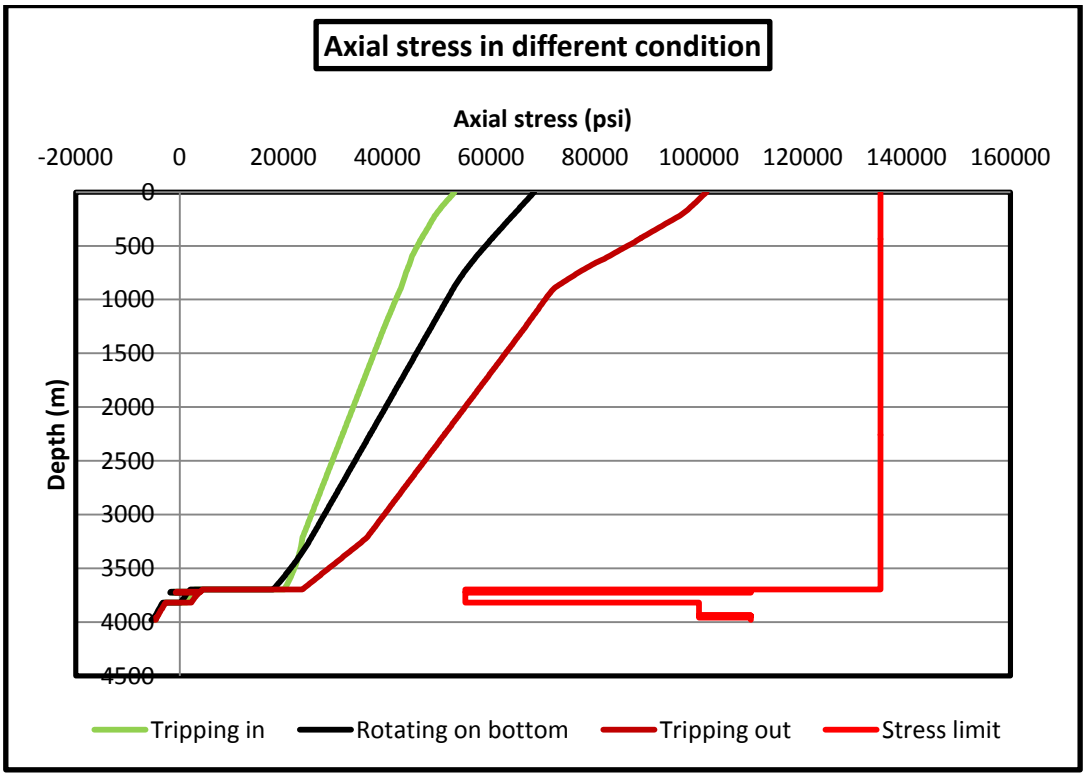

Figure 4.15: Axial stress in 12.25'' section with 900 gpm flowrate

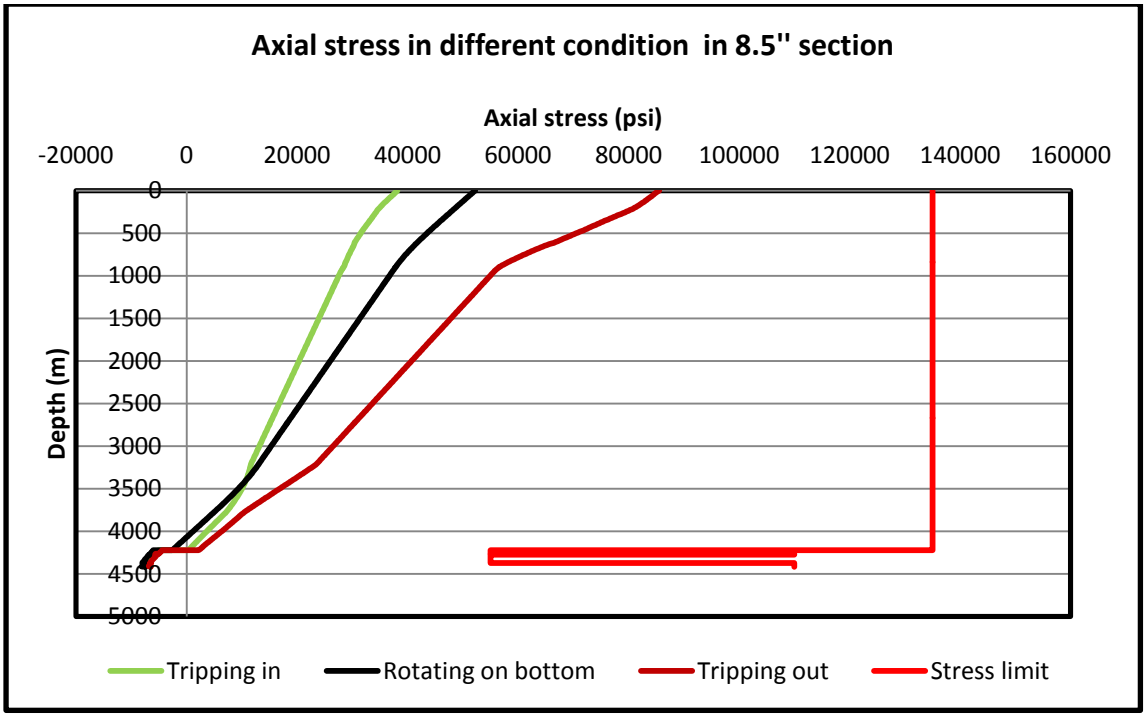

Figure 4.16 : Axial stress in 8.5'' section with 600 gpm flow rate

Comment on simulated Axial stress:

From the simulated graph it is clear that Axial stress have different values for Tripping in , Tripping out and Rotate on Bottom operation. It is also clear from the simulated graph that the axial stress varies for different flow rate. Last of all it is important to see from the simulated graph is that the predicted axial load develops during the various operation of the drilling is under the stress limit.

4.3.4 Torsional/shear stress of drill sting in Sangu 11 well

For a certain flow rate the shear stress is same for all conditions. Various simulated plot of Torsion stress regarding Sangu 11 is shown below

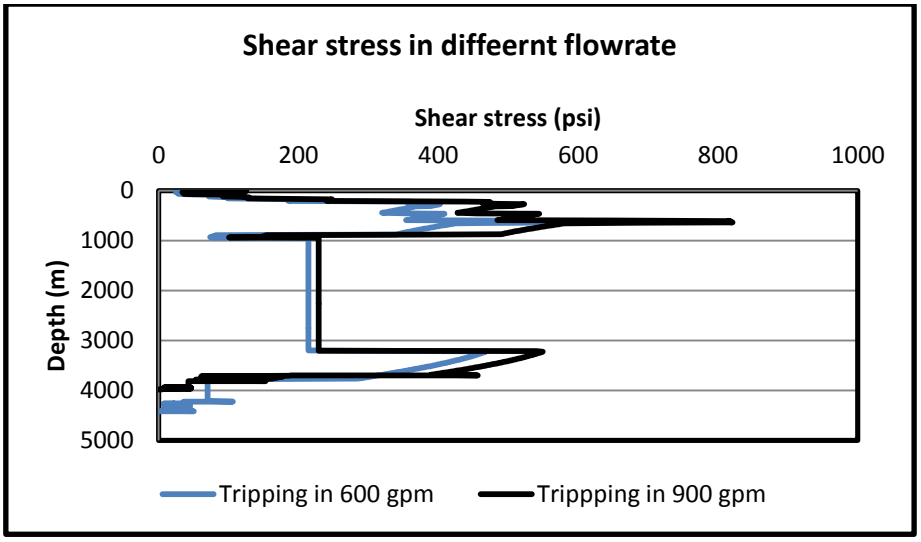

Figure 4.17 : shear stress in different flow rate

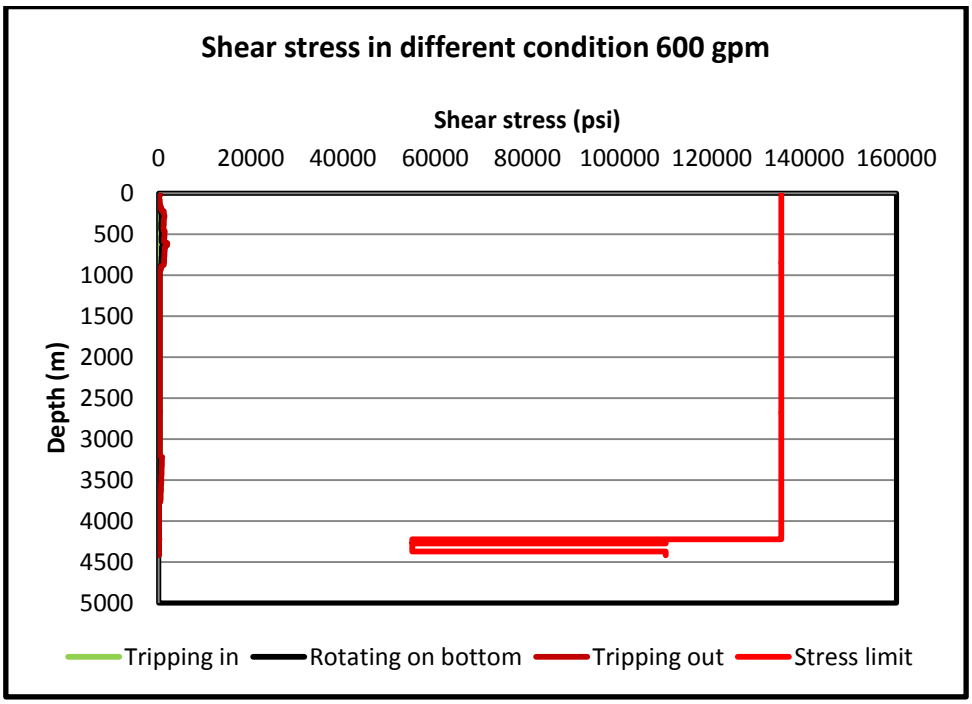

Figure 4.18 : Shear stress in 8.5'' section with 600 gpm flow rate

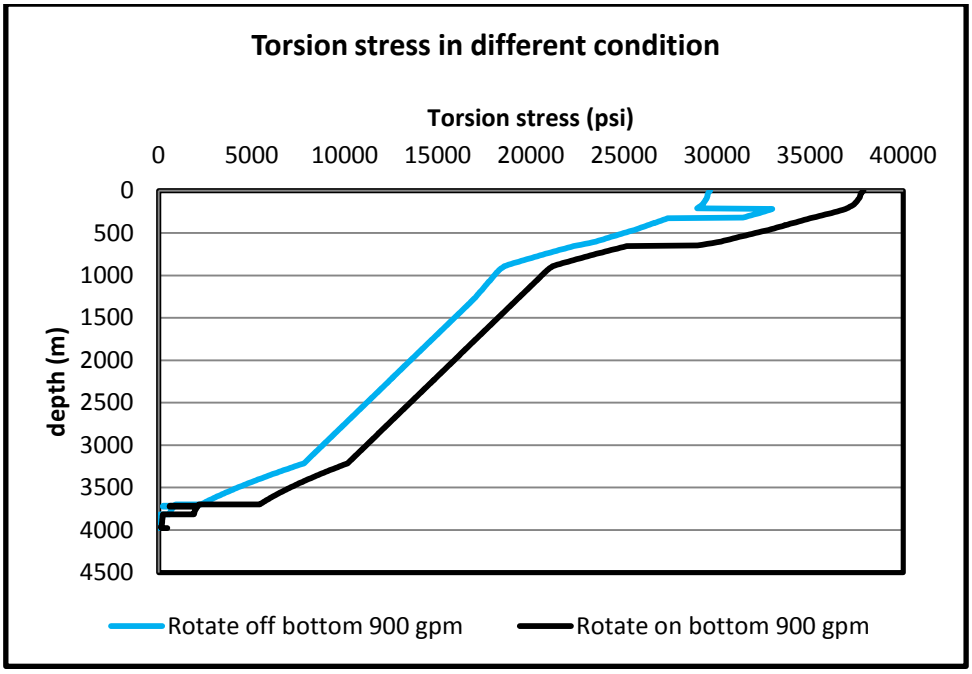

Figure 4.19: Torsion stress at different condition at 12.25'' section

Comment on Torsional/ shear stress

From the simulation it is clear that in tripping in and Tripping out doesn't produce any torsional stress as the simulated value is zero. But for a certain flow rate he rotate on bottom and rotate off bottom operation produces different torsional stress and the torsional stress develop due to roatate on bottom is greater than the rotate off bottom.

In case of shear stress rotating off bottom and Tripping out both have some value but negligible to the stress limit.

4.3.5 Von Mises stress of drill sting in Sangu 11 well

Different simulated plot for Von Mises stress are plotted below:

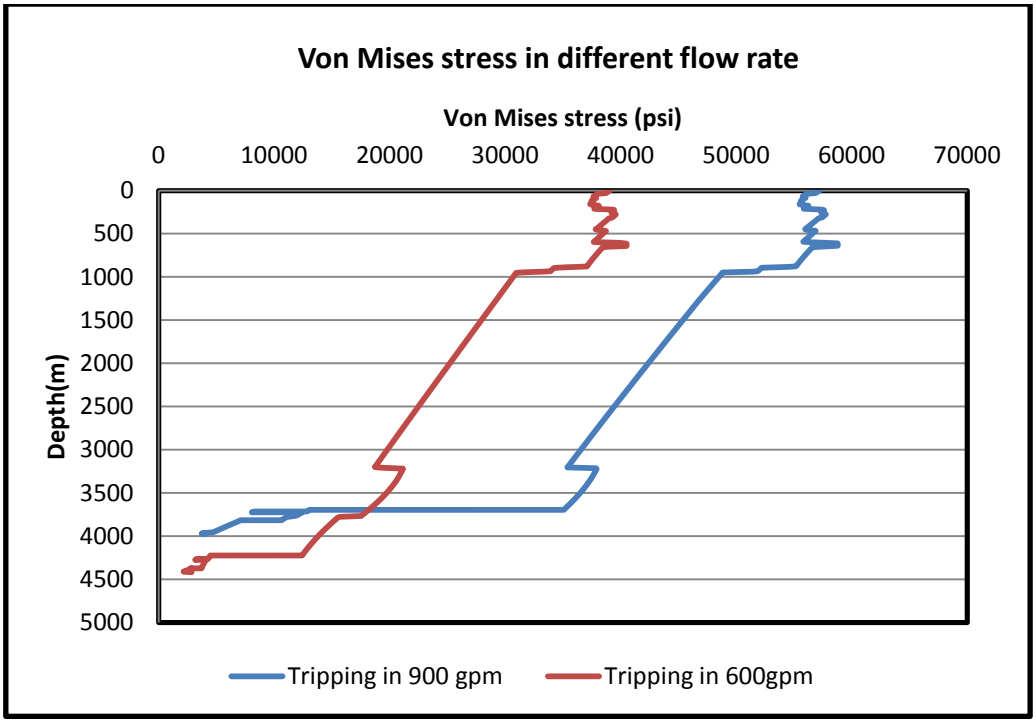

Figure4.20 : Von Mises stress in different flow rate

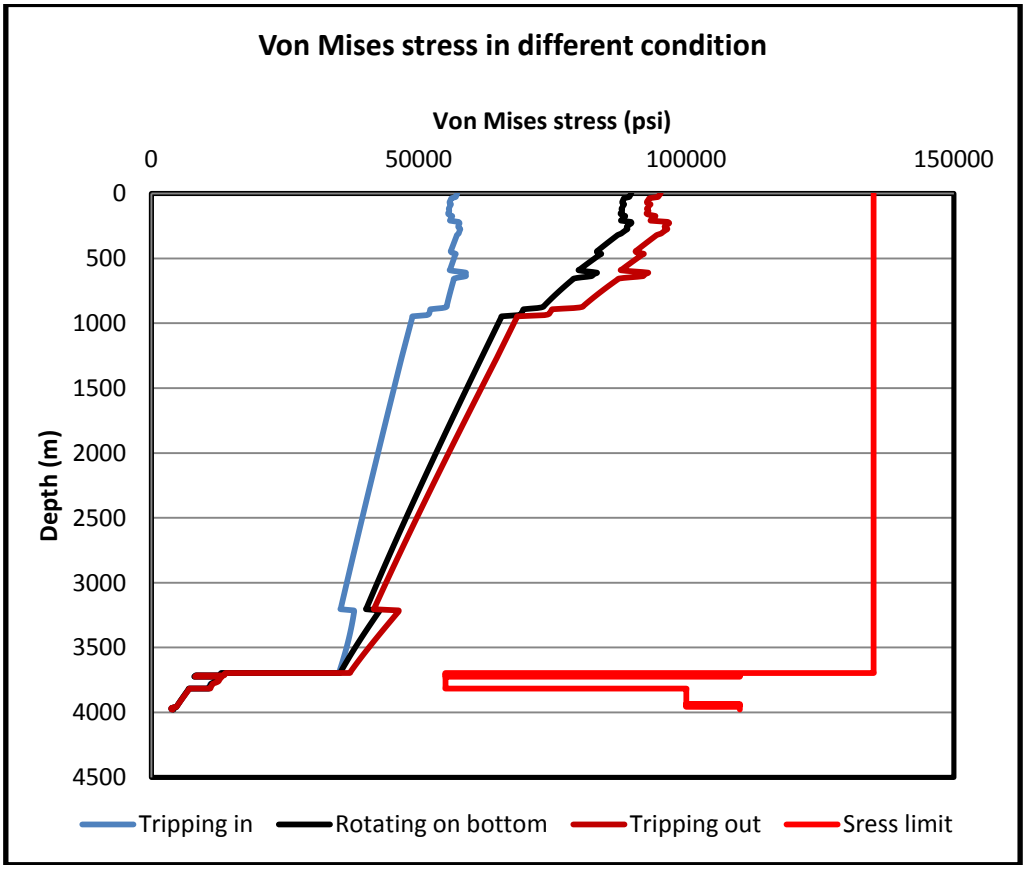

Figure4.21 : Von Mises stress in 12.25'' section with 900 gpm

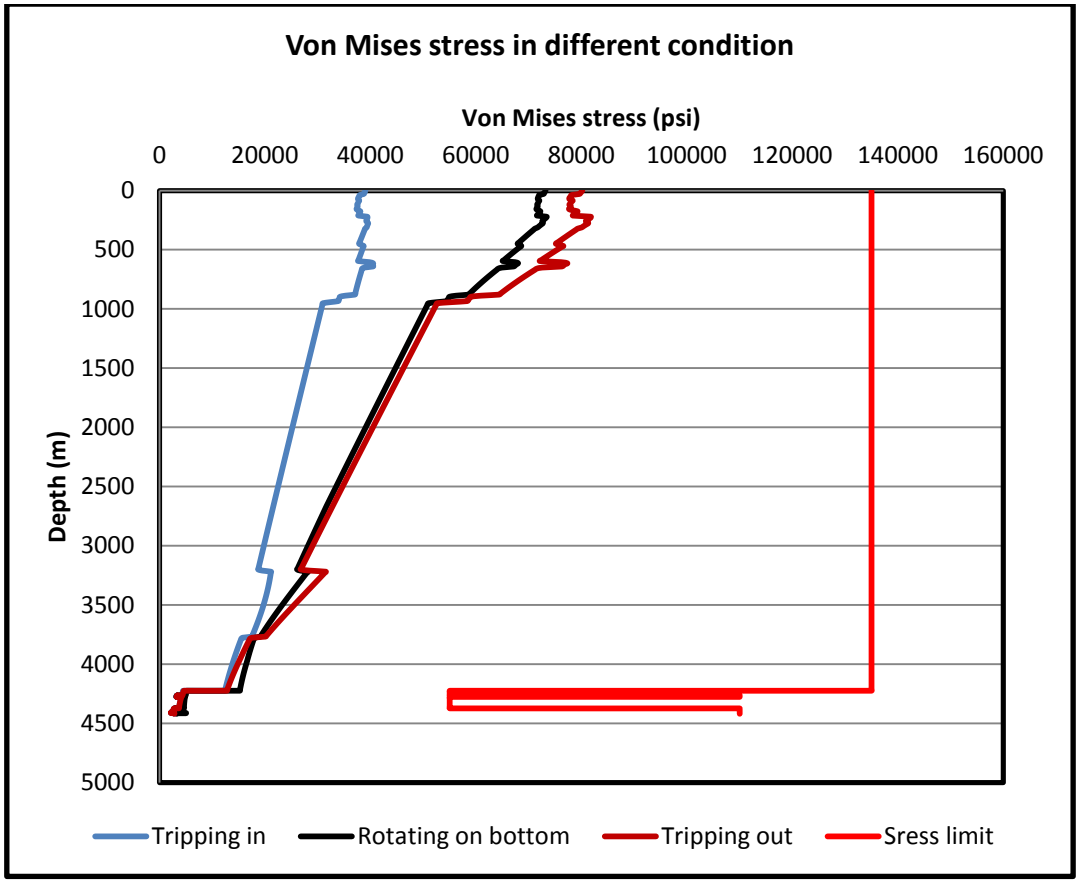

Figure4.22 : Von Mises stress in 8.5'' section with 600 gpm

Comment on Von Mises stress on Sangu 11

The Von Mises stress is also dependent on flow rate aswell as the mood of operation. For the same flow rate Von Mises stress is different for different operation. And it is clear that for the both section the Von Mises stress is under the stress limit

4.3.3 Buckling of drill sting in Sangu 11 well

The simulated plot of Sangu 11 for WOB to Buckling is shown below

4.3.3.1 WOB to buckling for 12.25" section

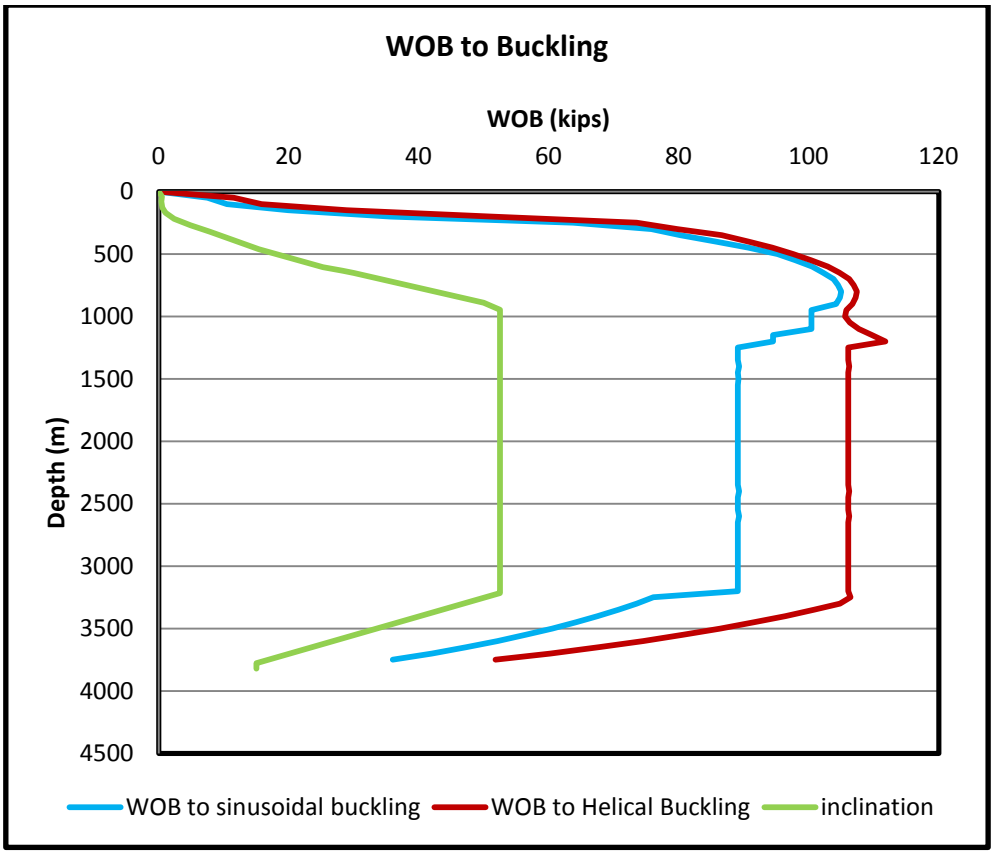

Figure 4.23 : WOB limit for buckling in 12.25'' section

Comment on WOB for 12.25" section :

From the simulation it is clear that the chance of buckling for first 200 m is very high. At the time of drilling we have to be careful about the Weight on Bit in this height. WOB buckling limit has a very good relation with the inclination. It changes with the change of inclination.

4.3.3.2 WOB to buckling for 8.5" section

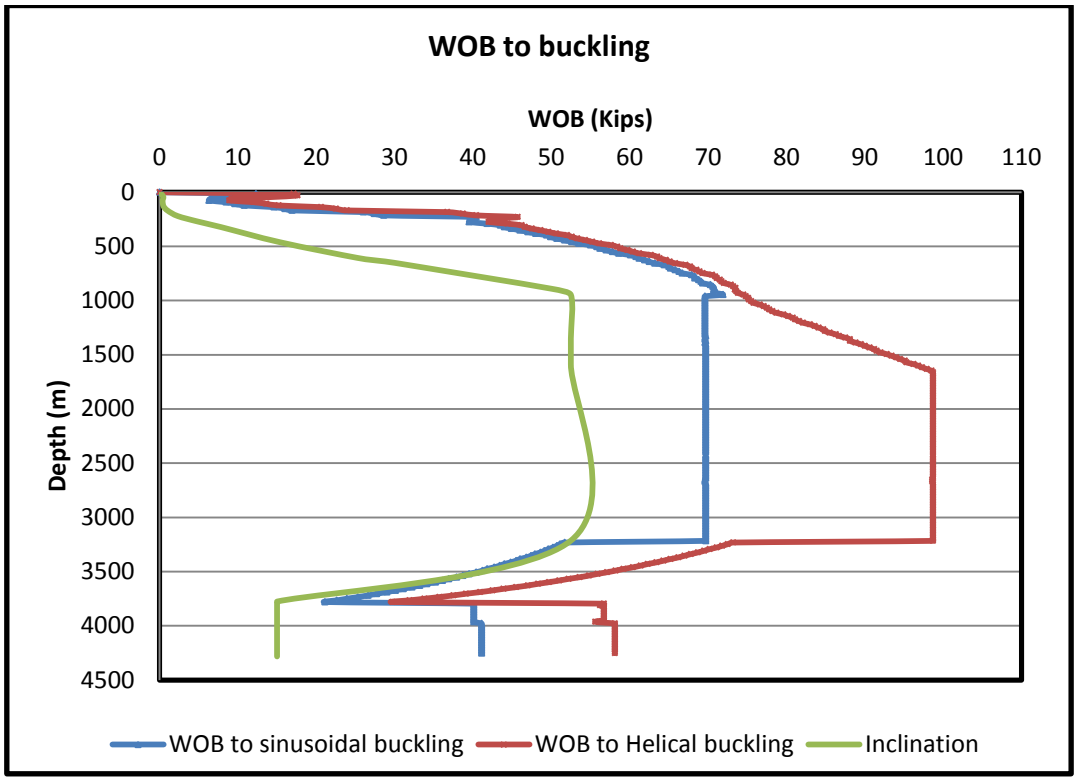

Figure 4.24: WOB limit for buckling in 8.5" section

Commment on WOB for 8.5" section

From the above simulation we have got the safe guideline to use the WOB during drilling. In this section also the WOB is very crucial for first 150 m. As in this depth somewhere the critical WOB is somewhere less than 6.

4.4 Simulation results in 12.25" section

4.2.1 Simulation of hook load

The simulated graph of Tripping in Tripping out and Free Rotating weight is plotted below for different friction factor from 0.2 to 0.4.

Corresponding Hook Load data is in Appendix

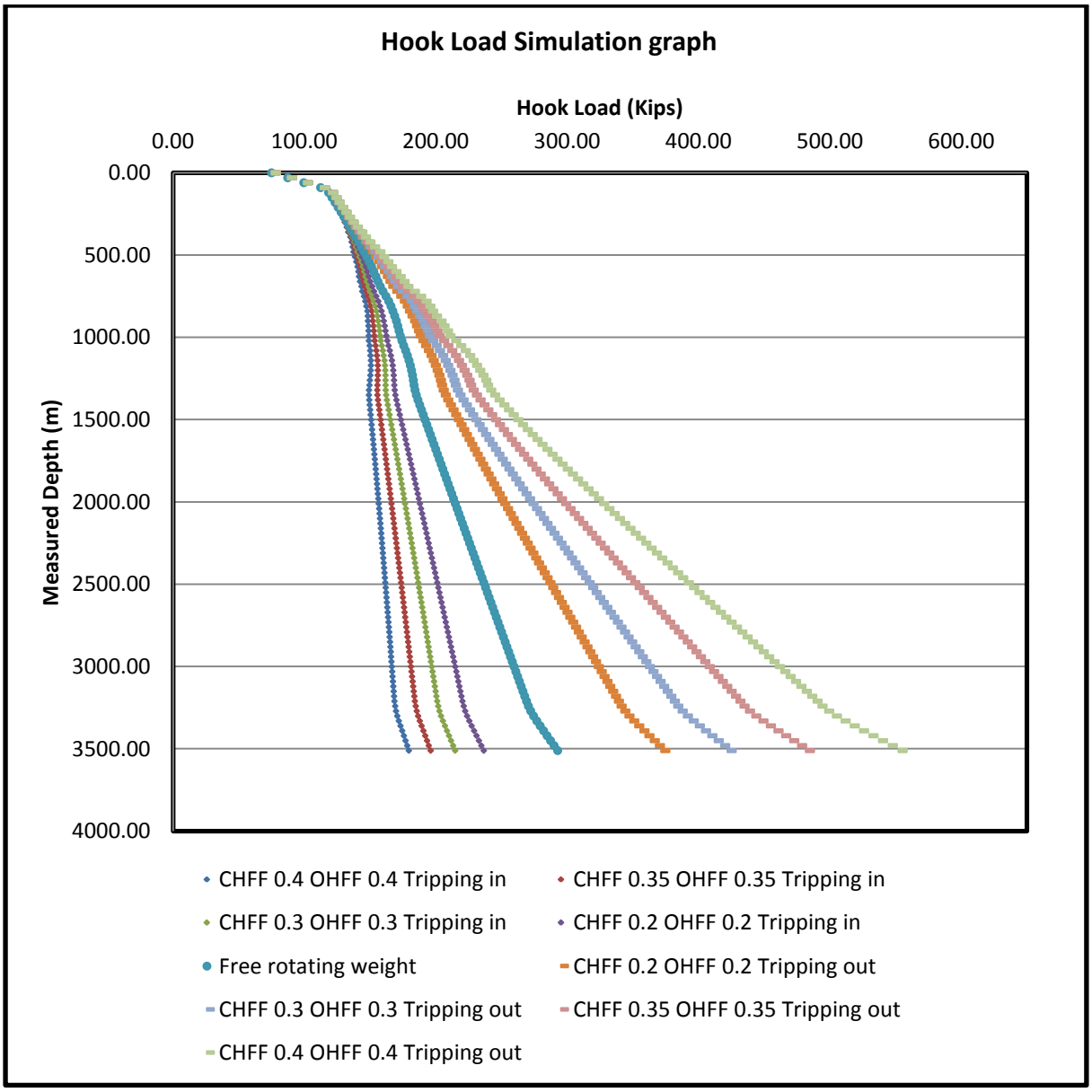

Figure 4.25: Simulated data of Hook Load for 12.25" section

4.2.2 Simulation of toque

The simulated graph of Torque for different friction factor from 0.2 to 0.5 is shown below. Corresponding Torque data is in Appendix.

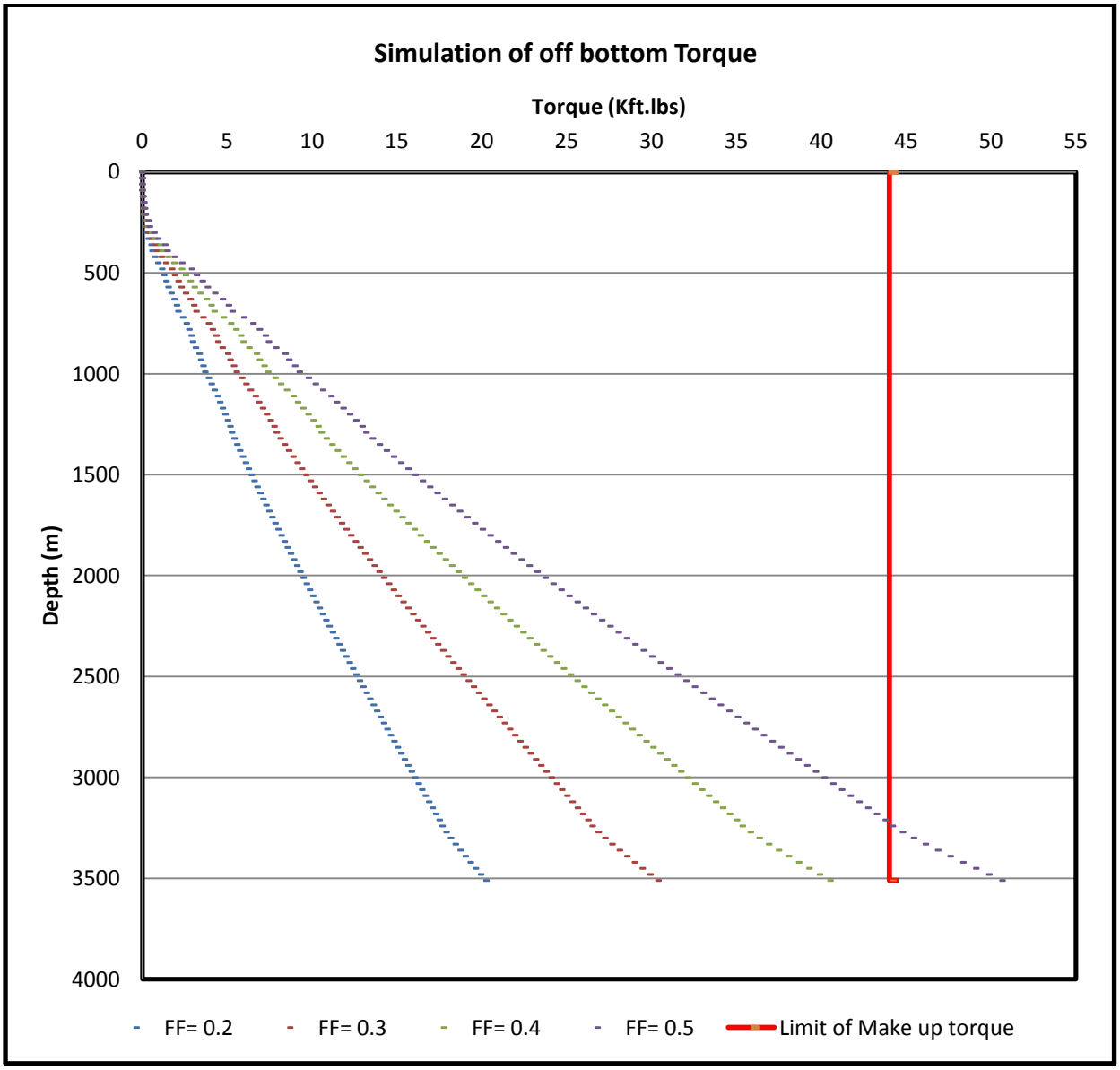

Figure 4.26: Simulated graph of Torque for 12.25'' section

4.2.3 Comparison of real time hook load data with simulated hook load

The real time data are plotted against the simulated Hook Load graph of 12.25'' section is shown below:

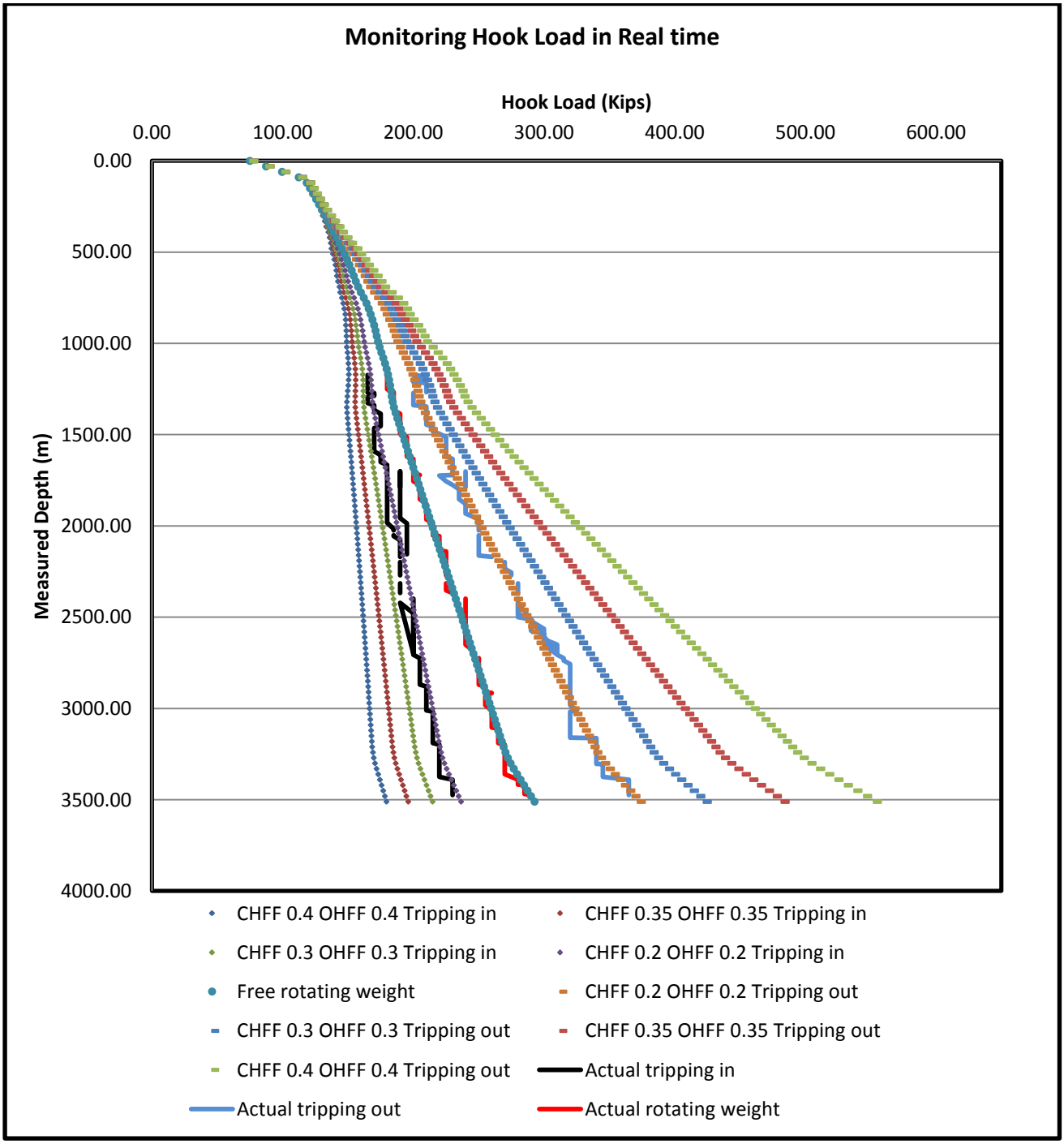

Figure 4.27: Plot of the real time data on Hook Load simulation of 12.25'' section

4.2.4 Comparison of real time torque data with simulated torque load

The real time data are plotted against the simulated Torque graph of 12.25'' section is shown below:

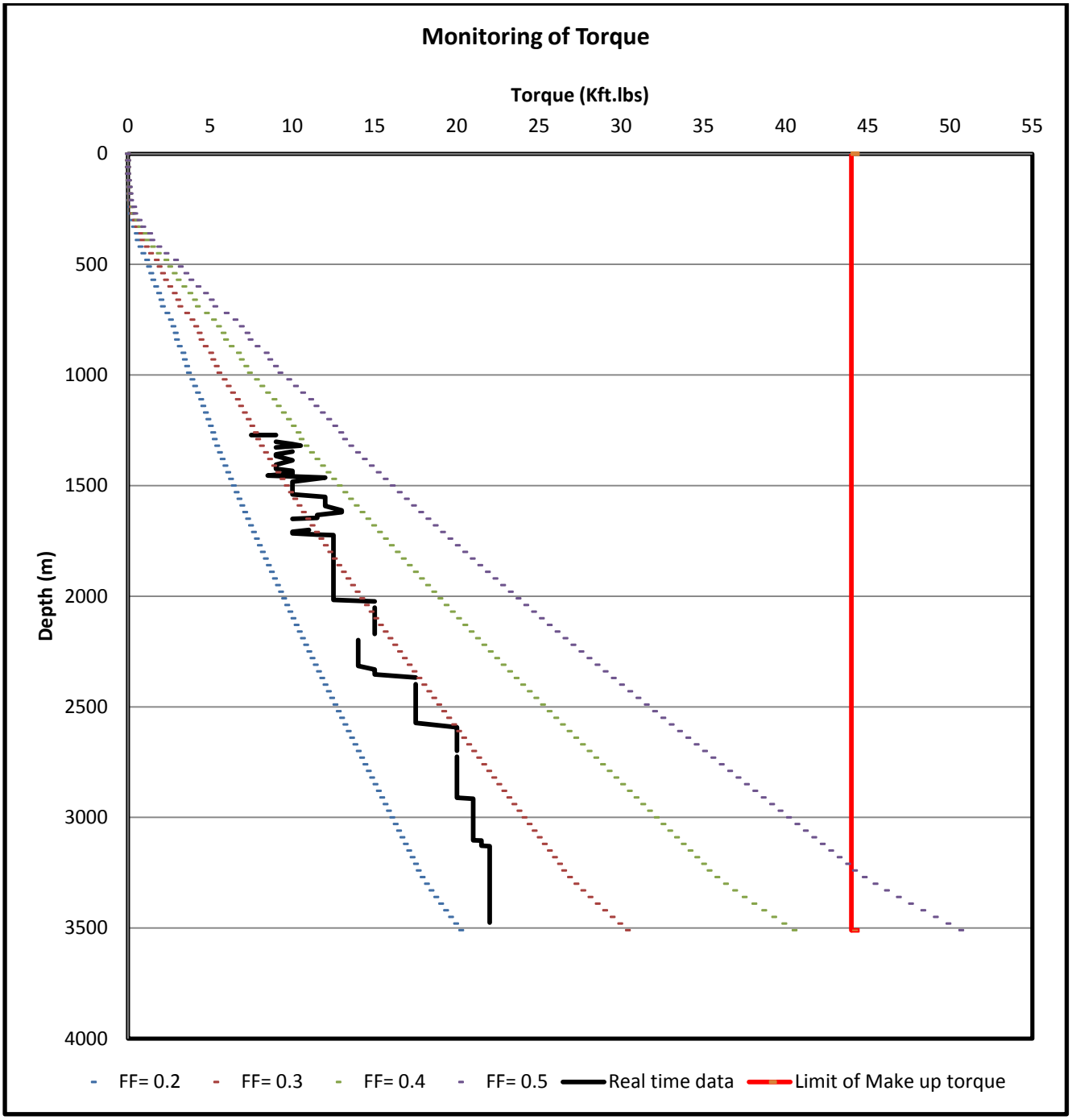

Figure 4.28: Plot of the real time data on Torque simulation of 12.25'' section

4.5 Monitoring of torque and drag in 12.5" section

We can divide this section in three different layer as three different zones. The zones are

Section	12.25 inches		
Run	Bottom Hole Type	Start Depth	Stop Depth
1	Motor BHA	1164 m	1726 m
2	RSS BHA	1726 m	3017 m
3	Rotary BHA with power drive	3017 m	3503 m

Run # 1 (1164 m -1726 m)

Operational Summary:

This section started with a contingency plan of running a motor BHA to avoid the repeat of earlier RSS run as the formation was still relatively soft. A 12 1/4" Smith mill tooth bit (IADC 1-1-7) was lowered with the string including Powerpak motor, float sub, ARC, Telescope, Sonic and SADN. The first shallow hole test was carried out with 700gpm and SPP of 650psi before loading radioactive source into the SADN. After loading radioactive source into the SADN the string was RIH to first stand of HWDP and perform second shallow hole test with 700 GPM and SPP of 800 psi.RIH to top of cement at 1045m and drilled out to float collar at 1066m. The float collar and cement was drilled out to shoe at 1103m using sea water and maintaining 2 to 10 klbs WOB, 40 RPM and flow rate of 800gpm. Resume drilling sliding to build angle and catch up with the plan. The flow rate was maintained at 800gpm to avoid washing the formation as it was still very soft sand. Continue drilling and gradually stage up flow rate to 950gpm and maintaining ROP below 50m/hr to improve hole cleaning while building angle and aligning azimuth as required by plan. At TD, pump Hi-vis and circulated bottoms up two times with the string being stage out after 30mins to avoid hole washout.

Observation from Torque and drag graph :

In this region the Hook Load shows a very good resemble with the simulated line bearing the FF 0.2 and 0.3.The real time data in Tripping in and Tripping out both shows the FF is in between 0.2 and 0.3. Moreover the real time Hook Load data doe6 not show any abnormal trend compared with the simulated line in the Tripping in and Tripping out graph. But from the Torque graph it shows that the initial value of the Torque is fluctuating frequently showing the FF 0.3 to 0.4 in this region. It shows the necessity of giving more effort in the hole cleaning at the beginning of this section.

Run#2 (1726 m -3017 m)

Operational Summary

This section was drilled with a RSS BHA. A 12 1/4" Smith MDi519 LPBX bit, PowerDrive X5, ARC, Telescope, Sonic and SADN was picked up. RIH and drilled from 1726 m to 2194 m. While drilling this section, flow rate of 950 gpm and string RPM of 140 was maintained throughout. Prior to connections each stand was washed up and reamed down and MWD survey was taken prior to making connections. At 2194 m it was decided to do a wiper trip.. Circulated at 950 gpm and 140 rpm for three bottoms up while raking back a stand every 30 minutes. After three circulations tried to trip out on elevator, observed 50 k overpull at 2100 m. RIH 5 meters and circulated for 20 minutes and tried to POOH on elevators. Observed, 50 k over-pull. Commence back-reaming. While back-reaming, torque was normal and there were no indications of hole cleaning or well bore stability issues. Back-reamed till 1986 m and then tried again to trip out on elevators. Observed 40-50 k overpull. Drilled ahead from 2194 m and gradually started to increase MW from 9.5 ppg to 10 ppg. Drilling parameters and connection procedures were maintained. Drilled to 2705 m and while washing up observed over-pull. Decision was made to do a wiper trip one stand earlier than originally planned. Circulated 4 bottoms up while racking back one stand every 45 minutes. RPM was kept constant at 140 rpm. After circulation, an attempt was made to trip out on elevators. It was taking 50 k overpull. Ream out of hole till 2166 m and then RIH to bottom without any issues.Drilled till 3017 m and decide to POOH to change LWD tools and pick up PBL sub. Ream out till 2506 m and then trip out till 2157 m. Ream out from 2157 m to 2081 m and then trip out of hole.

Observation from Torque and drag graph :

In this region the real time Hook Load data also shows a very good resemble with the predicted Hook Load having different FF. In the Tripping in case the real time Hook Load data matches with the simulated data showing the FF form 0.2 to 0.3 and in the Tripping out condition the real time Hook Load stands for the FF 0.2 for that region. From the Torque it is clear that the extra effort in hole cleaning operation changes the trend of the Torque which shows previously the FF ranges from 0.3 to 0.4. Now in this region the Torque shows the decreasing trend having the FF From 0.2 to 0.3. Now the FF in both Torque and Hook Load shows the same FF. So Torque and drag monitoring in this region showed that hole cleaning was good and no abnormal drag was observed.

Run#3 (3017 m-3503 m)

Operational summary:

Pick up new Power drive X5 tool along with LWD tools . Pick up PBL sub above SADN8. RIH to 3010 m. Circulated hole clean and dropped ball to open the PBL ports. Circulated for one hour at 1500 gpm, through the PBL sub. Closed PBL sub by dropping the ball and continued to drill ahead from 3017 m. While drilling, flow-rate was maintained at 1000 gpm and string rpm was 140 rpm. 23 stands of WWT drill pipe protectors (torque reducers) were in the in the drill string. Drill till 3503m. Section TD was declared based on geological correlation with offset well. Dropped ball to open PBL

sub ports and circulated through the PBL sub at 1500 gpm for one hour. Closed PBL sub and continued to circulate hole clean with 1000 gpm. Reamed out of hole till 2965 m. While reaming out Torque was erratic and higher than the previous wiper trips. Noticed the Ultrasonic calliper was reading almost a gauge hole, considerably less than what it was during drilling. RIH to 3503 m. Circulated for one hour and then trip out of hole without any problems to surface.

Observation from Torque and drag graph:

In this region both the Tripping in and Tripping out Hook Loa real time data shows a very good resemble with the simulated graph having the FF of 0.2.While drilling ahead observed that there was no increase in off bottom torque and gradually there was a reduction in off bottom Torque. Torque and drag measurements indicated that the Friction Factor was about 0.2.

4.6 Simulation results in 8.5'' section

4.6.1 Simulation of hook load

The simulated graph of Tripping in Tripping out and Free Rotating weight is plotted below for different friction factor from 0.2 to 0.5. Corresponding Hook Load data is in Appendix

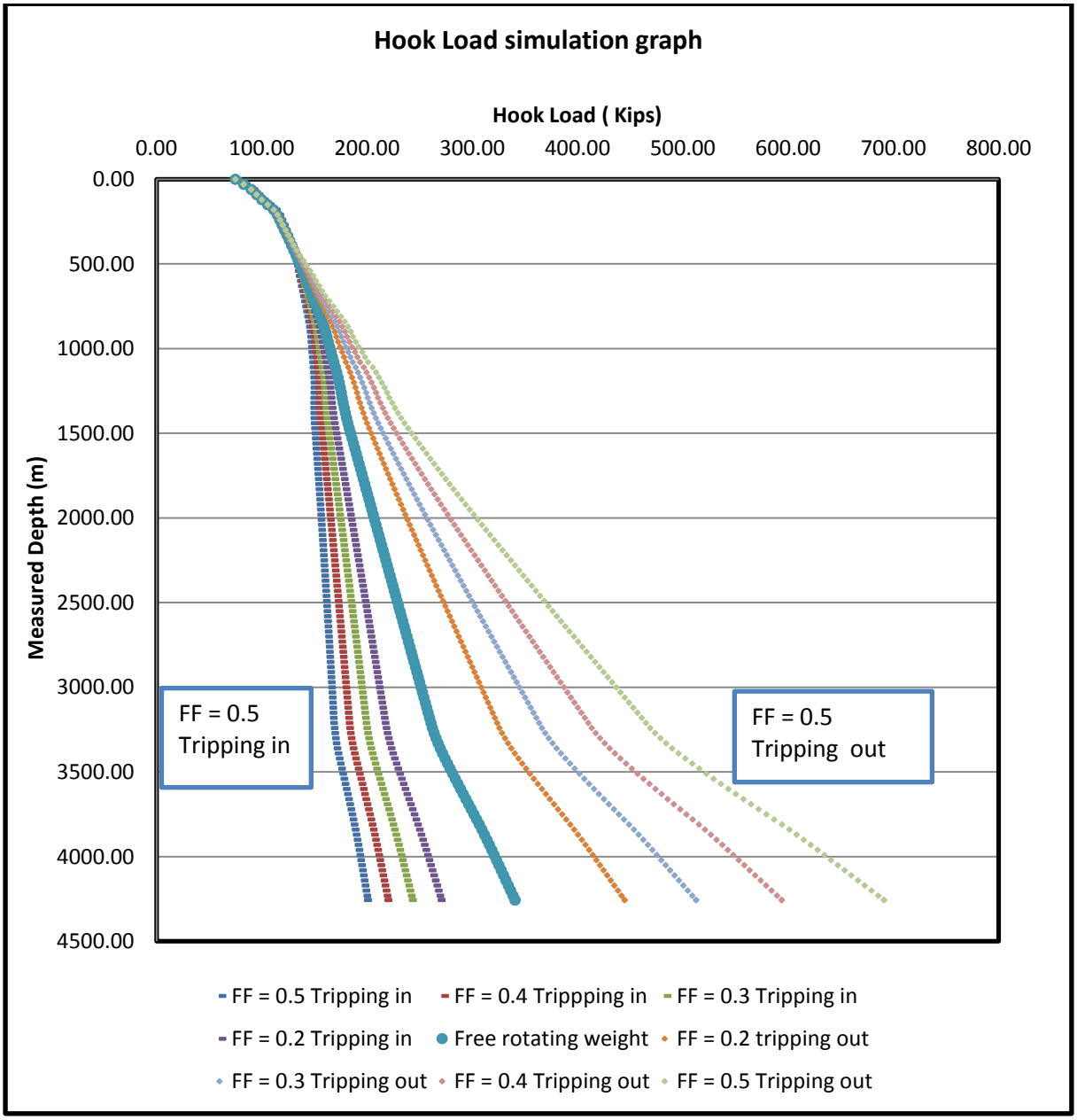

Figure 4.29: Simulated graph of Hook Load for 8.5'' section

4.6.2 Simulation of toque

The simulated graph of Torque for different friction factor from 0.2 to 0.5 is shown below. The corresponding Torque data is in Appendix

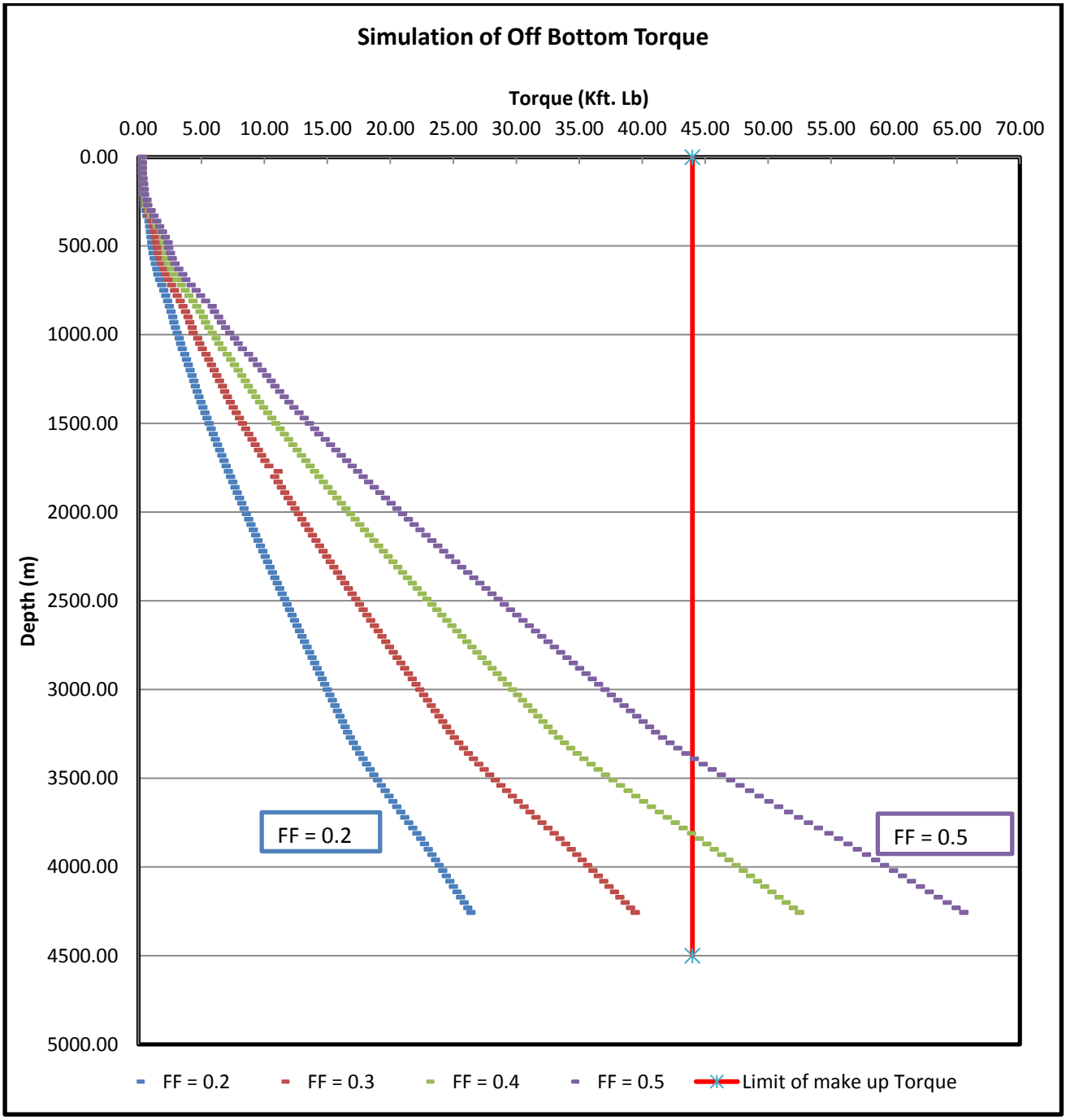

Figure 4.30: Simulated graph of Torque for 8.5'' section

4.6.3 Comparison of real time hook load data with simulated hook load

The real time data are plotted against the simulated Hook Load graph of 8.5'' section is shown below:

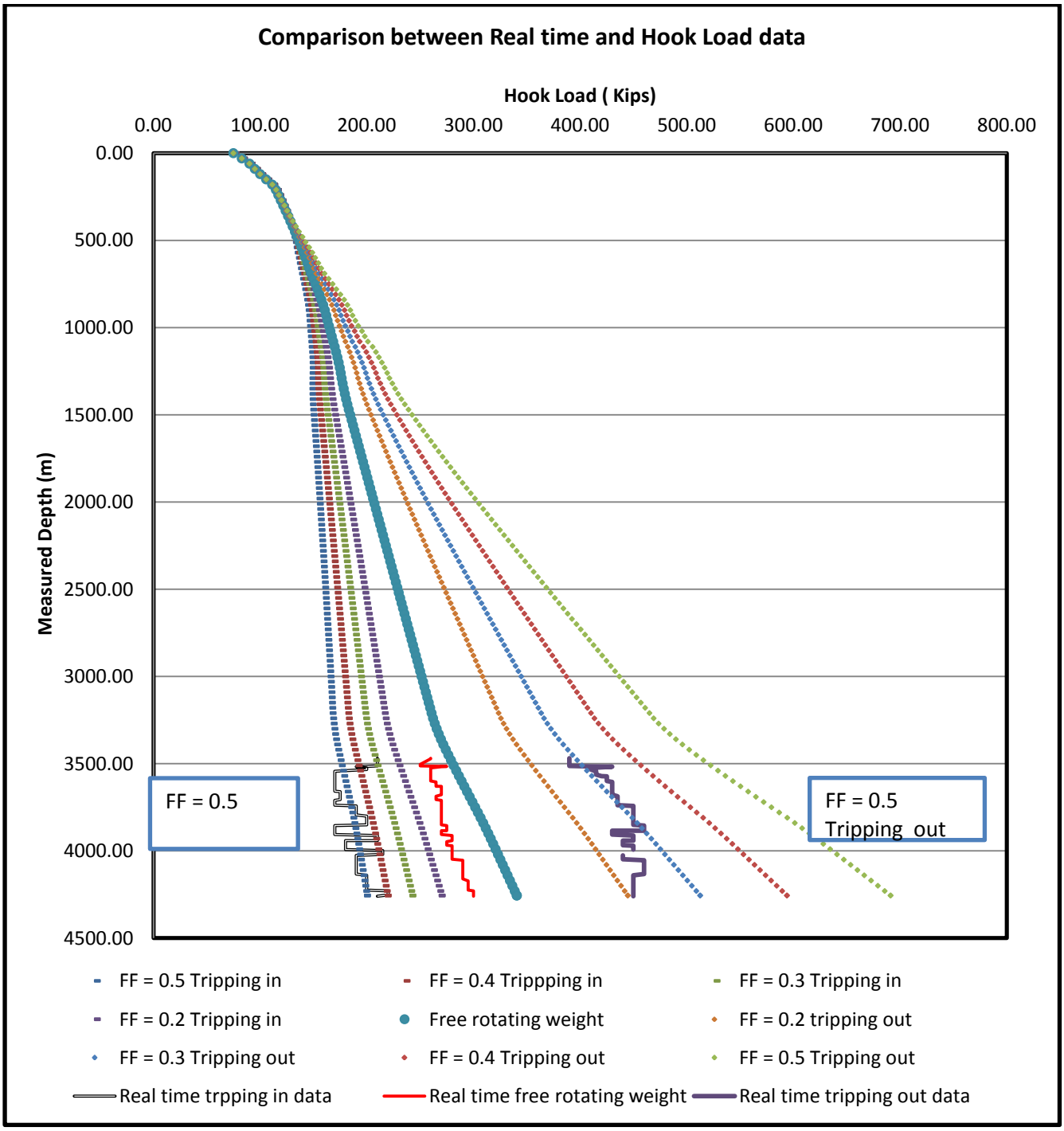

Figure 4.31: Plot of the real time data on Hook Load simulation of 8.5'' section

4.6.4 Comparison of real time torque data with simulated torque load

The real time data are plotted against the simulated Torque graph of 8.5'' section is shown below:

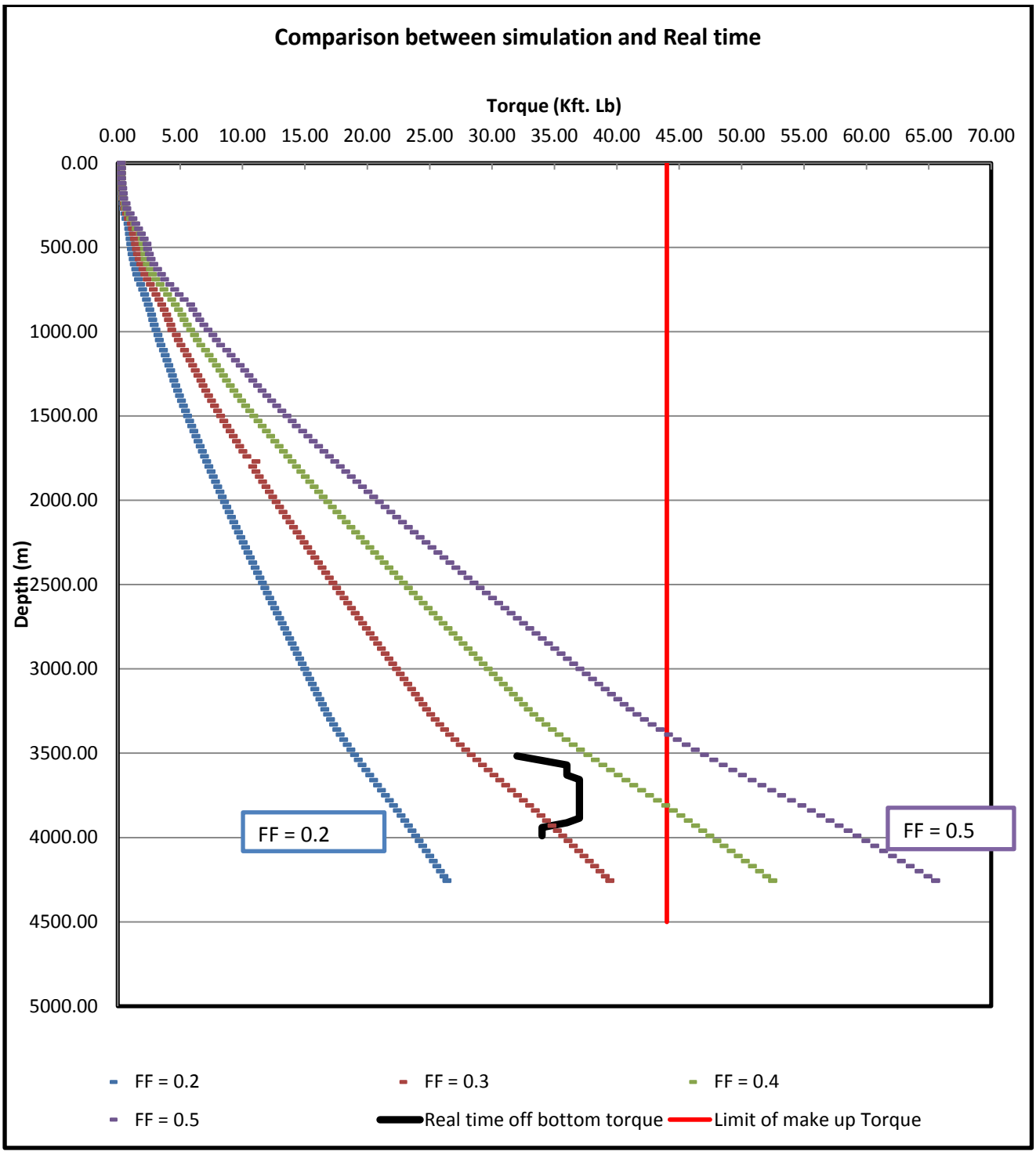

Figure 4.32: Plot of the real time data on Torque simulation of 8.5'' section

4.7 Monitoring of torque and drag in 8.5" section

Operational summary:

RSS BHA was made up and RIH. Slip and cut drill line at shoe. Drill 3 m of formation and perform LOT. A value of 19.1 ppg was recorded.

Drill ahead from 3503 m. Off bottom Torque recorded at the start of drilling the section was 32k ft-lbs. The free rotating weight was reading 20 kips lower than the computed weight. Pick up weight and Torque values were indicating that the open hole Friction Factor was about 0.35. Drill ahead to 3864 m. Off bottom torque was 37 k ft-lbs. Start adding Starglide lubricant into active system. After one complete circulation observed slight reduction in drag. No drag noticed while making connection however there was no change in off bottom torque. Continued drilling to 4000 m. Off-bottom torque gradually reduced to 34 k ft-lbs. At 4000m circulate bottoms up. Open PBL sub and circulate at 1000 gpm. During circulation observed off bottom Torque reduced to 30 k ft-lbs. Attempt to trip out on elevators. Observed gain in trip tank. RIH back to bottom and circulate bottoms up. No gas was recorded during circulation. Pump out of hole to avoid swabbing. Pump out without any problems to 3503 m. Service Top drive and pull back seven stands in order to install WWT non rotating protectors.RIH back to bottom and continue drilling ahead from 4000m. 32 stands of WWT non rotating protectors were in the drillstring. Drill to TD at 4260 m Torque remained constant at 36 kft-lbs. Circulate hole clean and pump out to 4000m. RIH back to bottom and take Stethoscope pre test as per program. During the entire process of pre test the well bore was stable. POOH to run 7" liner.

Observation from Torque and drag graph:

In this section the Tripping in Hook Load shows the higher FF of 0. Where as the Tripping out Hook Load shows a bit lower FF of 0.2 to 0.3.The free rotating weight shows 20 kips lower than the computed weight. From the torque graph it is observed that the Torque increases sharply at the beginning and accordingly after using the starglide lubricant it starts reducing the torque at the depth of 3883 m.

The most important thing in the Torque graph is the observation of the trend of higher torque at the beginning of the section. If the initiative of adding starglide is not taken in time the increasing trend may reach the limiting make up torque of 44 Kft-lb which can occur in the failure of drill string. The chance of crossing the limiting make up Torque is shown below

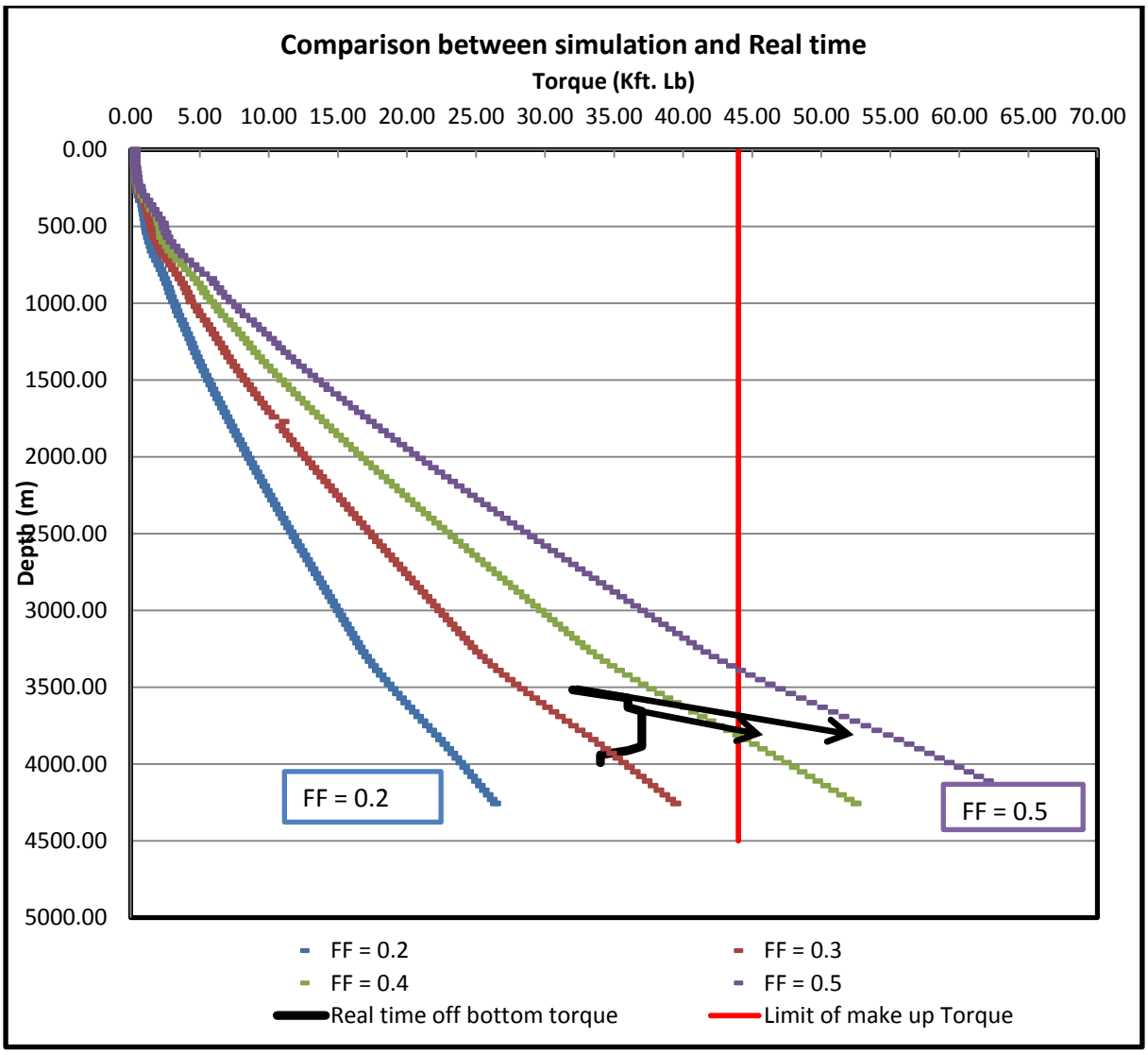
Comparison between simulation and Real time
Torque (Kft. Lb)
0.00 5.00 10.00 15.00 20.00 25.00 30.00 35.00 40.00 45.00 50.00 55.00 60.00 65.00 70.00
0.00
500.00
1000.00
1500.00
2000.00
2500.00
3000.00
3500.00
4000.00
4500.00
5000.00
Depth (m)
FF = 0.2
FF = 0.5
FF = 0.2
FF = 0.3
FF = 0.4
FF = 0.5
Real time off bottom torque
Limit of make up Torque

Chapter 5: Summary and conclusion

The analysis of Tripping in and tripping out real time Hook Load data shows the different friction factor value for the same depth. It can happen due to the manual filtering of the field data. The summary of the friction factor found in the South Sangu is show below :

Operation	12.25'' section	8.5'' section
Tripping in	0.2-0.35	0.2- greater than 0.4
Tripping out	0.2-0.4	0.3- greater than 0.4

From the above idea I have decided to simulate the Hook Load of the Sangu 11, 12.25'' section from 0.2 to 0.4 and 8.5'' section from 0.2 to 0.5.

In the case of Sangu 11, the main drawback of my study was to use the Motor BHA information in the case of simulating 12.25'' section. But a very close result was found from the filtered real time data found from the service company Weatherford from the rig "sea drill". My main achievement in the simulation phase was to identify the higher torque for higher friction factor which will cross the makeup torque limit and may cause the drill string failure. And in the real time data monitoring phase I trend of high torque was detected and was suggested to use the lubricant to reduce the increasing tendency of off bottom torque. The summary of observation in Sangu 11 is listed below:

- Predict the high Torque in simulation phase.
- Identify the increasing trend of Torque in monitoring phase.
- Identify that the non rotating protectors were not working in the case of 8.5'' section whether they reduce the Torque in 12.25'' section.
- Addition of lubricant (which was planned after analyzing the simulation) in the active system significantly helped in reducing the Torque as well drag.

References

Bernt S, Aadnoy; Iain Cooper; Stefan Z. Miska; Robert F. Mitchell and Michael L. Payne. " Advanced Drilling and Well Technology".SPE (2009),

Bernt S. Aadnoy. (2006) , ''Mechanics of drilling"

Mesfin Belayneh.(2006), " A review of Buckling in Oil Wells"

Mitchell R.F., Robello Samuel . " How good is the Torque/Drag model", SPE drilling and Completion , March, 2009. SPE/IADC 105068.

Robello Samuel, Halliburton (2010). "Friction Factors: What are they for Torque , Drag, Vibration, Bottom Hole Assembly and Transient Surge/Swab Analysis." IADC/SPE-128059, Drilling Conference and Exhibition, Louisiana, February 2010.

Bhalla, K., Walton, I.C., Schlumberger Dowell// The Effect of Fluid Flow on Coiled Tubing Reach// Journal SPE Production & Facilities February 1998. Society of Petroleum Engineers SPE 36464-PA

Aadnoy, B.S., Fazaelizadeh, M., Hareland, G. "A 3-Dimensional Analytica Model for Wellbore Friction", Journal of Canadian Petroleum Technology, 2010.

Aadnoy,B.S., Aasen,Jan A. "Three-dimensional well tubular design improves margins in critical well",journals of Petroleum Science and Engineering(2006),

Mirhaj, S.A., Fazaelizadeh, M., Kaarstad, E., Aadnoy, B.S. "New Aspects of Torque and Drag Modelling in Extended Reach Wells", SPE 135719, SPE Annual Technical Conference and Exhibition, Florence, Italy, September 2010.

Johancsik, C.A., Friesen, D.B., Dawson, R. Torque and Drag in Directional Wells -Prediction and Measurement. June 1984

Fazaelizadeh, M., Hareland, G., Aadnoy, B.S. "Application of New 3-D Analytical Model for Directional Wellbore Friction", Journal of Modern Applied Science, Vol. 4, No. 2, 2010

Cayeux, E., Daireaux, B., "Early Detection of Drilling Condition Deterioration Using Real Time Calibration of Computer Models: Field Example from North Sea Drilling Operations" SPE/IADC 119435, Drilling and Conference Exhibition, Amsterdam, The Netherlands, March, 2009.

Maidla, E.E., Wojtanowicz, A.K., "Field method of assessing borehole friction for directional well casing" SPE Middle East Oil Show, Manama, Bahrain, March, 1987.

Mirhaj, S.A., Kårstad, E., Aadnoy, B.S., "Minimizing Friction in Shallow Horizontal Wells", SPE 135812, IADC/SPE Asia Pacific Drilling Technology Conference and Exhibition, Ho Chi Minh City, Vietnam, November 2010.

Brett, J.F., Beckett, A.D., Holt, C.A., Smith, D.L., "Uses and Limitations of Drillstring Tension and Torque Models for Monitoring Hole Conditions", SPE Drilling Engineering, September 1989

Sakhalinproject/ http://www.ordons.com/asia/far-east/9976-sakhalin-1-project-drills-worlds-longest-extended-reach-well.html

Maersk project/ http://www.drillingcontractor.org/continuous-improvements-lead-to-maersk-oil-qatars-longest-horizontal-well-in-the-world-1924

Appendix

A. Survey data

Table 17: A1 Real Time survey data of South sangu 4

MD (m)	INC (°)	AZ (°)	TVD (m)	DLS (°/30m)	AbsTort (°/30m)	RelTort (°/30m)	VSect (m)	North (m)	East (m)
0	0	67.73	0	0	0	0	0	0	0
178.12	0.1	298	178.12	0.017	0.017	0	-0.1	0.07	-0.14
206.65	0.06	309.93	206.65	0.045	0.021	0	-0.12	0.09	-0.17
234.97	0.18	249.32	234.97	0.169	0.039	0	-0.17	0.09	-0.22
263.87	0.31	153.14	263.87	0.389	0.077	0	-0.21	0	-0.23
318.57	0.15	117.22	318.57	0.114	0.083	0	-0.15	-0.16	-0.1
346.96	0.06	222.3	346.96	0.185	0.092	0	-0.14	-0.19	-0.08
375.8	0.13	197.58	375.8	0.083	0.091	0	-0.18	-0.23	-0.1
403.91	0.15	167.42	403.91	0.08	0.09	0	-0.2	-0.3	-0.1
426.13	0.23	185.68	426.13	0.134	0.093	0	-0.23	-0.37	-0.1
460.68	0.32	176.78	460.68	0.086	0.092	0	-0.29	-0.54	-0.1
547.72	0.72	186.62	547.71	0.141	0.1	0	-0.64	-1.32	-0.15
576.56	0.93	177.96	576.55	0.253	0.108	0	-0.81	-1.74	-0.16
605.72	1.22	185.23	605.71	0.329	0.118	0	-1.03	-2.28	-0.18
634.38	1.41	184.71	634.36	0.199	0.122	0	-1.33	-2.94	-0.24
663.07	1.71	188.92	663.04	0.336	0.131	0	-1.71	-3.71	-0.33
692	1.99	186.52	691.95	0.301	0.138	0	-2.18	-4.64	-0.46
721.36	2.11	184.49	721.29	0.143	0.138	0	-2.67	-5.68	-0.56
749.99	2.04	180.63	749.91	0.164	0.139	0	-3.1	-6.72	-0.6
778.77	2.56	181.46	778.66	0.543	0.154	0	-3.56	-7.87	-0.63
806.64	2.68	180.81	806.5	0.133	0.154	0	-4.07	-9.15	-0.65
832.71	2.8	181.89	832.54	0.15	0.153	0	-4.57	-10.39	-0.68
861.25	2.81	181.18	861.05	0.038	0.15	0	-5.13	-11.79	-0.72
889.46	2.89	178.95	889.22	0.145	0.15	0	-5.66	-13.19	-0.72
946.23	3.32	181.26	945.91	0.237	0.155	0	-6.84	-16.27	-0.73
974.05	3.26	180.69	973.68	0.074	0.152	0	-7.47	-17.86	-0.76
1003.09	3.29	180.87	1002.68	0.033	0.149	0	-8.12	-19.52	-0.78
1032.32	3.24	181.77	1031.86	0.073	0.147	0	-8.78	-21.19	-0.82
1061.09	3.13	181.71	1060.59	0.115	0.146	0	-9.43	-22.78	-0.87
1089.8	3.22	179.61	1089.25	0.154	0.146	0	-10.05	-24.37	-0.88
1118.81	3.28	178.28	1118.21	0.1	0.145	0	-10.65	-26.02	-0.85
1147.3	3.42	178.59	1146.66	0.149	0.145	0	-11.24	-27.68	-0.81
1174.22	3.28	178.41	1173.53	0.156	0.145	0	-11.8	-29.25	-0.77
1203.29	3.18	179.06	1202.55	0.11	0.144	0	-12.38	-30.89	-0.73
1228.37	3.09	181.55	1227.6	0.195	0.145	0	-12.91	-32.26	-0.74
1254.88	2.9	179.33	1254.07	0.252	0.148	0	-13.44	-33.65	-0.75
1283.46	1.98	177.08	1282.62	0.971	0.166	0	-13.87	-34.86	-0.71
1339.8	0.41	144.38	1338.95	0.879	0.196	0	-14.15	-36	-0.55
1371.6	1.64	77.68	1370.75	1.439	0.225	0	-13.67	-35.99	-0.04
1397.54	4.25	68.48	1396.65	3.058	0.277	0	-12.35	-35.56	1.22
1425.54	5.5	66.47	1424.55	1.352	0.299	0	-9.97	-34.65	3.42

1455.11	5.47	65.41	1453.98	0.107	0.295	0	-7.14	-33.49	6
1483.82	8.2	72.15	1482.49	2.968	0.346	0	-3.73	-32.3	9.19
1510.93	9.73	68.56	1509.26	1.802	0.372	0	0.48	-30.87	13.16
1539.65	11.25	66.96	1537.5	1.616	0.396	0	5.71	-28.88	18
1571.17	13.44	69.7	1568.29	2.157	0.431	0	12.45	-26.41	24.27
1603.83	15.99	68.19	1599.88	2.368	0.47	0	20.74	-23.42	32
1628	17.94	66.03	1623	2.543	0.501	0	27.79	-20.67	38.5
1657.04	20.73	65.21	1650.4	2.896	0.543	0	37.4	-16.7	47.25
1673.5	21.77	65.44	1665.74	1.902	0.557	0	43.36	-14.21	52.67
1697.88	24.38	66.48	1688.16	3.25	0.595	0	52.91	-10.32	61.4
1721.73	26.55	66.19	1709.7	2.734	0.625	0	63.16	-6.2	70.79
1749.93	26.63	66.19	1734.91	0.085	0.616	0	75.78	-1.11	82.34
1782.24	26.74	62.77	1763.78	1.43	0.631	0	90.26	5.14	95.43
1810	26.38	62.89	1788.61	0.393	0.627	0	102.63	10.81	106.47
1836.87	25.79	63.01	1812.75	0.662	0.628	0	114.4	16.18	116.99
1865.55	25.47	63.45	1838.6	0.389	0.624	0	126.77	21.77	128.07
1893.61	25.15	63.59	1863.97	0.348	0.62	0	138.73	27.12	138.81
1920.54	24.98	64.19	1888.36	0.341	0.616	0	150.11	32.14	149.05
1949.85	25.72	64.27	1914.85	0.758	0.618	0	162.64	37.6	160.35
1977.6	26.43	65.34	1939.78	0.921	0.622	0	174.82	42.79	171.39
2006.28	26.64	65.78	1965.44	0.301	0.618	0	187.62	48.09	183.05
2035.86	26.22	67.7	1991.93	0.966	0.623	0	200.79	53.29	195.15
2064.79	26.23	67.67	2017.88	0.017	0.614	0	213.57	58.14	206.97
2091.13	25.74	68	2041.55	0.582	0.614	0	225.11	62.5	217.66
2119.41	25.33	68.18	2067.07	0.443	0.612	0	237.3	67.05	228.97
2150.93	24.73	68.13	2095.63	0.571	0.611	0	250.64	72.01	241.35
2179.6	24.53	68.98	2121.69	0.426	0.609	0	262.58	76.38	252.47
2208.06	23.62	68.32	2147.68	1	0.614	0	274.19	80.6	263.28
2227.36	23.69	68.09	2165.36	0.18	0.61	0	281.93	83.48	270.47
2255.55	24.53	68.31	2191.09	0.899	0.614	0	293.45	87.75	281.16
2283.22	25.89	67.26	2216.12	1.552	0.625	0	305.23	92.21	292.07
2312.15	27.11	66.96	2242.01	1.273	0.633	0	318.14	97.23	303.97
2341.4	27.72	66.36	2267.98	0.687	0.634	0	331.61	102.57	316.33
2372.85	28.19	65.79	2295.76	0.516	0.632	0	346.34	108.55	329.81
2397.62	27.61	66.06	2317.65	0.719	0.633	0	357.93	113.28	340.39
2428.6	27.9	65.66	2345.06	0.334	0.629	0	372.35	119.18	353.55
2454.3	28.21	65.41	2367.74	0.387	0.627	0	384.43	124.18	364.56
2485.56	28.71	64.98	2395.23	0.519	0.625	0	399.31	130.43	378.08
2514.03	29.33	64.88	2420.12	0.655	0.626	0	413.1	136.29	390.59
2539.73	29.54	64.86	2442.5	0.245	0.622	0	425.72	141.65	402.02
2568.09	29.43	63.48	2467.19	0.728	0.623	0	439.65	147.73	414.59
2596.06	28.66	64.83	2491.64	1.085	0.628	0	453.2	153.65	426.81
2624.36	29.23	64.27	2516.41	0.669	0.628	0	466.87	159.54	439.17
2652.71	28.52	64.76	2541.23	0.792	0.63	0	480.54	165.43	451.53
2681.46	28.81	64.82	2566.46	0.304	0.627	0	494.32	171.3	464.01
2709.49	28.76	46.95	2591.07	9.181	0.715	0	507.39	178.79	475.07
2738.84	28.09	64.81	2616.93	8.689	0.801	0	520.92	186.57	486.5
2770.93	27.59	64.58	2645.31	0.478	0.797	0	535.88	192.97	500.05
2795.08	27.13	64.17	2666.75	0.618	0.795	0	546.96	197.77	510.06
2823.66	26.96	63.84	2692.21	0.238	0.79	0	559.93	203.47	521.74
2854.68	25.68	63.24	2720.01	1.264	0.795	0	573.65	209.6	534.05
2860.77	25.43	63.12	2725.51	1.258	0.796	0	576.26	210.78	536.39

2888.46	23.77	63	2750.68	1.799	0.806	0	587.75	216	546.67
2910.79	22.36	62.4	2771.23	1.92	0.814	0	596.47	220.01	554.44
2939.64	22.33	64.24	2797.91	0.728	0.813	0	607.4	224.94	564.24
2967.46	23.25	56.05	2823.57	3.559	0.839	0	618.06	230.3	573.56
2996.81	25.18	67.26	2850.35	5.088	0.881	0	629.98	235.96	584.13
3024.89	26.74	66.35	2875.59	1.72	0.888	0	642.27	240.8	595.43
3054.37	26.39	69.8	2901.96	1.61	0.895	0	655.45	245.72	607.65
3082.47	26.8	70.64	2927.09	0.594	0.893	0	668.02	249.98	619.49
3109.56	25.97	70.79	2951.36	0.922	0.893	0	680.04	253.95	630.85
3137.74	27.16	66.41	2976.56	2.439	0.907	0	692.63	258.56	642.58
3167.35	27	66.47	3002.93	0.164	0.9	0	706.11	263.95	654.93
3169.4	28.36	68.64	3004.74	24.771	0.915	0	707.06	264.31	655.81
3224.01	29.49	64.84	3052.54	1.185	0.92	0	733.46	274.75	680.06
3252.9	29.19	65.49	3077.73	0.454	0.916	0	747.6	280.7	692.91
3281.48	33.1	69.66	3102.19	4.685	0.948	0	762.37	286.3	706.57
3310.09	36.13	69.25	3125.73	3.187	0.968	0	778.61	292.01	721.79
3338.8	35.22	67.54	3149.05	1.411	0.972	0	795.35	298.17	737.35
3365.94	34.45	64.7	3171.33	1.985	0.98	0	810.84	304.44	751.53
3395.66	31.91	62.37	3196.2	2.868	0.996	0	827.06	311.68	766.09
3427.66	31.2	63.1	3223.47	0.756	0.994	0	843.74	319.35	780.97

B. Hook Load data of South Sangu 4

B.1 Simulated and Real time Tripping in data for 12.25" section (Cased Hole)

Table 18:B1Simulated and Real time data for Cased hole 12.25" section (Tripping in)

Simulated data of 12.25 inches Cased hole section				Real Time data	
Run Measured Depth(m)	Tripping in CHFF 0.2 HKLD (KN)	Tripping in CHFF 0.3 HKLD (KN)	Tripping in CHFF 0.4 HKLD (KN)	Real time depth (m)	Real time HKLD (KN)
0	0	0	0	0	0
50	173.93	173.93	173.94	141	255.98
100	208.51	208.53	208.55	169.19	239.87
150	248.54	248.58	248.61	174.43	271.76
200	277.04	277.1	277.15	183.33	277.75
250	295.61	295.7	295.78	391.89	352.76
300	313.16	313.44	313.73	461.67	373.45
350	331.47	331.83	332.19	511.24	381.88
400	349.15	349.63	350.1	561.77	401.09
450	367.26	367.85	368.44	585.79	423.27
500	385.49	386.21	386.93	599.16	428.76
550	403.22	404.11	405	619.54	438.87
600	421.52	422.6	423.69	646.29	449.89
650	439.02	440.43	441.85	687.63	441.76
700	454.82	456.53	458.24	745.19	456.84
750	472.03	474.05	476.08	841.16	511.18
800	491.7	494.07	496.45	863.15	545.76
850	510.09	512.91	515.74	890.78	528.76
900	527.59	530.71	533.86	939.32	547.72
950	544.81	548.29	551.78	1010.91	611.17
1000	563.41	567.17	570.96	1089.64	601.15
1050	578.88	582.92	587	1117.13	608.85
1100	597.55	601.93	606.36	1242.82	649.86
1150	615.23	619.94	624.7	1246.84	656.43
1200	633.46	638.42	643.43		
1250	651.73	656.97	662.27		

B.2 Simulated and Real time Tripping in data for 12.25'' section (Open Hole)

Table 19: B2 Simulated and Real time data for open hole 12.25'' section (Tripping in)

Simulated data of 12.25 inches Open hole section				Real Time data			
Run Measured Depth(m)	Tripping in CHFF 0.2 HKLD (KN)	Tripping in CHFF 0.3 HKLD (KN)	Tripping in CHFF 0.4 HKLD (KN)	Real time depth(MD) (m)	Real time HKLD (KN)	Real time depth(MD) (m)	Real time HKLD (KN)
1250	649.94	649.94	649.94	1257.06	653.67	2058.26	819.92
1275	659.13	658.7	658.26	1267.48	657.84	2065.66	837.89
1300	668.69	667.79	666.89	1262.25	653.34	2073.91	825.21
1325	677.52	676.54	675.57	1256.71	652.87	2081.68	825.9
1350	686.65	685.57	684.5	1252.72	651.34	2110.94	835.34
1375	695.32	694.06	692.81	1254.66	652.79	2114.82	836.25
1400	702.58	700.8	699.02	1265.06	656.76	2119.78	842.23
1425	708.55	705.64	702.75	1290.22	664.34	2149.82	843.35
1450	715.88	711.99	708.16	1308.37	671.04	2155.26	844.3
1475	723.17	718.73	714.36	1322.30	676.44	2250.75	873.35
1500	730	725.09	720.26	1328.20	678.54	2254.99	866.74
1525	735.88	729.69	723.63	1337.72	681.43	2341.37	883.74
1550	742.21	735.23	728.41	1364.94	691.77	2344.89	893.36
1575	747.78	739.99	732.41	1373.76	696.08	2347.26	886.25
1600	752.88	744.29	735.96	1378.70	696.08	2393.75	894.15
1625	758.56	749.21	740.19	1413.40	703.45	2395.18	896.73
1650	763.35	753.11	743.25	1446.64	713.78	2423.81	902.34
1675	766.33	755.01	744.12	1457.18	716.89	2427.35	903.16
1700	769.7	757.41	745.6	1454.84	716.98	2476.49	911.71
1725	772.65	759.32	746.52	1464.38	718.67	2480.73	908.06
1750	775.22	760.82	747	1474.08	722.87	2503.91	911.07
1775	779.67	764.14	749.28	1480.20	724.98	2508.09	910.09
1800	783.92	767.2	751.32	1517.75	732.75	2521.44	912.76
1825	789.66	771.95	755.17	1517.42	733.43	2524.64	915.45
1850	794.78	775.87	758.12	1552.03	742.29	2557.97	920.63
1875	799.44	779.39	760.63	1565.01	746.79	2561.87	922.87
1900	803.93	782.72	762.99	1576.21	748.02	2573.72	925.09
1925	812.06	790.05	769.63	1580.35	749.08	2578.96	926.18
1950	817.59	794.89	773.85	1591.60	750.08	2599.89	900.66
1975	823.45	800.05	778.34	1612.65	754.89	2603.71	911.26
2000	829.68	805.63	783.33	1615.38	753.08	2609.67	912.74
2025	836.1	811.36	788.43	1624.78	757.09	2623.18	916.28

2050	842.35	816.87	793.26	1635.72	761.07	2626.99	918.23
2075	848.65	822.53	798.32	1649.81	764.65	2646.22	925.58
2100	855.59	828.83	804.04	1657.70	764.02	2650.50	925.97
2125	862.55	835.07	809.63	1672.41	756.84	2679.66	930.57
2150	868.67	840.52	814.48	1682.14	754.78	2679.66	930.57
2175	875.79	846.98	820.35	1686.91	755.84	2685.18	934.34
2200	883.04	853.5	826.22	1703.19	761.67	2685.18	934.34
2225	889.95	859.7	831.79	1730.19	763.89	2706.40	936.54
2250	896.78	865.85	837.3	1734.03	760.87	2709.14	936.88
2275	902.68	871.09	841.92	1743.69	759.88	2709.14	936.89
2300	908.43	876.13	846.32	1758.01	761.02	2747.02	945.58
2325	913.45	880.45	849.99	1766.98	763.38	2753.28	946.09
2350	917.95	884.32	853.26	1778.59	769.86	2758.44	946.59
2375	923.78	889.48	857.8	1802.77	781.65	2795.62	951.48
2400	929.93	894.92	862.57	1806.31	778.65	2801.20	952.67
2425	935.7	899.98	867	1814.92	771.04	2821.43	955.83
2450	941.29	904.92	871.36	1824.67	775.78	2821.43	954.98
2475	947	909.87	875.66	1824.67	773.34	2821.43	954.72
2500	952.77	915.01	880.21	1824.67	770.95	2817.98	953.21
2525	957.93	919.43	883.95	1824.67	771.89	2818.33	953.89
2550	962.66	923.53	887.46	1826.92	774.39	2825.49	956.74
2575	969.53	929.64	892.92	1836.52	772.98	2826.63	956.87
2600	975.78	935.18	897.82	1838.79	776.89	2848.87	962.34
2625	981.35	940.03	902.04	1838.63	773.06	2848.87	961.97
2650	987.39	945.41	906.82	1838.09	775.89	2848.87	961.89
2675	994.06	951.32	912.08	1840.66	774.78	2848.87	961.68
2700	1000.11	956.72	916.88	1842.09	789.87	2848.87	961.88
2725	1005.59	961.43	920.96	1855.00	775.65	2848.87	961.98
2750	1010.72	965.27	923.85	1855.00	778.89	2848.87	962.65
2775	1015.53	968.8	926.38	1868.19	781.35	2848.87	961.87
2800	1021.35	973.75	930.62	1869.74	776.76	2848.87	961.76
2825	1027.15	978.74	934.96	1871.04	778.01	2848.87	962.54
2850	1033.4	983.91	939.02	1909.20	784.56	2848.87	963.06
				1913.12	798.98	2848.87	961.76
				2000.20	811.09	2848.87	962.54
				2006.46	806.66	2848.87	963.06

B.3 Simulated and Real time Tripping out data for 12.25'' section (Cased Hole)

Table 20: B3 Simulated and Real time data for cased hole 12.25'' section (Tripping out)

Simulated data of 12.25 inches Cased hole section				Real Time data	
Run Measured Depth(m)	Tripping out CHFF 0.2 HKLD (KN)	Tripping out CHFF 0.3 HKLD (KN)	Tripping out CHFF 0.4 HKLD (KN)	Real time depth (m)	Tripping out Real time HKLD (KN)
0	0	0	0	0	0
50	174.73	174.74	174.74	141	283.79
100	209.33	209.35	209.37	169.19	255
150	249.38	249.41	249.45	174.43	280
200	277.9	277.95	278	183.33	284
250	296.5	296.58	296.67	391.89	366.08
300	314.24	314.53	314.82	461.67	378
350	332.63	332.99	333.36	511.24	393
400	350.43	350.9	351.38	561.77	434.59
450	368.65	369.24	369.83	585.79	410
500	387.01	387.73	388.46	599.16	435
550	404.91	405.8	406.69	619.54	468.75
600	423.4	424.49	425.58	646.29	469.89
650	442.93	444.35	445.78	687.63	488.84
700	459.03	460.74	462.46	745.19	501.11
750	476.55	478.58	480.62	841.16	543.21
800	496.57	498.95	501.34	863.15	550.76
850	515.41	518.24	521.1	890.78	553.21
900	533.21	536.36	539.54	939.32	559.64
950	550.79	554.28	557.81	1010.91	593.42
1000	569.67	573.46	577.29	1089.64	636.65
1050	587.72	591.8	595.91	1117.13	642.87
1100	606.73	611.16	615.62	1242.82	685.87
1150	624.74	629.5	634.31	1246.84	698.89
1200	643.22	648.23	653.3		
1250	661.77	667.07	672.42		

B.4 Simulated and Real time Tripping out data for 12.25'' section (Open Hole)

Table 21: B.4 Simulated and Real time data for open hole 12.25'' section (Tripping out)

Simulated data of 12.25'' Open hole section				Real Time data			
Run Measured Depth(m)	Tripping out CHFF 0.2 HKLD (KN)	Tripping out CHFF 0.3 HKLD (KN)	Tripping out CHFF 0.4 HKLD (KN)	Real time depth(MD) (m)	Tripping out Real time HKLD (KN)	Real time depth(MD) (m)	Tripping out Real time HKLD (KN)
1250	672.42	672.42	672.42	700.56	1286.96	1312.67	2484.66
1300	691.17	692.13	693.08	706.78	1296.80	1318.87	2491.37
1350	710.29	711.44	712.59	723.56	1333.14	1345.56	2582.06
1400	729.29	731.22	733.16	736.37	1373.95	1376.66	2611.95
1450	752.29	756.67	761.13	753.00	1446.76	1405.19	2696.80
1500	771.69	777.29	782.99	760.67	1446.82	1412.31	2701.59
1550	794.34	802.68	811.23	781.54	1482.38	1418.09	2703.75
1600	812.99	823.51	834.37	789.87	1512.44	1419.87	2731.91
1650	832.43	845.44	858.97	813.43	1566.81	1426.99	2736.90
1700	849.47	865.7	882.74	816.67	1572.04	1427.88	2761.44
1750	865.7	885.05	905.52	826.65	1621.78	1435.89	2772.45
1800	887.27	910.59	935.44	857.79	1676.94	1442.65	2782.67
1850	911.35	938.94	968.46	886.75	1763.39	1453.87	2797.82
1900	934.24	966.12	1000.37	901.45	1769.67		
1950	957.66	992.38	1029.8	911.38	1792.03		
2000	977.04	1013.81	1053.43	916.67	1819.68		
2050	997.38	1036.42	1078.52	932.22	1856.95		
2100	1018.32	1059.45	1103.82	965.26	1899.58		
2150	1040.09	1083.7	1130.82	968.56	1933.47		
2200	1062.59	1108.66	1158.53	999.56	1994.71		
2250	1084.68	1133.18	1185.77	1032.56	2021.51		
2300	1103.62	1154.24	1209.14	1088.84	2149.55		
2350	1120.64	1173.22	1230.24	1101.98	2234.73		
2400	1140.13	1194.89	1254.24	1109.98	2234.74		
2450	1159.77	1217.18	1279.58	1115.87	2234.85		
2500	1180.9	1241.52	1307.64	1109.83	2234.85		
2550	1199.42	1262.56	1331.47	1116.95	2235.04		
2600	1220.66	1286.44	1358.29	1132.07	2305.38		
2650	1240.79	1309.24	1384.07	1177.00	2350.94		
2700	1262.86	1334.05	1411.96	1233.05	2410.75		
2750	1289.53	1366.95	1452.38	1237.94	2438.42		
2800	1315.79	1399.38	1492.29	1265.52	2451.76		
2850	1339.57	1426.92	1524.16	1289.54	2472.58		

B.5 Simulated and Real time Tripping in data for 8.5'' section (Open Hole)

Table 22: B.5 Simulated and Real time data for open hole 8.5'' section (Tripping in)

Simulated data of 8.5'' Open hole section (Tripping in)				Corrected Simulated data			Real Time data			
Run Measured Depth(m)	Tripping in OHFF 0.2 HKLD (KN)	Tripping in OHFF 0.3 HKLD (KN)	Tripping in OHFF 0.4 HKLD (KN)	Tripping in OHFF 0.2 HKLD (KN)	Tripping in OHFF 0.3 HKLD (KN)	Tripping in OHFF 0.4 HKLD (KN)	Real time depth (m)	Tripping in Real time HKLD (KN)	Real time depth (m)	Tripping in Real time HKLD (KN)
2850	913.36	913.25	913.14	1003.36	1003.25	1003.14	2850	1003.72231	3150	1059.7145
2875	919.37	918.27	917.18	1009.37	1008.27	1007.18	2858	1002.39383	3158	1060.6619
2900	925.24	923.52	921.82	1015.24	1013.52	1011.82	2875	1001.66425	3170	1061.6637
2925	930.7	928.4	926.1	1020.7	1018.4	1016.1	2878	1005.37747	3175	1062.3171
2950	936.77	933.85	930.95	1026.77	1023.85	1020.95	2889	1007.84931	3188	1065.9105
2975	942.74	939.09	935.47	1032.74	1029.09	1025.47	2898	1009.28669	3203	1067.239
3000	947.94	943.65	939.39	1037.94	1033.65	1029.39	2902	1011.46453	3212	1069.7326
3025	952.91	947.87	942.87	1042.91	1037.87	1032.87	2925	1009.28669	3225	1069.3188
3050	959.36	953.68	948.06	1049.36	1043.68	1038.06	2932	1014.73128	3230	1069.9068
3075	965	958.72	952.5	1055	1048.72	1042.5	2940	1016.37555	3243	1069.3188
3100	969.62	962.94	956.33	1059.62	1052.94	1046.33	2950	1019.09785	3250	1070.9304
3125	974.6	967.58	960.66	1064.6	1057.58	1050.66	2959	1021.38458	3258	1072.444
3150	980.48	972.96	965.56	1070.48	1062.96	1055.56	2968	1021.49347	3273	1073.4131
3175	984.6	976.58	968.71	1074.6	1066.58	1058.71	2975	1023.67131	3278	1074.6436
3200	988.57	979.94	971.51	1078.57	1069.94	1061.51	2988	1027.26475	3288	1074.7634
3225	992.94	983.93	975.13	1082.94	1073.93	1065.13	2995	1033.12313	3300	1075.3514
3250	998.89	989.37	980.08	1088.89	1079.37	1070.08	3009	1034.56051	3313	1076.7997
3275	1003.18	993.09	983.27	1093.18	1083.09	1073.27	3021	1035.81276	3320	1075.8305
3300	1006.66	996.1	985.81	1096.66	1086.1	1075.81	3030	1040.17933	3328	1077.9648
3325	1010.71	999.85	989.24	1100.71	1089.85	1079.24	3045	1041.83449	3340	1079.5329
3350	1015.32	1003.86	992.69	1105.32	1093.86	1082.69	3050	1046.21194	3350	1080.7089
3375.01	1018.52	1006.45	994.73	1108.52	1096.45	1084.73	3058	1047.1593	3365	1080.9376
3400.01	1022.22	1009.76	997.69	1112.22	1099.76	1087.69	3075	1050.0885	3370	1081.7869
3425.01	1028.17	1015.25	1002.73	1118.17	1105.25	1092.73	3080	1050.56762	3383	1082.9956
3450.01	1032.48	1019.01	1005.98	1122.48	1109.01	1095.98	3088	1051.63476	3388	1085.1735
							3103	1051.27542	3398	1084.3895
							3115	1052.41878	3403	1085.413
							3120	1052.74546	3418	1079.7289
							3133	1054.9233	3425	1078.1173
							3143	1058.28806	3438	1076.9957

B.6 Simulated and Real time Tripping out data for 8.5'' section (Open Hole)

Table 23: B.6 Simulated and Real time data for open hole 8.5'' section (Tripping out)

Simulated data of 8.5" Open hole section (Tripping out)				Corrected Simulated data			Real Time data Tripping out data			
Run Measured Depth(m)	Tripping out OHFF 0.2 HKLD (KN)	Tripping out OHFF 0.3 HKLD (KN)	Tripping out OHFF 0.4 HKLD (KN)	Tripping out OHFF 0.2 HKLD (KN)	Tripping out OHFF 0.3 HKLD (KN)	Tripping out OHFF 0.4 HKLD (KN)	Real time depth (m)	Tripping out Real time HKLD (KN)	Real time depth (m)	Tripping out Real time HKLD (KN)
2850	1139.46	1139.62	1139.79	1254.46	1254.62	1254.79	2851	1242.23	3152	1402.39
2875	1150.89	1152.56	1154.22	1265.89	1267.56	1269.22	2860	1247.76	3160	1407.17
2900	1161.93	1164.58	1167.24	1276.93	1279.58	1282.24	2872	1255.93	3172	1413.18
2925	1174.90	1178.56	1182.25	1289.90	1293.56	1297.25	2880	1261.88	3180	1421.65
2950	1187.19	1191.86	1196.57	1302.19	1306.86	1311.57	2891	1266.73	3190	1424.65
2975	1198.50	1204.32	1210.19	1313.50	1319.32	1325.19	2900	1270.63	3205	1428.10
3000	1209.56	1216.47	1223.45	1324.56	1331.47	1338.45	2910	1276.44	3214	1441.04
3025	1221.24	1229.46	1237.76	1336.24	1344.46	1352.76	2922	1281.42	3229	1454.32
3050	1231.86	1241.09	1250.42	1346.86	1356.09	1365.42	2934	1286.50	3232	1461.72
3075	1241.67	1251.91	1262.30	1356.67	1366.91	1377.30	2942	1294.56	3245	1465.08
3100	1253.09	1264.25	1275.59	1368.09	1379.25	1390.59	2950	1299.60	3250	1471.30
3125	1265.03	1276.94	1289.07	1380.03	1391.94	1404.07	2961	1300.66	3260	1482.34
3150	1274.57	1287.34	1300.38	1389.57	1402.34	1415.38	2970	1307.19	3275	1490.55
3175	1284.89	1298.76	1312.96	1399.89	1413.76	1427.96	2981	1322.68	3280	1495.94
3200	1297.44	1312.79	1328.58	1412.44	1427.79	1443.58	2990	1324.87	3290	1500.47
3225	1309.47	1325.67	1342.35	1424.47	1440.67	1457.35	3000	1326.08	3305	1503.66
3250	1318.68	1335.78	1353.46	1433.68	1450.78	1468.46	3011	1331.25	3315	1507.57
3275	1329.40	1347.90	1367.10	1444.40	1462.90	1482.10	3023	1340.98	3322	1512.33
3300	1339.44	1358.86	1378.99	1454.44	1473.86	1493.99	3032	1349.03	3332	1515.75
3325	1348.82	1368.75	1389.40	1463.82	1483.75	1504.40	3047	1352.74	3342	1522.54
3350	1356.92	1378.03	1399.98	1471.92	1493.03	1514.98	3052	1353.64	3351	1526.10
3375	1367.26	1389.86	1413.43	1482.26	1504.86	1528.43	3060	1357.14	3364	1534.11
3400	1380.67	1404.59	1429.59	1495.67	1519.59	1544.59	3071	1359.80	3372	1536.76
3425	1389.70	1414.44	1440.39	1504.70	1529.44	1555.39	3082	1364.79	3385	1548.27
3450	1400.58	1426.77	1454.32	1515.58	1541.77	1569.32	3090	1373.95	3390	1555.92
							3105	1378.20	3400	1570.95
							3111	1384.70	3405	1577.58
							3122	1391.48	3420	1591.28
							3135	1398.40	3425	1609.52
							3145	1401.09	3440	1620.60

C. Simulated data of Sangu 11

C.1 All simulated Hook Load data of 12.25'' section of Sangu 11 (All operation)

Table 24: C.1 Simulated Hook Load data of 12.25'' section of Sangu 11 (all operation)

Simulated data									
MD (m RT)	Predicted Tripping in Wt (FF = 0.4)	Predicted Tripping in Wt (FF = 0.35)	Predicted Tripping in Wt (FF = 0.30)	Predicted Tripping in Wt (FF = 0.2)	Predicted Free Rot Wt	Predicted Tripping out Wt (FF = 0.2)	Predicted Tripping out Wt (FF = 0.3)	Predicted Tripping out Wt (FF = 0.35)	Predicted Tripping out Wt (FF = 0.4)
0.00	75.01	75.01	75.01	75.01	75.01	75.01	75.01	75.01	75.01
30.00	87.34	87.35	87.36	87.36	87.37	87.39	87.39	87.40	87.40
60.00	99.59	99.60	99.60	99.61	99.61	99.62	99.63	99.63	99.64
90.00	112.38	112.39	112.39	112.40	112.42	112.43	112.44	112.45	112.45
120.00	118.33	118.36	118.40	118.43	118.50	118.57	118.60	118.63	118.67
150.00	120.71	120.78	120.84	120.91	121.04	121.17	121.24	121.30	121.37
180.00	122.94	123.03	123.12	123.21	123.39	123.57	123.66	123.75	123.84
210.00	125.19	125.30	125.41	125.52	125.74	125.96	126.07	126.18	126.29
240.00	127.06	127.26	127.47	127.67	128.08	128.48	128.69	128.89	129.09
270.00	129.18	129.42	129.66	129.90	130.39	130.88	131.13	131.38	131.62
300.00	130.76	131.14	131.53	131.91	132.69	133.47	133.86	134.25	134.64
330.00	132.33	132.85	133.37	133.89	134.95	136.02	136.55	137.09	137.64
360.00	133.43	134.17	134.92	135.66	137.17	138.71	139.48	140.26	141.05
390.00	135.10	135.93	136.76	137.61	139.32	141.06	141.95	142.84	143.75
420.00	136.01	137.07	138.13	139.21	141.42	143.68	144.84	146.01	147.19
450.00	136.91	138.17	139.46	140.77	143.48	146.28	147.73	149.20	150.71
480.00	137.44	138.97	140.55	142.17	145.53	149.07	150.91	152.81	154.75
510.00	138.58	140.27	142.01	143.79	147.50	151.41	153.44	155.53	157.67
540.00	139.56	141.42	143.33	145.30	149.41	153.76	156.02	158.37	160.78
570.00	140.53	142.54	144.61	146.74	151.19	155.92	158.38	160.94	163.57
600.00	141.20	143.38	145.64	147.98	152.92	158.22	161.03	163.94	166.96
630.00	141.62	144.02	146.50	149.08	154.54	160.42	163.55	166.81	170.20
660.00	142.39	144.89	147.50	150.23	156.06	162.44	165.87	169.45	173.19
690.00	143.56	146.15	148.87	151.71	157.84	164.58	168.22	172.03	176.03
720.00	144.12	146.95	149.93	153.07	159.91	167.58	171.78	176.25	180.99
750.00	145.42	148.34	151.46	154.79	162.17	170.65	175.35	180.38	185.77
780.00	146.42	149.51	152.81	156.36	164.26	173.40	178.49	183.96	189.88
810.00	147.25	150.47	153.95	157.67	165.97	175.55	180.88	186.60	192.77
840.00	148.04	151.40	154.99	158.85	167.42	177.26	182.73	188.57	194.87
870.00	148.31	151.86	155.68	159.75	168.80	179.19	184.95	191.13	197.81
900.00	148.43	152.16	156.19	160.50	170.10	181.21	187.40	194.06	201.28
930.00	148.84	152.70	156.83	161.27	171.16	182.62	189.04	195.99	203.57
960.00	148.93	152.96	157.25	161.84	172.10	184.09	190.84	198.20	206.19
990.00	149.10	153.30	157.74	162.49	173.07	185.40	192.33	199.85	208.05
1020.00	149.15	153.56	158.23	163.20	174.32	187.48	195.02	203.32	212.42
1050.00	149.79	154.30	159.05	164.14	175.67	189.54	197.57	206.44	216.24

1080.00	150.18	154.87	159.80	165.10	177.13	191.66	200.10	209.43	219.75
1110.00	150.38	155.26	160.39	165.91	178.48	193.69	202.52	212.29	223.11
1140.00	150.72	155.75	161.04	166.72	179.68	195.38	204.49	214.57	225.73
1170.00	150.74	155.96	161.43	167.31	180.72	196.95	206.35	216.79	228.33
1200.00	150.57	156.00	161.67	167.74	181.59	198.35	208.06	218.84	230.77
1230.00	150.32	155.95	161.81	168.08	182.37	199.66	209.68	220.83	233.18
1260.00	149.90	155.77	161.83	168.30	183.01	200.81	211.13	222.61	235.34
1290.00	149.63	155.68	161.91	168.53	183.56	201.67	212.16	223.81	236.71
1320.00	149.27	155.55	161.99	168.82	184.28	202.94	213.74	225.77	239.09
1350.00	149.20	155.69	162.32	169.34	185.27	204.53	215.72	228.22	242.12
1380.00	149.44	156.09	162.89	170.11	186.51	206.41	218.04	231.00	245.52
1410.00	149.79	156.60	163.56	170.97	187.85	208.42	220.49	233.98	249.14
1440.00	150.15	157.11	164.23	171.84	189.21	210.43	222.92	236.92	252.66
1470.00	150.53	157.62	164.91	172.71	190.56	212.45	225.36	239.87	256.22
1500.00	150.88	158.12	165.58	173.58	191.92	214.47	227.82	242.83	259.79
1530.00	151.24	158.63	166.25	174.44	193.28	216.50	230.27	245.78	263.32
1560.00	151.60	159.13	166.92	175.30	194.63	218.53	232.74	248.78	266.98
1590.00	151.97	159.62	167.59	176.16	195.99	220.58	235.24	251.81	270.68
1620.00	152.32	160.12	168.25	177.02	197.34	222.63	237.74	254.86	274.39
1650.00	152.67	160.61	168.91	177.88	198.70	224.68	240.25	257.93	278.14
1680.00	153.01	161.09	169.57	178.73	200.05	226.74	242.77	261.03	281.91
1710.00	153.34	161.58	170.23	179.59	201.41	228.81	245.31	264.14	285.78
1740.00	153.70	162.06	170.88	180.44	202.76	230.88	247.86	267.27	289.58
1770.00	154.01	162.55	171.53	181.29	204.12	232.95	250.42	270.42	293.47
1800.00	154.37	163.03	172.18	182.14	205.47	235.03	252.99	273.58	297.37
1830.00	154.70	163.51	172.83	182.99	206.83	237.12	255.57	276.79	301.29
1860.00	155.03	163.98	173.48	183.83	208.18	239.22	258.16	280.01	305.21
1890.00	155.36	164.46	174.12	184.68	209.54	241.31	260.77	283.23	309.15
1920.00	155.69	164.94	174.77	185.52	210.89	243.42	263.39	286.46	313.20
1950.00	156.02	165.41	175.41	186.36	212.25	245.53	266.03	289.70	317.17
1980.00	156.34	165.88	176.05	187.20	213.60	247.65	268.67	292.95	321.14
2010.00	156.66	166.35	176.69	188.04	214.96	249.79	271.31	296.20	325.11
2040.00	156.99	166.82	177.33	188.87	216.31	251.92	273.96	299.46	329.10
2070.00	157.31	167.29	177.97	189.71	217.67	254.04	276.61	302.72	333.09
2100.00	157.62	167.76	178.61	190.54	219.02	256.18	279.26	305.99	337.09
2130.00	157.94	168.22	179.24	191.37	220.38	258.32	281.92	309.26	341.09
2160.00	158.26	168.68	179.87	192.20	221.74	260.46	284.59	312.54	345.10
2190.00	158.57	169.14	180.50	193.03	223.09	262.61	287.25	315.82	349.12
2220.00	158.88	169.60	181.13	193.85	224.45	264.76	289.92	319.10	353.14
2250.00	159.19	170.05	181.76	194.68	225.80	266.91	292.59	322.39	357.17
2280.00	159.51	170.51	182.39	195.50	227.16	269.06	295.26	325.68	361.20
2310.00	159.81	170.97	183.01	196.32	228.51	271.21	297.94	328.98	365.23
2340.00	160.12	171.42	183.64	197.14	229.87	273.36	300.62	332.28	369.28
2370.00	160.43	171.88	184.26	197.96	231.22	275.52	303.30	335.58	373.33
2400.00	160.74	172.33	184.88	198.78	232.58	277.68	305.98	338.88	377.38
2430.00	161.05	172.78	185.50	199.60	233.93	279.84	308.66	342.19	381.43
2460.00	161.35	173.23	186.12	200.41	235.29	281.99	311.35	345.50	385.26
2490.00	161.66	173.68	186.73	201.22	236.64	284.16	314.03	348.81	389.53
2520.00	161.96	174.13	187.35	202.04	238.00	286.32	316.72	352.13	393.59
2550.00	162.27	174.58	187.96	202.85	239.35	288.48	319.41	355.45	397.65
2580.00	162.57	175.03	188.57	203.66	240.71	290.69	322.10	358.77	401.72
2610.00	162.87	175.48	189.18	204.47	242.06	292.85	324.80	362.09	405.78

2640.00	163.18	175.92	189.79	205.28	243.42	294.97	327.49	365.42	409.86
2670.00	163.48	176.36	190.40	206.09	244.77	297.19	330.19	368.74	413.93
2700.00	163.78	176.81	191.01	206.89	246.13	299.31	332.89	372.06	418.01
2730.00	164.08	177.25	191.61	207.70	247.48	301.52	335.58	375.39	422.09
2760.00	164.38	177.69	192.22	208.50	248.84	303.69	338.29	378.72	426.17
2790.00	164.68	178.13	192.82	209.30	250.19	305.81	340.99	382.05	430.25
2820.00	164.97	178.57	193.43	210.10	251.55	307.98	343.69	385.38	434.34
2850.00	165.27	179.00	194.03	210.90	252.90	310.21	346.39	388.71	438.43
2880.00	165.56	179.44	194.63	211.70	254.26	312.38	349.09	392.05	442.51
2910.00	165.85	179.88	195.23	212.50	255.61	314.55	351.80	395.39	446.60
2940.00	166.04	180.31	195.83	213.34	256.97	316.67	354.51	398.73	450.69
2970.00	166.33	180.74	196.42	214.14	258.32	318.90	357.21	402.07	454.78
3000.00	166.62	181.18	197.02	214.89	259.68	321.02	359.92	405.41	458.88
3030.00	166.91	181.61	197.62	215.73	261.03	323.19	362.63	408.75	462.97
3060.00	167.19	182.04	198.21	216.52	262.39	325.36	365.34	412.10	467.07
3090.00	167.48	182.47	198.81	217.26	263.74	327.60	368.05	415.44	471.16
3120.00	167.77	182.90	199.40	218.04	265.10	329.72	370.76	418.78	475.26
3150.00	168.05	183.32	199.99	218.83	266.45	331.95	373.48	422.13	479.36
3180.00	168.34	183.75	200.58	219.62	267.81	334.13	376.19	425.48	483.46
3210.00	168.62	184.17	201.17	220.41	269.16	336.31	378.90	428.82	487.56
3240.00	169.20	184.84	201.97	221.37	270.61	338.40	381.50	431.96	491.32
3270.00	169.82	185.59	202.88	222.49	272.39	341.20	384.88	436.11	496.39
3300.00	170.76	186.63	204.08	223.92	274.53	344.35	388.82	440.92	502.27
3330.00	171.96	187.92	205.53	225.61	276.98	347.98	393.25	446.33	508.89
3360.00	173.23	189.30	207.07	227.40	279.55	351.79	397.91	452.01	515.84
3390.00	174.52	190.68	208.61	229.28	282.17	355.73	402.64	457.79	522.93
3420.00	175.79	192.06	210.16	231.10	284.81	359.57	407.43	463.66	530.12
3450.00	177.06	193.45	211.71	232.94	287.48	363.61	412.28	469.76	537.42
3480.00	178.32	194.73	213.27	234.78	290.16	367.52	417.18	475.78	544.82
3510.00	179.56	196.21	214.83	236.64	292.87	371.65	422.13	481.69	552.31

C.2 All simulated Hook Load data of 8.5" section of Sangu 11 (All operation)

Table 25: C.2 Simulated Hook Load data of 8.5" section of Sangu 11 (all operation)

Simulated Hook Loa data for 8.5 inches section									
MD (m RT)	Predicted Tripping in Wt (FF = 0.5)	Predicted Tripping in Wt (FF = 0.4)	Predicted Tripping in Wt (FF = 0.30)	Predicted Tripping in Wt (FF = 0.2)	Predicted Free Rot Wt	Predicted Tripping out Wt (FF = 0.2)	Predicted Tripping out Wt (FF = 0.3)	Predicted Tripping out Wt (FF = 0.4)	Predicted Tripping out Wt (FF = 0.5)
0.00	75.00	75.00	75.00	75.00	75.00	75.00	75.00	75.00	75.00
30.00	82.86	82.86	82.86	82.86	82.86	82.86	82.86	82.86	82.86
60.00	90.08	90.08	90.08	90.08	90.08	90.08	90.08	90.08	90.08
90.00	95.03	95.04	95.05	95.06	95.08	95.10	95.11	95.11	95.12
120.00	100.02	100.03	100.04	100.05	100.08	100.10	100.11	100.12	100.13
150.00	105.55	105.58	105.61	105.64	105.69	105.74	105.77	105.80	105.82
180.00	111.15	111.19	111.23	111.27	111.35	111.43	111.47	111.51	111.55
210.00	114.57	114.62	114.68	114.73	114.84	114.95	115.00	115.06	115.11
240.00	116.64	116.74	116.85	116.95	117.15	117.36	117.46	117.56	117.67
270.00	118.77	118.90	119.04	119.18	119.45	119.73	119.87	120.01	120.14
300.00	120.60	120.83	121.05	121.28	121.74	122.21	122.45	122.69	122.93
330.00	122.62	122.90	123.17	123.45	124.01	124.58	124.87	125.16	125.45
360.00	124.34	124.72	125.10	125.48	126.26	127.05	127.45	127.85	128.26
390.00	126.24	126.67	127.11	127.55	128.44	129.35	129.81	130.28	130.75
420.00	127.71	128.27	128.84	129.42	130.60	131.81	132.43	133.06	133.70
450.00	129.24	129.92	130.61	131.31	132.74	134.22	134.97	135.74	136.53
480.00	130.28	131.16	132.06	132.97	134.84	136.79	137.79	138.81	139.85
510.00	131.60	132.62	133.66	134.72	136.88	139.14	140.30	141.49	142.70
540.00	132.33	133.59	134.87	136.17	138.87	141.67	143.12	144.60	146.11
570.00	133.28	134.72	136.19	137.70	140.79	144.02	145.67	147.37	149.10
600.00	134.43	136.02	137.63	139.28	142.66	146.18	147.99	149.85	151.74
630.00	135.32	137.07	138.86	140.69	144.46	148.40	150.45	152.53	154.67
660.00	136.36	138.22	140.12	142.08	146.16	150.46	152.71	155.03	157.41
690.00	137.32	139.33	141.40	143.53	148.00	152.76	155.26	157.84	160.49
720.00	138.33	140.50	142.75	145.08	150.04	155.42	158.28	161.26	164.36
750.00	139.38	141.68	144.09	146.61	152.02	157.98	161.19	164.55	168.07
780.00	140.35	142.79	145.36	148.06	153.90	160.39	163.91	167.61	171.53
810.00	141.28	143.85	146.56	149.42	155.71	162.84	166.76	170.93	175.38
840.00	142.19	144.88	147.73	150.77	157.49	165.18	169.44	173.99	178.89
870.00	142.99	145.83	148.86	152.09	159.22	167.39	171.90	176.73	181.91
900.00	143.62	146.62	149.83	153.25	160.79	169.40	174.15	179.23	184.67
930.00	144.16	147.31	150.67	154.23	162.08	170.99	175.90	181.13	186.73
960.00	144.47	147.77	151.30	155.05	163.30	172.70	177.89	183.43	189.37
990.00	144.88	148.34	152.03	155.95	164.59	174.47	179.94	185.80	192.10
1020.00	145.23	148.88	152.75	156.87	165.97	176.47	182.35	188.70	195.59
1050.00	145.70	149.51	153.54	157.82	167.27	178.20	184.34	190.98	198.21
1080.00	146.08	150.07	154.27	158.74	168.61	180.04	186.48	193.50	201.14
1110.00	146.44	150.60	154.98	159.63	169.99	182.27	189.29	197.04	205.57
1140.00	146.83	151.16	155.70	160.52	171.29	184.12	191.50	199.67	208.67
1170.00	147.12	151.63	156.34	161.34	172.54	185.90	193.58	202.09	211.46
1200.00	147.31	152.00	156.88	162.07	173.71	187.61	195.61	204.46	214.22
1230.00	147.38	152.26	157.32	162.70	174.76	189.19	197.50	206.70	216.83

1260.00	147.27	152.35	157.60	163.18	175.67	190.62	199.22	208.74	219.23
1290.00	147.17	152.44	157.88	163.62	176.49	191.88	200.74	210.54	221.33
1320.00	147.07	152.55	158.18	164.11	177.43	193.39	202.60	212.81	224.08
1350.00	147.09	152.76	158.57	164.70	178.46	194.95	204.47	215.01	226.65
1380.00	147.16	153.02	159.01	165.33	179.54	196.59	206.45	217.37	229.44
1410.00	147.29	153.34	159.50	166.01	180.67	198.33	208.56	219.92	232.51
1440.00	147.53	153.74	160.07	166.77	181.90	200.17	210.78	222.61	235.74
1470.00	147.86	154.22	160.72	167.60	183.21	202.13	213.15	225.48	239.23
1500.00	148.22	154.74	161.37	168.46	184.54	204.09	215.50	228.29	242.58
1530.00	148.58	155.25	162.05	169.32	185.88	206.09	217.94	231.20	246.11
1560.00	148.95	155.75	162.74	170.18	187.22	208.07	220.34	234.09	249.59
1590.00	149.31	156.25	163.40	171.04	188.56	210.06	222.75	237.01	253.13
1620.00	149.67	156.75	164.07	171.90	189.90	212.06	225.16	239.92	256.64
1650.00	150.02	157.25	164.70	172.75	191.24	214.06	227.60	242.89	260.23
1680.00	150.37	157.74	165.36	173.60	192.57	216.07	230.05	245.88	263.85
1710.00	150.72	158.23	166.01	174.45	193.91	218.08	232.52	248.89	267.50
1740.00	151.07	158.72	166.69	175.30	195.25	220.11	235.01	251.92	271.16
1770.00	151.42	159.21	167.31	176.14	196.59	222.14	237.50	254.96	274.85
1800.00	151.76	159.69	167.99	176.99	197.93	224.18	240.00	258.01	278.56
1830.00	152.10	160.17	168.64	177.83	199.27	226.23	242.52	261.08	282.30
1860.00	152.43	160.65	169.29	178.67	200.60	228.28	245.04	264.16	286.08
1890.00	152.77	161.13	169.93	179.51	201.94	230.34	247.57	267.25	289.90
1920.00	153.10	161.60	170.57	180.34	203.28	232.40	250.11	270.37	293.75
1950.00	153.43	162.07	171.21	181.18	204.62	234.47	252.65	273.51	297.61
1980.00	153.75	162.54	171.85	182.01	205.96	236.54	255.20	276.68	301.48
2010.00	154.08	163.01	172.49	182.84	207.29	238.61	257.77	279.86	305.36
2040.00	154.40	163.48	173.12	183.67	208.63	240.69	260.34	283.04	309.25
2070.00	154.72	163.94	173.76	184.50	209.97	242.77	262.94	286.24	313.15
2100.00	155.04	164.41	174.39	185.33	211.31	244.86	265.54	289.44	317.06
2130.00	155.36	164.87	175.02	186.16	212.65	246.95	268.15	292.65	320.98
2160.00	155.68	165.33	175.65	186.98	213.99	249.05	270.76	295.86	324.91
2190.00	155.99	165.79	176.27	187.80	215.32	251.15	273.38	299.08	328.84
2220.00	156.31	166.25	176.90	188.62	216.66	253.26	276.00	302.31	332.78
2250.00	156.62	166.70	177.52	189.44	218.00	255.38	278.62	305.54	336.72
2280.00	156.93	167.16	178.14	190.26	219.34	257.49	281.25	308.77	340.67
2310.00	157.25	167.61	178.76	191.08	220.68	259.61	283.88	312.01	344.62
2340.00	157.56	168.07	179.38	191.89	222.01	261.73	286.51	315.25	348.58
2370.00	157.87	168.52	180.00	192.71	223.35	263.85	289.15	318.49	352.55
2400.00	158.18	168.97	180.62	193.52	224.69	265.98	291.78	321.74	356.52
2430.00	158.48	169.42	181.24	194.33	226.03	268.10	294.42	324.99	360.50
2460.00	158.79	169.87	181.85	195.14	227.37	270.23	297.07	328.24	364.48
2490.00	159.09	170.31	182.46	195.95	228.71	272.35	299.71	331.50	368.46
2520.00	159.40	170.76	183.08	196.76	230.04	274.48	302.36	334.76	372.45
2550.00	159.70	171.20	183.69	197.56	231.38	276.61	305.01	338.03	376.44
2580.00	160.00	171.65	184.30	198.36	232.72	278.75	307.66	341.29	380.43
2610.00	160.30	172.09	184.90	199.16	234.06	280.88	310.31	344.56	384.43
2640.00	160.60	172.53	185.51	199.96	235.40	283.01	312.96	347.83	388.43
2670.00	160.90	172.97	186.12	200.76	236.73	285.15	315.62	351.11	392.43
2700.00	161.19	173.41	186.72	201.56	238.07	287.28	318.28	354.38	396.68
2730.00	161.49	173.85	187.32	202.36	239.41	289.42	320.93	357.66	400.69
2760.00	161.78	174.29	187.93	203.15	240.75	291.56	323.60	360.94	404.71
2790.00	162.08	174.72	188.53	203.95	242.09	293.69	326.26	364.22	408.72

2820.00	162.37	175.16	189.12	204.74	243.43	295.83	328.92	367.51	412.74
2850.00	162.67	175.59	189.72	205.53	244.76	297.97	331.58	370.79	416.76
2880.00	162.96	176.02	190.32	206.33	246.10	300.11	334.25	374.08	420.79
2910.00	163.25	176.46	190.92	207.12	247.44	302.26	336.92	377.37	424.81
2940.00	163.54	176.89	191.51	207.91	248.78	304.40	339.58	380.65	428.84
2970.00	163.83	177.32	192.10	208.70	250.12	306.54	342.25	383.94	432.87
3000.00	164.12	177.75	192.69	209.49	251.45	308.69	344.92	387.24	436.90
3030.00	164.41	178.18	193.28	210.28	252.79	310.83	347.59	390.53	440.93
3060.00	164.70	178.60	193.87	211.06	254.13	312.98	350.26	393.82	444.96
3090.00	164.99	179.03	194.45	211.85	255.47	315.12	352.94	397.11	448.99
3120.00	165.28	179.46	195.04	212.63	256.81	317.27	355.61	400.41	453.03
3150.00	165.45	179.88	195.62	213.42	258.15	319.41	358.28	403.71	457.06
3180.00	165.74	180.31	196.21	214.20	259.48	321.56	360.96	407.00	461.10
3210.00	166.02	180.73	196.79	214.98	260.82	323.71	363.63	410.30	465.14
3240.00	166.56	181.27	197.47	215.85	262.22	325.87	366.28	413.54	469.07
3270.00	167.07	181.91	198.27	216.85	263.83	328.38	369.39	417.35	473.72
3300.00	167.75	182.70	199.22	218.01	265.63	331.14	372.79	421.51	478.81
3330.00	168.40	183.59	200.27	219.28	267.56	334.08	376.40	425.93	484.22
3360.00	169.27	184.58	201.42	220.65	269.62	337.19	380.22	430.61	489.93
3390.00	170.26	185.68	202.69	222.14	271.84	340.51	384.29	435.59	496.03
3420.00	171.35	186.87	204.04	223.74	274.18	344.00	388.56	440.81	502.43
3450.00	172.46	188.09	205.43	225.44	276.58	347.58	392.95	446.18	509.01
3480.00	173.57	189.31	206.83	227.03	279.01	351.20	397.39	451.62	515.68
3510.00	174.69	190.54	208.24	228.77	281.46	354.88	401.90	457.15	522.49
3540.00	175.81	191.78	209.65	230.46	283.94	358.59	406.45	462.74	529.37
3570.00	176.92	193.02	211.08	232.15	286.44	362.33	411.06	468.40	536.33
3600.00	178.03	194.26	212.50	233.86	288.96	366.20	415.71	474.12	543.38
3630.00	179.14	195.38	213.94	235.58	291.50	370.01	420.39	479.88	550.50
3660.00	180.24	196.61	215.37	237.30	294.04	373.85	425.11	485.69	557.67
3690.00	181.32	197.83	216.80	239.02	296.59	377.70	429.85	491.53	564.91
3720.00	182.40	199.05	218.23	240.74	299.15	381.56	434.62	497.63	572.20
3750.00	183.46	200.25	219.65	242.45	301.70	385.43	439.39	503.53	579.49
3780.00	184.51	201.44	221.07	244.16	304.26	389.30	444.17	509.44	586.81
3810.00	185.48	202.57	222.43	245.82	306.79	393.20	449.02	515.49	594.36
3840.00	186.47	203.70	223.79	247.47	309.25	396.93	453.62	521.19	601.39
3870.00	187.41	204.79	225.11	249.07	311.64	400.57	458.11	526.73	608.24
3900.00	188.33	205.86	226.39	250.63	314.00	404.15	462.53	532.19	614.98
3930.00	189.22	206.90	227.66	252.17	316.33	407.68	466.89	537.57	621.62
3960.00	190.09	207.91	228.89	253.68	318.61	411.15	471.16	542.85	628.13
3990.00	190.94	208.91	230.11	255.17	320.86	414.57	475.39	548.05	634.54
4020.00	191.77	209.90	231.32	256.64	323.10	417.99	479.60	553.25	640.95
4050.00	192.61	210.89	232.52	258.12	325.34	421.40	483.81	558.44	647.34
4080.00	193.44	211.88	233.73	259.60	327.59	424.81	488.01	563.63	653.73
4110.00	194.26	212.87	234.94	261.08	329.83	428.22	492.22	568.82	660.13
4140.00	195.08	213.85	236.14	262.55	332.07	431.64	496.43	574.01	666.52
4170.00	195.90	214.84	237.35	264.03	334.31	435.05	500.63	579.20	672.91
4200.00	196.71	215.82	238.55	265.51	336.56	438.46	504.84	584.39	679.30
4230.00	197.52	216.81	239.76	266.98	338.80	441.87	509.05	589.58	685.70
4255.77	198.21	217.65	240.79	268.25	340.73	444.81	512.67	594.04	691.19
4255.78	198.21	217.65	240.79	268.25	340.73	444.81	512.67	594.04	691.19

C.3 All simulated Off Bottom Torque data of 12.25'' section of Sangu 11

Table 26: C.3 Simulated off bottom torque data of 12.25'' section of Sangu 11

Simulated data				
Off Bottom Torque Output				
Bit Depth	CSG 0.2 OPH 0.2	CSG 0.3 OPH 0.3	CSG 0.4 OPH 0.4	CSG 0.5 OPH 0.5
m	1000 ft.lbf	1000 ft.lbf	1000 ft.lbf	1000 ft.lbf
0	0	0	0	0
30.00	0.01	0.01	0.01	0.01
60.00	0.00	0.01	0.01	0.01
90.00	0.01	0.01	0.01	0.02
120.00	0.03	0.04	0.05	0.06
150.00	0.05	0.07	0.09	0.12
180.00	0.06	0.10	0.13	0.16
210.00	0.08	0.12	0.16	0.20
240.00	0.15	0.23	0.31	0.38
270.00	0.18	0.27	0.36	0.45
300.00	0.28	0.43	0.57	0.71
330.00	0.37	0.56	0.75	0.94
360.00	0.54	0.81	1.08	1.35
390.00	0.60	0.89	1.19	1.49
420.00	0.76	1.15	1.53	1.91
450.00	0.94	1.41	1.88	2.35
480.00	1.17	1.76	2.34	2.93
510.00	1.29	1.93	2.57	3.21
540.00	1.42	2.13	2.85	3.56
570.00	1.54	2.32	3.09	3.86
600.00	1.72	2.58	3.44	4.29
630.00	1.90	2.85	3.80	4.75
660.00	2.04	3.06	4.08	5.10
690.00	2.13	3.19	4.25	5.32
720.00	2.40	3.61	4.81	6.01
750.00	2.62	3.93	5.24	6.54
780.00	2.77	4.16	5.54	6.93
810.00	2.91	4.36	5.82	7.27
840.00	2.98	4.48	5.97	7.46
870.00	3.16	4.73	6.31	7.89
900.00	3.38	5.06	6.75	8.44
930.00	3.46	5.20	6.93	8.66
960.00	3.60	5.40	7.20	9.00
990.00	3.71	5.57	7.42	9.28
1020.00	3.92	5.89	7.85	9.81
1050.00	4.09	6.13	8.18	10.22
1080.00	4.26	6.39	8.53	10.66
1110.00	4.46	6.69	8.92	11.15
1140.00	4.59	6.88	9.18	11.47
1170.00	4.74	7.11	9.49	11.86
1200.00	4.90	7.35	9.79	12.24
1230.00	5.04	7.57	10.09	12.61

1260.00	5.19	7.79	10.38	12.98
1290.00	5.28	7.92	10.56	13.21
1320.00	5.43	8.15	10.87	13.58
1350.00	5.60	8.40	11.20	14.00
1380.00	5.76	8.65	11.53	14.41
1410.00	5.93	8.90	11.87	14.83
1440.00	6.10	9.15	12.20	15.26
1470.00	6.27	9.41	12.54	15.68
1500.00	6.44	9.66	12.88	16.11
1530.00	6.61	9.92	13.23	16.53
1560.00	6.79	10.18	13.57	16.96
1590.00	6.96	10.44	13.92	17.40
1620.00	7.13	10.70	14.27	17.84
1650.00	7.31	10.97	14.62	18.28
1680.00	7.49	11.23	14.98	18.72
1710.00	7.67	11.50	15.33	19.17
1740.00	7.85	11.77	15.69	19.61
1770.00	8.03	12.04	16.05	20.06
1800.00	8.21	12.31	16.41	20.52
1830.00	8.39	12.58	16.78	20.97
1860.00	8.57	12.86	17.15	21.43
1890.00	8.76	13.14	17.51	21.89
1920.00	8.94	13.41	17.88	22.36
1950.00	9.13	13.69	18.26	22.82
1980.00	9.32	13.97	18.63	23.29
2010.00	9.50	14.25	19.01	23.76
2040.00	9.69	14.54	19.38	24.23
2070.00	9.88	14.82	19.76	24.70
2100.00	10.07	15.11	20.14	25.18
2130.00	10.26	15.39	20.52	25.65
2160.00	10.45	15.68	20.91	26.13
2190.00	10.65	15.97	21.29	26.61
2220.00	10.84	16.26	21.68	27.10
2250.00	11.03	16.55	22.07	27.59
2280.00	11.23	16.84	22.46	28.07
2310.00	11.43	17.14	22.85	28.56
2340.00	11.62	17.43	23.25	29.06
2370.00	11.82	17.73	23.64	29.55
2400.00	12.02	18.03	24.04	30.05
2430.00	12.22	18.33	24.44	30.55
2460.00	12.42	18.63	24.84	31.05
2490.00	12.62	18.93	25.25	31.56
2520.00	12.82	19.24	25.65	32.06
2550.00	13.03	19.54	26.05	32.57
2580.00	13.23	19.84	26.46	33.07
2610.00	13.43	20.15	26.86	33.58
2640.00	13.63	20.45	27.27	34.09
2670.00	13.84	20.76	27.67	34.59
2700.00	14.04	21.06	28.08	35.10
2730.00	14.24	21.37	28.49	35.61
2760.00	14.45	21.67	28.89	36.12
2790.00	14.65	21.98	29.30	36.63

2820.00	14.85	22.28	29.71	37.14
2850.00	15.06	22.59	30.12	37.65
2880.00	15.26	22.90	30.53	38.16
2910.00	15.47	23.20	30.94	38.67
2940.00	15.67	23.51	31.34	39.18
2970.00	15.88	23.82	31.75	39.69
3000.00	16.08	24.12	32.16	40.21
3030.00	16.29	24.43	32.57	40.72
3060.00	16.49	24.74	32.99	41.23
3090.00	16.70	25.05	33.40	41.75
3120.00	16.90	25.36	33.81	42.26
3150.00	17.11	25.66	34.22	42.77
3180.00	17.32	25.97	34.63	43.29
3210.00	17.52	26.28	35.04	43.80
3240.00	17.69	26.53	35.38	44.22
3270.00	17.93	26.89	35.85	44.81
3300.00	18.19	27.28	36.38	45.47
3330.00	18.47	27.70	36.93	46.17
3360.00	18.76	28.13	37.51	46.89
3390.00	19.05	28.58	38.10	47.63
3420.00	19.35	29.03	38.70	48.38
3450.00	19.65	29.48	39.31	49.14
3480.00	19.96	29.94	39.93	49.91
3510.00	20.27	30.41	40.55	50.68

C.4 All simulated Off Bottom Torque data of 8.5'' section of Sangu 11

Table 27: C.4 Simulated off bottom torque data of 8.5'' section of Sangu 11

Simulated data				
Off Bottom Torque Output				
Bit Depth	CSG 0.2 OPH 0.2	CSG 0.3 OPH 0.3	CSG 0.4 OPH 0.4	CSG 0.5 OPH 0.5
m	1000 ft.lbf	1000 ft.lbf	1000 ft.lbf	1000 ft.lbf
0.00	0.00	0.00	0.00	0.00
30.00	0.01	0.01	0.01	0.01
60.00	0.00	0.01	0.01	0.01
90.00	0.01	0.01	0.01	0.02
120.00	0.03	0.04	0.05	0.06
150.00	0.05	0.07	0.09	0.12
180.00	0.06	0.10	0.13	0.16
210.00	0.08	0.12	0.16	0.20
240.00	0.15	0.23	0.31	0.38
270.00	0.18	0.27	0.36	0.45
300.00	0.28	0.43	0.57	0.71
330.00	0.37	0.56	0.75	0.94
360.00	0.54	0.81	1.08	1.16
390.00	0.60	0.89	1.19	1.39
420.00	0.65	0.97	1.53	1.61
450.00	0.70	1.06	1.68	1.84
480.00	0.76	1.14	1.74	2.06
510.00	0.81	1.22	1.86	2.11
540.00	0.87	1.30	1.89	2.25
570.00	0.96	1.43	1.91	2.39
600.00	1.04	1.56	2.09	2.61
630.00	1.16	1.74	2.33	2.91
660.00	1.24	1.89	2.51	3.22
690.00	1.38	2.08	2.77	3.47
720.00	1.55	2.33	3.11	3.89
750.00	1.71	2.57	3.42	4.28
780.00	1.87	2.78	3.71	4.64
810.00	2.02	3.02	4.04	5.04
840.00	2.16	3.24	4.33	5.56
870.00	2.29	3.44	4.59	5.74
900.00	2.43	3.64	4.86	6.07
930.00	2.52	3.78	5.03	6.29
960.00	2.64	3.97	5.29	6.62
990.00	2.78	4.05	5.56	6.95

1020.00	2.94	4.41	5.87	7.34
1050.00	3.05	4.57	6.09	7.62
1080.00	3.18	4.78	6.37	7.96
1110.00	3.38	5.07	6.75	8.45
1140.00	3.52	5.28	7.04	8.80
1170.00	3.66	5.50	7.33	9.15
1200.00	3.81	5.72	7.62	9.53
1230.00	3.96	5.93	7.91	9.89
1260.00	4.10	6.14	8.19	10.24
1290.00	4.22	6.38	8.43	10.54
1320.00	4.37	6.55	8.74	10.92
1350.00	4.51	6.77	9.03	11.28
1380.00	4.66	7.00	9.33	11.66
1410.00	4.82	7.23	9.64	12.05
1440.00	4.98	7.47	9.96	12.45
1470.00	5.15	7.72	10.29	12.87
1500.00	5.31	7.96	10.62	13.28
1530.00	5.48	8.22	10.96	13.70
1560.00	5.65	8.47	11.29	14.02
1590.00	5.81	8.72	11.63	14.54
1620.00	5.98	8.98	11.97	14.96
1650.00	6.15	9.23	12.31	15.38
1680.00	6.32	9.49	12.65	15.81
1710.00	6.50	9.75	12.99	16.24
1740.00	6.67	10.07	13.34	16.68
1770.00	6.84	10.79	13.69	17.11
1800.00	7.02	10.53	14.04	17.55
1830.00	7.20	10.79	14.39	17.99
1860.00	7.37	11.06	14.74	18.43
1890.00	7.55	11.33	15.10	18.88
1920.00	7.73	11.59	15.46	19.32
1950.00	7.91	11.86	15.82	19.77
1980.00	8.09	12.14	16.18	20.23
2010.00	8.27	12.41	16.55	20.68
2040.00	8.46	12.68	16.91	21.14
2070.00	8.64	12.96	17.28	21.60
2100.00	8.83	13.24	17.65	22.07
2130.00	9.01	13.52	18.03	22.53
2160.00	9.20	13.80	18.40	23.00
2190.00	9.39	14.09	18.78	23.48
2220.00	9.58	14.37	19.16	23.95
2250.00	9.77	14.65	19.54	24.42
2280.00	9.96	14.94	19.92	24.90
2310.00	10.15	15.23	20.30	25.38
2340.00	10.34	15.51	20.68	25.86

2370.00	10.53	15.80	21.07	26.34
2400.00	10.73	16.09	21.45	26.82
2430.00	10.92	16.38	21.84	27.30
2460.00	11.11	16.67	22.23	27.78
2490.00	11.31	16.96	22.62	28.27
2520.00	11.50	17.26	23.01	28.76
2550.00	11.70	17.55	23.40	29.25
2580.00	11.90	17.85	23.80	29.75
2610.00	12.10	18.15	24.20	30.25
2640.00	12.30	18.45	24.59	30.74
2670.00	12.50	18.74	24.99	31.24
2700.00	12.69	19.04	25.39	31.74
2730.00	12.89	19.34	25.79	32.24
2760.00	13.09	19.64	26.19	32.74
2790.00	13.29	19.94	26.59	33.24
2820.00	13.49	20.24	26.99	33.74
2850.00	13.70	20.54	27.39	34.24
2880.00	13.90	20.84	27.79	34.74
2910.00	14.10	21.15	28.20	35.24
2940.00	14.30	21.45	28.60	35.75
2970.00	14.50	21.75	29.00	36.25
3000.00	14.70	22.05	29.40	36.76
3030.00	14.90	22.36	29.81	37.26
3060.00	15.11	22.66	30.21	37.77
3090.00	15.31	22.96	30.62	38.27
3120.00	15.51	23.27	31.02	38.78
3150.00	15.71	23.57	31.43	39.28
3180.00	15.92	23.87	31.83	39.79
3210.00	16.12	24.18	32.24	40.29
3240.00	16.31	24.46	32.62	40.77
3270.00	16.53	24.80	33.06	41.33
3300.00	16.77	25.15	33.54	41.92
3330.00	17.02	25.52	34.03	42.54
3360.00	17.27	25.91	34.54	43.18
3390.00	17.54	26.31	35.08	43.86
3420.00	17.82	26.73	35.64	44.56
3450.00	18.11	27.16	36.22	45.27
3480.00	18.40	27.60	36.80	46.00
3510.00	18.70	28.04	37.39	46.74
3540.00	18.99	28.49	37.99	47.48
3570.00	19.30	28.94	38.59	48.24
3600.00	19.60	29.40	39.20	49.01
3630.00	19.91	29.87	39.82	49.78
3660.00	20.22	30.33	40.44	50.55
3690.00	20.54	30.80	41.07	51.34

3720.00	20.85	31.28	41.70	52.13
3750.00	21.17	31.75	42.33	52.92
3780.00	21.48	32.23	42.97	53.71
3810.00	21.82	32.72	43.63	54.54
3840.00	22.12	33.18	44.24	55.30
3870.00	22.42	33.63	44.85	56.06
3900.00	22.72	34.08	45.44	56.80
3930.00	23.01	34.52	46.02	57.53
3960.00	23.30	34.95	46.60	58.25
3990.00	23.58	35.38	47.17	58.96
4020.00	23.87	35.80	47.74	59.67
4050.00	24.15	36.23	48.31	60.38
4080.00	24.44	36.66	48.87	61.09
4110.00	24.72	37.08	49.44	61.80
4140.00	25.01	37.51	50.01	62.51
4170.00	25.29	37.93	50.58	63.22
4200.00	25.57	38.36	51.15	63.94
4230.00	25.86	38.79	51.72	64.65
4255.77	26.10	39.15	52.21	65.26
4255.78	26.10	39.15	52.21	65.26